

UNCLASSIFIED

AD NUMBER
ADB282264
NEW LIMITATION CHANGE
TO Approved for public release, distribution unlimited
FROM Distribution authorized to U.S. Gov't. agencies only; Proprietary Information; Aug 2001. Other requests shall be referred to US Army Medical Research and Materiel Command, 504 Scott Street, Fort Detrick, MD 21702
AUTHORITY
USAMRMC ltr, 21 Feb 2003

THIS PAGE IS UNCLASSIFIED

AD _____

Award Number: DAMD17-99-1-9025

TITLE: Identification of Novel Prognostic Genetic Marker in
Prostate Cancer

PRINCIPAL INVESTIGATOR: Jeremy Squire, Ph.D.

CONTRACTING ORGANIZATION: Ontario Cancer Institute
Toronto, M5G 2M9, Canada

REPORT DATE: August 2001

TYPE OF REPORT: Final

PREPARED FOR: U.S. Army Medical Research and Materiel Command
Fort Detrick, Maryland 21702-5012

DISTRIBUTION STATEMENT: Distribution authorized to U.S. Government
agencies only (proprietary information, Aug 01). Other requests
for this document shall be referred to U.S. Army Medical Research
and Materiel Command, 504 Scott Street, Fort Detrick, Maryland
21702-5012.

The views, opinions and/or findings contained in this report are
those of the author(s) and should not be construed as an official
Department of the Army position, policy or decision unless so
designated by other documentation.

20020910 033

NOTICE

USING GOVERNMENT DRAWINGS, SPECIFICATIONS, OR OTHER DATA INCLUDED IN THIS DOCUMENT FOR ANY PURPOSE OTHER THAN GOVERNMENT PROCUREMENT DOES NOT IN ANY WAY OBLIGATE THE U.S. GOVERNMENT. THE FACT THAT THE GOVERNMENT FORMULATED OR SUPPLIED THE DRAWINGS, SPECIFICATIONS, OR OTHER DATA DOES NOT LICENSE THE HOLDER OR ANY OTHER PERSON OR CORPORATION; OR CONVEY ANY RIGHTS OR PERMISSION TO MANUFACTURE, USE, OR SELL ANY PATENTED INVENTION THAT MAY RELATE TO THEM.

LIMITED RIGHTS LEGEND

Award Number: DAMD17-99-1-9025
Organization: Ontario Cancer Institute

Those portions of the technical data contained in this report marked as limited rights data shall not, without the written permission of the above contractor, be (a) released or disclosed outside the government, (b) used by the Government for manufacture or, in the case of computer software documentation, for preparing the same or similar computer software, or (c) used by a party other than the Government, except that the Government may release or disclose technical data to persons outside the Government, or permit the use of technical data by such persons, if (i) such release, disclosure, or use is necessary for emergency repair or overhaul or (ii) is a release or disclosure of technical data (other than detailed manufacturing or process data) to, or use of such data by, a foreign government that is in the interest of the Government and is required for evaluational or informational purposes, provided in either case that such release, disclosure or use is made subject to a prohibition that the person to whom the data is released or disclosed may not further use, release or disclose such data, and the contractor or subcontractor or subcontractor asserting the restriction is notified of such release, disclosure or use. This legend, together with the indications of the portions of this data which are subject to such limitations, shall be included on any reproduction hereof which includes any part of the portions subject to such limitations.

THIS TECHNICAL REPORT HAS BEEN REVIEWED AND IS APPROVED FOR PUBLICATION.

11/10/2014 con Kelly

26/05/02

REPORT DOCUMENTATION PAGE			Form Approved OMB No. 074-0188	
Public reporting burden for this collection of information is estimated to average 1 hour per response, including the time for reviewing instructions, searching existing data sources, gathering and maintaining the data needed, and completing and reviewing this collection of information. Send comments regarding this burden estimate or any other aspect of this collection of information, including suggestions for reducing this burden to Washington Headquarters Services, Directorate for Information Operations and Reports, 1215 Jefferson Davis Highway, Suite 1204, Arlington, VA 22202-4302, and to the Office of Management and Budget, Paperwork Reduction Project (0704-0188), Washington, DC 20503				
1. AGENCY USE ONLY (Leave blank)	2. REPORT DATE August 2001	3. REPORT TYPE AND DATES COVERED Final (4 Jan 99 - 3 Jul 01)		
4. TITLE AND SUBTITLE Identification of Novel Prognostic Genetic Marker in Prostate Cancer		5. FUNDING NUMBERS DAMD17-99-1-9025		
6. AUTHOR(S) Jeremy Squire, Ph.D.				
7. PERFORMING ORGANIZATION NAME(S) AND ADDRESS(ES) Ontario Cancer Institute Toronto, Ontario, Canada E-Mail: jeremy.squire@utoronto.ca		8. PERFORMING ORGANIZATION REPORT NUMBER		
9. SPONSORING / MONITORING AGENCY NAME(S) AND ADDRESS(ES) U.S. Army Medical Research and Materiel Command Fort Detrick, Maryland 21702-5012		10. SPONSORING / MONITORING AGENCY REPORT NUMBER		
11. SUPPLEMENTARY NOTES Report contains color				
12a. DISTRIBUTION / AVAILABILITY STATEMENT Distribution authorized to U.S. Government agencies only (proprietary information, Aug 01). Other requests for this document shall be referred to U.S. Army Medical Research and Materiel Command, 504 Scott Street, Fort Detrick, Maryland 21702-5012.			12b. DISTRIBUTION CODE	
13. Abstract (<i>Maximum 200 Words</i>) (<i>abstract should contain no proprietary or confidential information</i>) Prostate cancer (PCa) has become the most commonly diagnosed cancer in men in North America. A critical issue in the management of PCa has been the lack of DNA-based markers for early detection and subsequent cure, before the disease can disseminate and become life-threatening. Our research premise is that analysis of chromosomal alterations in PCa, when correlated with clinical parameters, will provide a better understanding of the disease initiation and progression. FISH analyses of HPIN samples showed that the overall level of numeric chromosomal abnormalities, especially of chromosome 8, increased in patients that subsequently progressed to carcinoma. The presence of p53 mutation in HPIN was associated with the presence of CIN as determined by FISH. SKY analyses of PCa cell lines identified a consistent pattern of CIN underlying tumorigenesis with recurrent submicroscopic deletions occurring on chromosome 8p. In addition, CGH analyses of microdissected DOP-PCR amplified PCa foci demonstrated a more complete repertoire of aberrations as well as a better phenotype-genotype correlation. Presently, we are developing a high-resolution microarray CGH approach to focus on gene dosage changes on chromosome 8. Together, these results will aid in tumor suppressor gene(s) discovery that will eventually be used as prognostic markers of PCa progression.				
14. SUBJECT TERMS Molecular cytogenetics, Cancer genes, Prognostic markers, Chromosome anomalies			15. NUMBER OF PAGES 178	
			16. PRICE CODE	
17. SECURITY CLASSIFICATION OF REPORT Unclassified	18. SECURITY CLASSIFICATION OF THIS PAGE Unclassified	19. SECURITY CLASSIFICATION OF ABSTRACT Unclassified	20. LIMITATION OF ABSTRACT Unlimited	

TABLE OF CONTENTS

pg.2 **INTRODUCTION**

pg.3 **BODY**

pg.9 **KEY RESEARCH ACCOMPLISHMENTS**

pg.10 **REPORTABLE OUTCOMES**

pg.11 **CONCLUSIONS**

pg. 12 **REFERENCES**

pg 16 **APPENDICES**

INTRODUCTION:

Prostate cancer (PCa) has become the most commonly diagnosed cancer in men in North America with a mortality rate second only to lung cancer. As humans develop a longer life expectancy, the negative impact of PCa will rise dramatically. For example, at autopsy, a very large fraction (up to 30%) of elderly men in some cultures have evidence of PCa although there had been no clinical symptoms during life. With a longer life expectancy an increasing number of men will develop PCa and at present, the treatment of this disease is particularly problematic. Despite its prevalence, our understanding of the cellular and genetic basis for prostate tumorigenesis and metastasis remains limited. PCa appears to be distributed across a very broad spectrum of aggressiveness, and there are no reliable predictors of tumor behavior. A critical issue in the management of PCa has been the lack of DNA-based markers for early detection and subsequent cure. Since PCa is curable when it is organ-confined, but is not easily curable when it has spread beyond the prostate, prognostic indicators of aggressive disease are essential for increased survival. There are likely to be a number of genetic factors that together may affect the probability of development and progression of PCa. **We hypothesize that analysis of chromosomal alterations in PCa when correlated with clinical parameters will provide a greater understanding of PCa oncogenesis and tumor progression.**

Acquisition of genetic mutations of oncogenes and tumor suppressor genes underlie most cancers, and the challenge for cancer researchers is to isolate these causative genes and to determine their role in the malignant process. There are now many examples of human cancers where a molecular genetic approach has yielded valuable information that helps with the management of cancer patients. Chromosomal analysis of tumors has proven to be the best place to commence a strategy of identification of genes associated with specific tumors. In general, classical cytogenetic techniques have not been effective in detecting chromosomal aberrations in PCa due to the intratumor heterogeneity, and poor cell viability and chromosome quality. This report will address our progress in the context of the 'Statement of work'. It will identify the successful components of this study and will also point out some of the limitations of the approach that was originally proposed in our grant application and indicate how we have addressed some of the difficulties encountered in the funding period. Our recent progress highlights how we have addressed some of the technical challenges associated with studying the genetic basis of PCa oncogenesis. Our experimental design was based on the assumption that PCa-specific recurrent chromosomal changes will lead to loss of function of tumor suppressor gene(s) and/or activation of oncogenes and that clues concerning the location of such changes will be detected by using the most up to date molecular cytogenetic screening methods. Our experiments have focused on early human PCa and on patient cohorts in which we can correlate cytogenetic findings with poor outcome. We believe that identification of critical chromosomal regions recurrently involved in PCa will ultimately lead to the recognition of the key molecular pathways that will offer excellent opportunities for new diagnostic gene-based testing and novel therapeutic interventions.

BODY:**Aim 1. Evidence for specific chromosome translocation(s)/rearrangement(s) in early PCa?**

We were the first group in North America to apply SKY methodologies to PCa [*Mol. Diagn.* 5: 23 (2000); *Cancer. Genet. Cytogenet.* 120:50(2000)] (Appendices 1 and 2). In these two papers, our SKY analysis of PCa cell lines and tumor-derived immortalized prostate epithelial cell lines identified a large number of structural aberrations suggesting there was an underlying chromosomal instability and subsequent accumulation of cytogenetic alterations that confer a selective growth advantage. We utilized a combination of conventional and SKY techniques and allelotyping analysis (performed by Dr. Macoska's laboratory) to assess numerical and structural chromosomal alterations. These studies revealed trisomy for chromosome 20 and rearrangements involving chromosomes 3, 8, 10, 18, 19, 20 or 21. Interestingly, allelotyping data disclosed loss of 8p sequences in two of the five cell lines, and the spectral karyotyping data revealed that the loss of 8p sequences in these tumor-derived cell lines was directly due to i(8q) chromosome formation and/or other structural alterations of chromosome 8. The allelotyping showed that molecular changes not apparent by cytogenetic methods were present in these PCa cell lines. This study provided intriguing evidence that 8p loss in human prostate tumors could, in some cases, result from complex structural rearrangements involving chromosome 8. Culture conditions developed in this phase of the study were essential for in vitro growth of the immortalized PCa cell lines and short-term culture of patient samples.

To determine whether similar cytogenetic aberrations were present in patient tumors we have evaluated tumor tissue derived from 30 surgical resections using different modifications of conventional cytogenetic methods for solid tumors. Firstly, we varied the constituents of the culture media using suggestions from Dr. D. Peehl [1] and investigators working in the laboratory of Dr. S. Heim [2]. Secondly, we have used an irradiated murine feeder cell line S17 as a source of paracrine cytokines to stimulate epithelial cell growth [3]. While this substrate appeared to produce improved growth it was technically difficult to process additional quiescent cells and metaphase preparations obtained from these samples contained primarily normal karyotypes. However we noticed that a significant proportion of metaphase cells had random losses of chromosomes and in the light of the observations made in Appendices 1 and 2 we further investigated numerical cell-to-cell variation of chromosome 8 aneusomy in the LNCaP, DU145, and PC-3 cell lines and a patient cohort of 15 PCa primary tumors by interphase fluorescence *in situ* hybridization (FISH). Our analysis showed that a high frequency of numerical alteration affecting chromosome 8 was present in both *in vitro* and PCa tissues. In comparison to normal controls, the patient cohort had a statistically significant ($p < 0.05$) greater frequency of cells with one and three centromere 8 copies. These data suggest that a chromosomal instability (CIN) process may be contributing towards the generation of *de novo* numerical and structural chromosome abnormalities in PCa [*Neoplasia* 3 No. 1 62-69 (2001)] (Appendix 3). Taken together with the data presented in Appendices 1 and 2 these observations were consistent with a pattern of CIN

underlying tumorigenesis in PCa with recurrent submicroscopic deletions occurring on the short arm of chromosome 8.

Aim 2. Evidence for consistent predictive chromosomal changes (numerical and structural gains and/or losses) in pre-neoplastic and/or early preinvasive carcinoma

Concurrently with the above SKY and interphase FISH studies we have been retrospectively analyzing numerical chromosomal changes in paraffin sections by interphase FISH using prostate biopsy sections to determine levels of intratumor cytogenetic heterogeneity and to determine whether interphase FISH can be used as an additional predictor of increased risk of carcinoma. It is well-established that high-grade prostrate intraepithelial neoplasia HPIN is the most likely precursor of PCa. Many patients with HPIN diagnosis in a prostate needle core biopsy, if left untreated they will progress to invasive cancer. Currently there is no available clinical, immunohistochemical or morphological criteria that are predictive of this progression but our progress has allowed us to develop a biological model to address the early genetic steps in the transition from HPIN to neoplasia.

p53 has been found to be associated with genomic instability leading to chromosomal rearrangement, which in turn has been demonstrated as a feature of many neoplastic and preneoplastic (dysplastic) human epithelia. The transition from preinvasive disease to invasive carcinoma was shown to be associated with changes in the number of chromosome copy and that coincide with the loss of *TP53* function. Whether there is a role of CIN in the progression of HPIN foci to invasive cancer and whether is that influenced by heterogeneity in the p53 expression between different HPIN foci is still unknown. p53 mutation has been shown to be associated with CIN in many human dysplastic and neoplastic lesions. However the precise role of p53 in the pathogenesis of PCa is unknown. In this component of our study we used topographic analysis of p53 alteration using immunohistochemistry on 35 archived prostatectomy specimens containing PCa foci; high-grade prostrate intraepithelial neoplasia (HPIN) foci intermingled with cancer (HPINI) and foci situated away (HPINA). Specimens from 2 patients were topographically genotyped using laser capture microdissection, PCR amplification and direct sequencing of p53 exons 5-9. CI was evaluated in the same tissue foci by interphase *in situ* hybridization using centromere probes for chromosome 7, 8 and Y. p53 immunoreactivity was found in 20%, 17%, 0%, and 0% in PCa, HPINI, HPINA, and benign epithelium respectively. p53 molecular analysis in the specimens examined confirmed the IHC findings. interphase FISH revealed numerical chromosomal alterations in keeping with CIN in 71% and 25% of p53+ve and p53-ve PCa respectively ($P=0.1$), 67% and 0% of p53+ve and p53-ve HPIN respectively ($P<0.02$) and in 27% and 0% of HPINI and HPINA respectively. We concluded that p53 mutation is an early change in at least a subset of PCa. HPINI foci tend to have higher overall p53 immunoreactivity and CIN than HPINA. The presence of p53 mutation in HPIN was associated with the presence of CIN as determined by interphase FISH. Our study also provided additional evidence in support of the concept that HPIN might be the earliest precursor of cancer. Furthermore our studies identify genomic similarities in HPINI and

PCa, implying that carcinoma may arise from progression of certain HPIN foci that most likely harbor p53 mutation and/or more CIN [accepted in *Arch. Path.* pending minor revisions] (Appendix 4).

To determine whether chromosomal changes in these precursor lesions could increase its predictive value an interphase *in situ* hybridization analysis was performed on archived prostate needle core biopsies from 54 patients with initial diagnosis of isolated HPIN and follow-up of 3 years or more. We utilized commercially available centromere probes for chromosomes 4, 7, 8, 10. We had interpretable results in 44 patients as follows: 1) group A: 24 HPIN patients with persistent HPIN and/or benign lesions in the follow-up biopsies, and 2) group B: 20 HPIN patients with progression to prostate carcinoma. Twenty five percent of the patients in group B displayed numerical chromosomal aberrations. Only 8.3 % of the patients from group A had chromosomal abnormalities ($P=0.1$). The overall chromosomal changes in HPIN were higher than normal or hyperplastic epithelium with statistically significant difference ($P<0.05$). All aberrations were detected in the form of chromosomal gain. Overall, the commonest aberration was gain of chromosome 8, followed by gains of chromosomes 7 and 10. These results indicated that while no single numeric chromosomal abnormality could be assigned as a predictor of HPIN progression to carcinoma, the overall level of numeric chromosomal abnormalities show a trend of elevation in HPIN patients that subsequently progressed to carcinoma [accepted in *Modern Pathology* pending minor revisions] (Appendix 5). Taken together the results of Appendices 4 and 5 are also important mechanistically since they suggest that CIN is more common in HPIN foci that progress to and/or are situated adjacent to carcinoma foci and that p53 mutation associated with HPIN was more likely to lead to CIN developing.

The overall molecular approach that we are taking to study HPIN in PCa is reviewed in Appendix 6. In the initial phase of this study we applied comparative genomic hybridization (CGH) and interphase FISH to twenty one early stage pT1/pT2 PCa specimens in order to: 1) evaluate the utility of CGH for examining bulk-extracted genomic DNA from early stage PCa specimens; 2) identify all regions of chromosomal gain and loss present in each patient sample; 3) determine whether there are any consistent genomic dosage changes, common to the patient cohort; and 4) verify any aberrations found by CGH using interphase FISH. To investigate the effect of tumor heterogeneity on the analysis of genomic aberration, we compared the results of CGH analysis using DNA extracted from tumor bulk, against that of DNA amplified by degenerate oligonucleotide primed PCR (DOP-PCR) from homogeneous cell population obtained by laser capture microdissection of discrete, individual tumor foci. Sampling by microdissection, positive aberrations were observed in 3 of 3 foci of carcinoma involved with prostatic capsule, and in 2 of 3 HPIN foci examined. Carcinoma foci consistently exhibited more extensive aberrations than the HPIN samples obtained from the same tumor. Microfoci of epithelial acini from the same tumour, separated by no more than 3mm exhibit significantly different CGH profiles, indicating high extent of CIN within PCa tumours. Between the different tumor samples, gain of 8q was the only consistent feature while HPIN showed no consistent aberration. Using bulk extracted DNA, CGH detected aberrations in only 3 of the 21 samples interrogated, despite the known trisomy

8 status, as revealed by FISH. The results presented in Appendix 7 [currently under review in *Prostate*] demonstrate that CGH analysis using bulk dissected fresh tissue is not sufficiently sensitive to fully detect the chromosomal numerical aberrations in PCa. Given the considerable intratumor genomic heterogeneity, CGH in conjunction with microdissection and DOP-PCR amplification provides a more complete repertoire of aberrations as well as a better phenotype-genotype correlation in prostate tumors.

Aim 3. Positional mapping to identify putative candidate genes, which may be useful as prognostic indicators of early disease.

Aims 1 and 2 of our research program drew attention to the importance of microdeletions and LOH implicating and localizing the regions containing candidate tumor suppressor genes on the short arm of chromosome 8. In addition they highlighted the need to use laser capture microdissection to obtain purer populations of homogeneous tissue so that the earliest genetic alterations associated with PCa can be clearly resolved. Our model does not support the idea that recurrent chromosomal translocations are involved in PCa (one component of our original hypothesis). Thus rather than use large YACs to detect genomic disruption (as originally proposed) we have used microarray CGH from the short arm of human chromosome 8 to detect by high resolution the precise location of deletions in PCa DNA originally identified in Aims 1 and 2 by conventional 'chromosome CGH'.

The reason we chose to use microarray methods is because recent significant advances in microarray technology have circumvented some of the resolution limitations we experienced with chromosome target CGH. An emerging platform that addresses the shortcomings of chromosome CGH couples the technique to microarray expression technology, and is generally referred to as "array CGH". Instead of using chromosome targets, CGH is applied to arrayed short DNA sequence targets bound to glass slides thus significantly increasing resolution for localizing regions of imbalance. To date, several other groups have published results using array CGH. Pinkel et al. [4] detected genomic imbalances within a sub-band of chromosome 20 in breast cancer, that had failed to be observed using chromosome CGH. In another study, array CGH was used to examine neurofibromatosis type 2 (*NF2*) patients and determined the extent and frequency of deletions around the *NF2* locus on chromosome 22q [5]. Further refinements have permitted retrospective analysis using genomic DNA from archival samples as we are doing in this study. Daigo et al. have adapted array CGH for amplicon profiling of formalin-fixed paraffin-embedded tumour samples [6], using DOP-PCR for whole genome amplification of the extracted DNA.

At present, we are constructing a genomic DNA tiling path along chromosome 8p23 to identify copy number changes by array CGH experiments. This region of the genome is highly pertinent to PCa for two reasons: 1) Previous publications [7-10] have mapped a homozygous deletion in this region, suggesting the presence of a tumor suppressor gene(s); and 2) this region is poorly characterised, as there are 30-40 *in silico* predicted genes from the Human Genome Project (see Table 1 below) with no ascribed function or

with a postulated function based on homology. Currently, our genomic array is derived from 129 bacterial artificial chromosomes (BACs) that cover approximately 13 Mb from the telomere of chromosome 8 (8pter) to cytoband 8p22. These BACs were identified using the MapViewer resource at the NCBI (http://www.ncbi.nlm.nih.gov/cgi-bin/Entrez/hum_srch). Genomic DNA from BACs derived from chromosomes 3, 2p24 (*MYCN*), 8q, 11, X, and Y will also be included onto the array and will serve as controls. After the BACs were obtained from the RPCI-11 library, genomic DNA was extracted using a mini prep kit, column purified, followed by two rounds of whole-genome amplification using degenerate oligonucleotide primed-PCR (DOP-PCR), and finally spotted onto glass slides. We are using protocols similar to those described in Appendix 8 [from "*Molecular Cytogenetics: Protocols and Applications*" Humana Press (to be published 2002) chapter called "*Microarray CGH*"] for performing array CGH. While we are presently optimizing the technique with control samples having known copy number changes, our end goal is to examine DNA extracted from microdissected DOP-PCR patient tumors to eventually identify progression prognosticators. Concurrently, we have developed custom softwares for normalizing and analyzing microarray results. During analysis of array CGH results, we will recognize submicroscopic deletions by a normalized fluorescence signal decrease to ~ 0.5 - 0.6 by ratio analysis. Bioinformatics sequence analyses of this region, including *in silico* screening of prostate expression libraries, will complement the array CGH to provide supporting evidence for genes of interest. To confirm such deletions we will use genomic probes that map to the deleted region(s) of chromosome 8 for direct FISH analysis of paraffin sections. We anticipate being in a strong position to localize the region(s) and gene(s) involved in the development of PCa and poor disease outcome as this research program continues. An example of the results we have obtained using cDNA array targets (methods described in Appendix 8) and characterizing genomic imbalance of chromosome 8 is shown below in Figure 1.

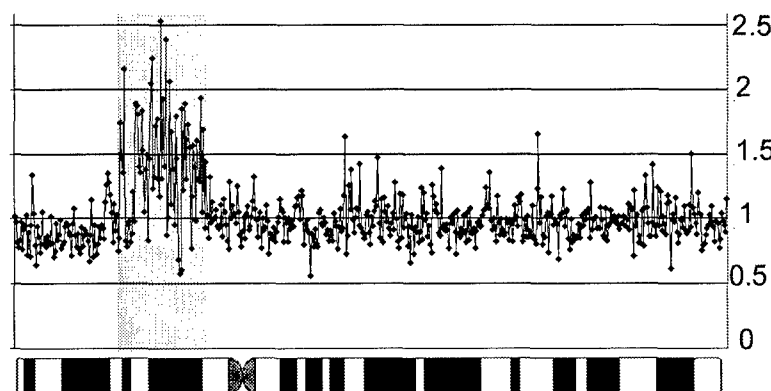


Figure 1 Array CGH analysis of gain of chromosome 8. In this analysis the increased resolution of copy number imbalance using cDNA microarrays is well illustrated. In Appendix 8 of this progress report the application of array CGH is reviewed. This approach is being used to localise chromosomal losses in band 8p23 (D8S1781-D8S262) to determine the minimal region that contains a PCa-specific tumor suppressor gene.

Gene Symbol	band	Megabase from Telomere (Mb)	Gene Orientation	Predicted Function
LOC91979	8p23.3	0.1	-	?
LOC91980	8p23.3	0.2	+	?
LOC91981	8p23.3	0.25	-	?
FLJ12847	8p23.2	5.2	+	?; protein exists
LOC90913	8p23.2	5.3	+	?
FLJ11210	8p23.1	5.8	-	Member of the phospholipid and glycerol acyltransferase family; may be involved in phospholipid metabolism
LOC90912	8p23.1	5.95	+	?
LOC82134	8p23.1	5.95	+	Sequence containing defensin, alpha 1, myeloid-related regions
LOC91819	8p23.1	6.7	-	?
LOC91048	8p23.1	6.9	+	?
LOC91049	8p23.1	6.9	-	?
LOC90448	8p23.1	7.3	-	?
LOC90449	8p23.1	7.55	-	?
LOC90453	8p23.1	7.6	-	?
LOC90454	8p23.1	7.65	-	?
MGC16279	8p23.1	7.65	-	?; protein exists
LOC90455	8p23.1	7.65	+	?
LOC90456	8p23.1	7.8	+	?
LOC90459	8p23.1	8.55	+	?
DKFZP434K171	8p23.1	9.55	+	Low similarity to a region of myotubularins
LOC90823	8p23.1	9.7	-	?
MGC10442	8p23.1	9.75	+	Non-receptor protein tyrosine kinase with SH3 and SH2 domains
LOC92938	8p23.1	10.1	-	?
LOC92939	8p23.1	10.1	-	?
LOC90911	8p23.1	10.3	-	?
LOC91782	8p23.1	10.7	+	?
PRO1496	8p23.1	10.9	-	?; protein exists
LOC51312	8p23.1	11	+	Mitochondrial solute carrier
PRO1584	8p23.1	11	+	?; protein exists
KIAA0717	8p22	12.15	+	Ras-like gene
KIAA0062	8p22	12.2	+	?; protein exists
LOC59346	8p22	12.5	+	LIM protein mystique
FLJ10351	8p22	12.55	+	Highly similar to <i>PIWI</i> ; may be required for germ-line stem cell division
FLJ14107	8p22	12.55	+	?; protein exists
LOC57805	8p22	12.55	-	p30 DBC protein
FLJ11125	8p22	12.9	-	?; protein exists
FLJ21801	8p22	12.95	+	?; protein exists
FLJ22494	8p22	13	-	?; protein exists

Table 1. Gene and their putative function (if known) predicted to be in the 13 Mb region covered by our array, from 8pter – 8p22 (source: http://www.ncbi.nlm.nih.gov/cgi-bin/Entrez/hum_srch).

The size of biological samples obtained from PCa biopsies is, in most cases, very limited, particularly when obtained by fine needle biopsies or laser-capture microdissection, and therefore acquiring sufficient amounts of RNA to carry out subsequent expression analyses and mutational studies of the above candidate genes could be problematic. We have therefore used modified cDNA synthesis approach to generate, directly during the PCR step, fluorescently labeled probes immediately usable for cDNA microarray hybridization expression analysis. Our statistical analysis of gene expression using microarray analysis demonstrated the fidelity of this new amplification/labeling approach to that of the standard T7-amplification method (*manuscript in preparation*) and indicate that we will be able to continue our analysis of patient samples at both the DNA and RNA level as we search for candidate genes in these regions of chromosome 8p. This research work was recently an invited platform presentation at the NIH annual laser capture microdissection meeting in Washington DC.

KEY RESEARCH ACCOMPLISHMENTS:

- First SKY paper analyzing PCa (selected as the cover feature for the issue).
- First delineation of chromosome 8 alterations by SKY in PCa cell lines.
- Optimization of *in vitro* conditions for short-term culture and SKY analysis of patient PCa tissue.
- Characterization of CIN phenotype in PCa cell lines and patient samples and development of a model to explain the differential rate of CIN *in vitro*.
- Identified p53 mutation as an early change in a subset of PCa. HPIN close to invasive foci of carcinoma tend to have higher overall p53 immunoreactivity and elevated level of CIN compared to HPIN away from carcinoma.
- The presence of p53 mutation in HPIN was associated with the presence of CIN as determined by interphase FISH.
- Our studies provided additional evidence in support of the concept that HPIN might be the earliest precursor of cancer.
- Our work identified genomic similarities in HPIN close to invasive carcinoma and in the PCa tumor implying that carcinoma may arise from progression of certain HPIN foci that most likely harbor p53 mutation and/or elevated CIN.
- Interphase FISH analysis of HPIN indicated that while no single numeric chromosomal abnormality could be assigned as a predictor of HPIN progression to carcinoma, the overall level of numeric chromosomal abnormalities show a trend of elevation in HPIN patients that subsequently progressed to carcinoma.
- Development of a model that indicates that CIN is more common in HPIN foci that progress to and/or are situated adjacent to carcinoma foci, and that p53 mutation associated with HPIN was more likely to lead to developing CIN.
- CGH analysis of PCa patient tumors identifies a low frequency of chromosomal copy number aberration in bulk-extracted tissue.
- Development of laser capture microdissection and DOP-PCR methods for CGH analysis of tumor microfoci.

- Development of glass slide-based microarray for analysis of gene copy number and expression by CGH.
- Development of RNA amplification methods following laser capture microdissection for gene expression analysis.

REPORTABLE OUTCOMES:

- 3 papers published (Appendices 1-3)
- 2 papers accepted pending minor revisions (Appendices 4-5)
- 1 paper in press (Appendix 6)
- 1 paper under review (Appendix 7)
- 1 invited chapter review (Appendix 8)
- 14 abstracts.
- Three graduate students are working on this project. Dr. Jaudah Al-Maghrabi is a M.D. Pathologist on a training fellowship from Saudi Arabia. He completed his M.Sc. based on the data presented in Appendices 4 and 5 in December 2000. His fellowship support derived from Saudi Arabia.
- Ben Beheshti recently reclassified to become a predoctoral student. His student stipend is supported by the Paul Starita Fellowship and University of Toronto Open Scholarships.
- Bisera Vukovic is a new PhD student who is supported by an NCIC prostate cancer studentship. Her thesis work that has developed directly from the discoveries made by this project and it centers on the role of telomere erosion in eliciting the genomic instability associated with early HPIN lesions in PCa.
- Dr. Paul Park derived part of his stipend from the American Foundation for Urological Diseases. Dr. Park is the first Canadian to receive an AFUD scholarship award for his work on prostate cancer. He is now training to be a clinician scientist at the University of Toronto.
- Development of chromosome 8 EST database for gene discovery/ LOH analysis.
- Co-op training BSc Rotation student third year from University of Waterloo, London Ontario. Craig Platt. Working with Ben Beheshti on CGH Analysis of prostate cancer cell line and tumours using high density EST microarray. April 2000-August 2000.
- Successful grant application to National Cancer Institute of Canada (NCIC) for research funding of microarray analysis to detect prognostic differential gene expression in PCa.
- Co-op training BSc Rotation student third year from University of Waterloo, London Ontario. Karen Kwon. Working with Ben Beheshti on CGH Analysis of prostate cancer cell line and tumours using high density EST microarray. September 2000-December 2000.
- Co-Applicant of successful grant application to NCIC for research grant supporting National Network of Prostate Cancer researchers in Canada for more effective utilization of resources and infrastructure.
- Co-Applicant of successful grant application to NCIC to support research training in prostate cancer.

- Two month academic research visit from Dr. Monica Nunes (University of Sao Paulo) to study HPIN in PCa.
- Development of collaboration with Dr. J. Macoska for 8p allelotyping
- Co-op training BSc Rotation student third year from University of Waterloo, London Ontario. Ilan Braude. Working with Ben Beheshti on CGH Analysis of prostate cancer cell line and tumours using high density EST microarray. January 2001-August 2001.

CONCLUSIONS:

Our studies have demonstrated the value of using the most sensitive molecular cytogenetic LOH detection methods to study DNA alterations in early PCa lesions. SKY has shown that long-term cell lines have a much greater complexity of aberration than short-term cultures. This study provided evidence that 8p loss in human prostate tumors could, in some cases, result from complex structural rearrangements involving chromosome 8. We detected a high frequency of numerical alteration affecting chromosome 8 by interphase FISH was present in both *in vitro* and PCa tissues. In comparison to normal controls, the patient cohort had a statistically significant ($p < 0.05$) greater frequency of cells with one and three centromere 8 copies. The results of our first Aim were consistent with a pattern of CIN underlying tumorigenesis in PCa with recurrent submicroscopic deletions occurring on the short arm of chromosome 8.

We also concluded that p53 mutation is an early change in at least a subset of PCa. HPIN situated near invasive foci tend to have higher overall p53 immunoreactivity and CIN than HPIN situated away from carcinoma. The presence of p53 mutation in HPIN was associated with the presence of CIN as determined by interphase FISH. Our study also provided additional evidence in support of the concept that HPIN might be the earliest precursor of cancer. Furthermore our studies identify genomic similarities in HPIN close to invasive carcinoma and PCa, implying that carcinoma may arise from progression of certain HPIN foci that most likely harbor p53 mutation and/or more CIN. Our interphase FISH results indicated that while no single numeric chromosomal abnormality could be assigned as a predictor of HPIN progression to carcinoma, the overall level of numeric chromosomal abnormalities show a trend of elevation in HPIN patients that subsequently progressed to carcinoma. These findings are also important mechanistically since they suggest that CIN is more common in HPIN foci that progress to and/or are situated adjacent to carcinoma foci and that p53 mutation associated with HPIN was more likely to lead to CIN developing. In addition the results indicate that laser capture microdissection is the best way to obtain homogeneous nucleic acid for further study to better understand early genetic changes in PCa. In the latter phase of Aim 2 we demonstrated that CGH analysis using bulk dissected fresh tissue was not sufficiently sensitive to fully detect the chromosomal numerical aberrations in PCa. Given the considerable intratumor genomic heterogeneity, CGH in conjunction with microdissection and DOP-PCR amplification provides a more complete repertoire of aberrations as well as a better phenotype-genotype correlation in prostate tumors.

In Aim 1 we found that some deletions of chromosome arm 8p will be submicroscopic since they are apparent by molecular analysis such as LOH but by cytogenetic methods cannot be seen. We have therefore developed high-resolution CGH microarrays as part of the second phase of this work to characterize the copy number from the telomere of chromosome (8pter) to band 8p22 using DNA extracted from microdissected DOP-PCR patient tumors. Our genomic array currently has 129 BACs that cover approximately 13 Mb almost contiguously, starting from the telomere of chromosome 8p. At present, it is clear that this region has many uncharacterized genes that are of interest to cancer research. Together with our bioinformatics analyses of this region, our array CGH approach will aid in tumor suppressor gene(s) discovery that may eventually be used as prognostic markers of PCa progression.

REFERENCES:

1. Peehl, D.M., et al., *In vitro studies of human prostatic epithelial cells: attempts to identify distinguishing features of malignant cells*. Growth Factors, 1989. **1**(3): p. 237-50.
2. Teixeira, M., et al. *High frequency of clonal chromosome abnormalities in prostatic neoplasms sampled by prostatectomy or ultrasound-guided needle biopsy*. in *Proceedings of the Eighth International Workshop on Chromosomes in Solid Tumors*. 2000. Tucson, AZ, USA.
3. Kurosaka, D., T.W. LeBien, and J.A. Pribyl, *Comparative studies of different stromal cell microenvironments in support of human B-cell development*. Exp Hematol, 1999. **27**(8): p. 1271-81.
4. Pinkel, D., et al., *High resolution analysis of DNA copy number variation using comparative genomic hybridization to microarrays*. Nat Genet, 1998. **20**(2): p. 207-11.
5. Bruder, C.E., et al., *High resolution deletion analysis of constitutional DNA from neurofibromatosis type 2 (NF2) patients using microarray-CGH*. Hum Mol Genet, 2001. **10**(3): p. 271-82.
6. Daigo, Y., et al., *Degenerate oligonucleotide primed-polymerase chain reaction-based array comparative genomic hybridization for extensive amplicon profiling of breast cancers : a new approach for the molecular analysis of paraffin-embedded cancer tissue*. Am J Pathol, 2001. **158**(5): p. 1623-31.
7. Perincher, G., et al., *Loss of two new loci on chromosome 8 (8p23 and 8q12-13) in human prostate cancer*. Int J Oncol, 1999. **14**(3): p. 495-500.
8. Sun, P.C., et al., *Homozygous deletions define a region of 8p23.2 containing a putative tumor suppressor gene*. Genomics, 1999. **62**(2): p. 184-8.
9. Sunwoo, J.B., et al., *Localization of a putative tumor suppressor gene in the sub-telomeric region of chromosome 8p*. Oncogene, 1999. **18**(16): p. 2651-5.
10. Wright, K., et al., *Frequent loss of heterozygosity and three critical regions on the short arm of chromosome 8 in ovarian adenocarcinomas*. Oncogene, 1998. **17**(9): p. 1185-8.

BIBLIOGRAPHY:

papers

Beheshti, B., Karaskova, J., Park, P., **Squire, J.A.**, Beatty, B.G., Identification of a High Frequency of Chromosomal Rearrangements in the Centromeric Regions of Prostate Cancer Cell Lines by Sequential Giemsa Banding and Spectral Karyotyping. *Molecular Diagnosis* 5(1) 23-32 (2000). APPENDIX 1

Squire, J.A. Genetic characterization of immortalized human prostate epithelial cell cultures: Evidence for structural rearrangements of chromosome 8 and i(8q) chromosome formation in primary tumor-derived cells. *Cancer Genet Cytogenet.* Jul 1;120(1):50-7 (2000) APPENDIX 2

Beheshti B., Park P., Sweet J., Trachtenberg J., Jewett M. A. S., **Squire JA.** Evidence of chromosomal instability in prostate cancer determined by spectral karyotyping (SKY) and interphase FISH analysis. *Neoplasia* 3(1)62-69 (2001) APPENDIX 3

Al-Maghrabi J., Vorobyova L., Toi A., Jothy S., Chapman W., Jewett M., Zielenska M., Sweet J., Trachtenberg J., Banarjee D. and **Squire J A.** Identification of numerical chromosomal changes detected by interphase FISH in high-grade prostrate intraepithelial neoplasia (HPIN) as a predictor of carcinoma. *Arch. Path and Lab Medicine* APPENDIX 4.

Al-Maghrabi J., Vorobyova L., Toi A., Chapman W., Zielenska M.. and **Squire JA.** p53 alteration in prostatic high intraepithelial neoplasia (HPIN) and concurrent carcinoma: Immunohistochemistry, interphase *in situ* hybridization (FISH), and sequencing analysis of laser captured microdissected specimens. *Modern Pathology* APPENDIX 5

J. Trachtenberg, JA. **Squire, JA.** Sweet, T.J. Brown. Prostatic Intraepithelial Neoplasia: Molecular Considerations. *Urology* 2001 (In Press) APPENDIX 6

Beheshti B, Marrano P **Squire JA** and Park PC. Resolution of genotypic heterogeneity in prostate tumors using DOP-PCR and CGH on microdissected carcinoma and PIN foci. (Under review *Prostate*) APPENDIX 7

Beheshti B, Marrano P **Squire JA** and Park PC: Microarray CGH. Book chapter in Molecular Cytogenetics: Protocols and Applications. Series: *Methods In Molecular Medicine* Humana Press (to be published 2002) APPENDIX 8

abstracts

Comparative microarray study of T7-based and PCR-based RNA amplification approaches: a pilot study for the expression profiling of laser capture microdissected prostate cancer samples. Albert M, Ijuria I, Park P, **Squire JA** and Macgregor P.

Presented at Laser Capture Microdissection Annual Meeting. NIH Washington July 2001.

B. Beheshti, P.C. Park, C. Lu, I. Braude, C. Platt, K. Kwon, J. Woodgett, **J.A. Squire**. Analysis of Chromosome 8p23.2 in Prostate Cancer by *in silico* Study of Biological Databanks and High-Resolution Comparative Genomic Hybridization on DNA Microarrays. Proceedings of the 92nd Annual Meeting of the American Association for Cancer Research. New Orleans, March 2001. 42:67.

P.C. Park, B. Beheshti, P. Marrano, J. Bayani, J. Sweet, J. Trachtenberg, **J.A. Squire**. Identification of Chromosomal Aberrations and Intratumor Genotypic Heterogeneity by Comparative Genomic Hybridisation in Laser-Capture Microdissected Prostate Tissue. Proceedings of the 92nd Annual Meeting of the American Association for Cancer Research. New Orleans, March 2001. 42:150.

B. Beheshti, P.C. Park, L.R. Kapusta, L. Klotz, **J.A. Squire**. Analysis of Prostate Cancer Cell Lines and Tumours Using High-Density EST Microarrays. Proceedings of the Human Genome Meeting 2000 (poster 275); and Canadian Genetics Diseases Network. Vancouver, April 2000.

J. Trachtenberg, **J.A. Squire**, J. Sweet, T.J. Brown. Prostatic Intraepithelial Neoplasia: Molecular Considerations. Annual Prostate Cancer Meeting. Lake Tahoe (2000)

Beheshti B, Karaskova J, Beatty BG, Park PC, Beheshti M, Trachtenberg J, Sweet J, Jewett, Rhim JS, Hukku B, **Squire JA**, Macoska J. Chromosomal aberrations in early-stage prostate cancer patients and virus-immortalized cell lines identified by combined CGH, SKY, and Allelotyping techniques. Proceedings of the American Association of Cancer Research. March 41:513 (2000)

B. Beheshti, J. Karaskova, B.G. Beatty, P.C. Park, J. Sweet, M. Beheshti, J. Trachtenberg, J.S. Rhim, B. Hukku, **J.A. Squire**, J.A. Macoska. Chromosomal Aberrations in Early Stage Prostate Cancer Patients and Virus-Immortalised Cell Lines Identified by Combined Comparative Genomic Hybridization, Spectral Karyotyping, and Allelotyping Techniques. Abstract accepted in the 8th International Workshop on Chromosomes in Solid Tumors, Tucson, AZ, USA. January 2000.

J.A. Squire, B. Beheshti, L.R. Kapusta, L. Klotz, P.C. Park, Identification of early prognostic markers in CaP by subtractive hybridization and microarray analysis. Abstract accepted in the 8th International Workshop on Chromosomes in Solid Tumors, Tucson, AZ, USA. January 2000.

P.C. Park, B. Beheshti, L.R. Kapusta, L. Klotz, **J.A. Squire**. Identification of early prognostic markers in CaP by subtractive hybridization and microarray analysis. Abstract accepted in the American Association for Cancer Research 91st Annual Meeting, San Francisco, CA, USA. April 2000.

B. Beheshti, B.G. Beatty, P.C. Park, J. Karaskova, J. Sweet, M.A.S. Jewett, M. Beheshti, and **J.A. Squire**. Chromosomal abnormalities associated with aggressive prostate cancer as identified by interphase FISH, comparative genomic hybridization and spectral karyotyping. Proceedings of the American Association for Cancer Research. March 1999. 40:235.

B. Beheshti, B.G. Beatty, J. Bayani, J. Sweet, M.A.S. Jewett, P.C. Park, and **J.A. Squire**. Chromosomal abnormalities associated with aggressive prostate cancer as identified by interphase fluorescence *in situ* hybridization (FISH), comparative genomic hybridization (CGH) and spectral karyotyping (SKY). 54th Annual Canadian Urological Association Meeting. June 1999. Can. J Urol., 6(3):775.

B. Beheshti, B.G. Beatty, J. Bayani, J. Sweet, M.A.S. Jewett, P.C. Park, and **J.A. Squire**. Chromosomal abnormalities associated with aggressive prostate cancer as identified by interphase FISH, comparative genomic hybridization and spectral karyotyping. (3rd prize poster; University of Toronto Laboratory Medicine and Pathobiology Student Research Day, February and May 1999).

B. Beheshti, B.G. Beatty, J. Bayani, J. Sweet, M.A.S. Jewett, P.C. Park, and **J.A. Squire**. Identification of common chromosomal rearrangements in pericentric regions of prostate cancer cell lines by sequential Giemsa-banding, spectral karyotyping, and interphase FISH. (2nd prize poster; Hospital for Sick Children Department of Paediatric Laboratory Medicine Research Day, June 1999).

B. Beheshti, BG Beatty, PC Park, J Karaskova, P Marrano, J Bayani, J Sweet, MAS Jewett, M Beheshti, J Trachtenberg, and **JA Squire**. Chromosomal aberrations associated with aggressive prostate cancer as identified by interphase FISH, comparative genomic hybridization and spectral karyotyping. 54th Annual Canadian Urological Association, June 20-23 1999. (London, Ontario).

Paul Park AFUD (award recipient's presentation) **Jeremy Squire** (Mentor). Identification of novel prognostic markers in early prostate cancer. American Foundation for Urological Disease, Annual Research Scholar Meeting. May Dallas, Texas, U.S.A. (1999).

list of personnel

Dr. J. Squire

Dr. B. Beatty

Dr. P. Park

Paula Marrano

Jana Karaskova

Zong-Mei Zhang

Lada Vorobyova

DAMD17-99-1-9025:

J. A. SQUIRE



APPENDICES:

Original Research

Identification of a High Frequency of Chromosomal Rearrangements in the Centromeric Regions of Prostate Cancer Cell Lines by Sequential Giemsa Banding and Spectral Karyotyping

B. BEHESHTI, BSc,*[†] J. KARASKOVA, MSc,* P. C. PARK, PhD,*[†]
J. A. SQUIRE, PhD,*[†] B. G. BEATTY, PhD*[†]

Toronto, Canada

Background: Currently, prostate cancer (CaP) cytogenetics is not well defined, largely because of technical difficulties in obtaining primary tumor metaphases.

Methods and Results: We examined three CaP cell lines (LNCaP, DU145, PC-3) using sequential Giemsa banding and spectral karyotyping (SKY) to search for a common structural aberration or translocation breakpoint. No consistent rearrangement common to all three cell lines was detected. A clustering of centromeric translocation breakpoints was detected in chromosomes 4, 5, 6, 8, 11, 12, 14, and 15 in DU145 and PC-3. Both these lines were found to have karyotypes with a greater level of complexity than LNCaP.

Conclusion: The large number of structural aberrations present in DU145 and PC-3 implicate an underlying chromosomal instability and subsequent accumulation of cytogenetic alterations that confer a selective growth advantage. The high frequency of centromeric rearrangements in these lines indicates a potential role for mitotic irregularities associated with the centromere in CaP tumorigenesis.

Key words: cytogenetics, fluorescence *in situ* hybridization, translocation breakpoint, centromere.

From the *Ontario Cancer Institute, Princess Margaret Hospital, University Health Network; and the [†]Departments of Laboratory Medicine and Pathobiology and Medical Biophysics, Faculty of Medicine, University of Toronto, Toronto, Canada.

Supported in part by the US Army Medical Research and Materiel Command Prostate Cancer Research Program; and a grant from the American Foundation for Urologic Diseases/American Urologic Association Research Scholar Program and Imclone Systems, Inc (P.C.P.).

Reprint requests: Jeremy Squire, PhD, Senior Scientist, Ontario Cancer Institute, University Health Network, 610 University Ave, Toronto, Ontario M5G 2M9, Canada. Email: jeremy.squire@utoronto.ca

Copyright © 2000 by Churchill Livingstone®
1084-8592/00/0501-0006\$10.00/0

Prostate cancer (CaP) has the leading incidence of cancer and is the second most common cause of cancer mortality in men in North America [1]. However, our understanding of the molecular genetic changes that underlie the progression of this disease remains at an early stage. Because it is well known that chromosomal translocation can lead to disruption of tumor-suppressor gene function, as well as activation of proto-oncogenes [2], the identification of such rearrangements is a critical step toward understanding the development of this tumor. There are numerous examples in leukemias and soft-tissue sarcomas in which detailed cytoge-

netic analysis has identified consistent chromosomal aberrations leading to the isolation of causative genes [3,4].

The cytogenetics of solid tumors has been hampered in comparison to that of hematologic malignancies because of poor success in short-term culture and inadequate representative metaphase spreads of good quality. CaP has been particularly problematic in this regard because the tumor is slow growing, with a low mitotic index, and consequently there is a greater risk that normal stromal cell overgrowth will occur within a short duration of culture [5–7]. To circumvent some of these difficulties, a variety of different tissue culture protocols have been implemented, including selection in favor of tumor cells and against normal cell overgrowth [8–12]. Using such procedures, a number of consistent cytogenetic alterations have been identified, generally affecting chromosomes 7, 8, 10, and Y [5,13–15]. Nevertheless, no consistent structural chromosome aberrations have been identified in CaP, and it remains conceivable that technical limitations on the quality of the cytogenetic preparations derived from primary tumor material have precluded identification of causative structural chromosomal alterations in this tumor.

In light of these difficulties, the detailed study of CaP cell lines has provided some insight into the progression of the disease, and classic Giemsa banding (G-banding) analysis of three of the commonly studied CaP cell lines, LNCaP, DU145, and PC-3, has provided useful information on the extent of cytogenetic change and karyotype evolution [16–19]. Cytogenetic analysis of LNCaP using standard G-banding methods showed a relatively simple karyotype involving one reciprocal and one nonreciprocal translocation and three deletions [17]. The t(6;16)(p21;q22) translocation was recently shown to result in the production of a novel chimeric fusion transcript, Tpc-Hpr, that is believed to interfere with normal ribosomal function [20]. This translocation appears to be an isolated finding because neither DU145 nor PC-3 has this rearrangement. However, both these lines have highly aberrant karyotypes in comparison to LNCaP and show many marker chromosomes and complex rearrangements with compound regions that cannot be identified by G-banding [18,19]. Although the use of chromosome painting has helped in the identification of some of the complex marker chromosomes in these two cell lines, the origin(s) of many of these

highly abnormal chromosomes remains unknown [21].

To more accurately define the karyotypes of these three cell lines, we used the new technique of spectral karyotyping (SKY) in combination with G-banding. SKY is a 24-color fluorescence *in situ* hybridization (FISH) approach that uniquely identifies each chromosome based on its specific spectral color composition [22], and the technique allows for the unambiguous identification of individual chromosome fragments involved in complex chromosomal rearrangements and marker chromosomes. By analyzing SKY results in conjunction with the findings from conventional G-banding using the same metaphase spread, it is possible to identify individual regions of specific chromosomes and accurately define all structural rearrangements present.

In this study, we applied sequential G-banding and SKY to the three CaP cell lines, LNCaP, DU145, and PC-3, to (1) search for all previously unidentified structural chromosomal rearrangements in each cell line, (2) determine if there are consistent rearrangements or cryptic or masked chromosomal changes common to all three cell lines, and (3) fully characterize the more complex chromosomal rearrangements present in DU145 and PC-3.

Materials and Methods

Tissue Culture and Cytogenetic Preparations

LNCaP (CRL-1740), DU145 (HTB-81), and PC-3 (CRL-1435) were obtained from the American Type Culture Collection (Rockville, MD). LNCaP, an androgen-dependent cell line originating from a lymph node metastasis [16,23], was grown in RPMI 1640 with 2 mM L-glutamine, 1.5 g/L sodium bicarbonate, 4.5 g/L glucose, 10 mM HEPES, 1.0 mM sodium pyruvate, and 10% fetal bovine serum. DU145, an androgen-independent cell line obtained from a metastasis to the bone [18], was grown in F15K minimum essential medium with 1.5 g/L sodium bicarbonate and 10% fetal bovine serum. PC-3, also an androgen-independent cell line and originated from a brain metastasis [19], was grown in Ham's F12K with 2 mM L-glutamine, 1.5 g/L sodium bicarbonate, and 10% fetal bovine serum.

Cytogenetic preparations of LNCaP (passage

23), DU145 (passage 83), and PC-3 (passage 38) were made according to standard protocols [24] using colcemid and KCl hypotonic treatment. The slides were karyotyped following a standard G-banding protocol [24], and images of 10 metaphases in which there was minimal chromosome overlap, long chromosome length, little or no cytoplasm, and high banding resolution were selected for detailed analysis. Microscope coordinates of all digitized G-banded preparations were recorded so the metaphase cells analyzed by G-banding could be analyzed concurrently by SKY methods.

SKY

The SKY KIT probe cocktail from Applied Spectral Imaging (Carlsbad, CA) was hybridized to metaphase spreads from each CaP cell line according to standard protocols [22,25,26] and the manufacturer's instructions. Briefly, after destaining the G-banded slides with methanol for 10 minutes, the slides were rehydrated in a descending ethyl alcohol series (100%, 90%, 70%) and fixed with 1% formaldehyde in 50 mM $MgCl_2$ /phosphate buffer solution for 10 minutes. The slides were then dehydrated using an ascending ethyl alcohol series and denatured for 30 to 45 seconds in 70% formamide/ $2\times SSC$ at 75°C. The SKY probe was denatured for 7 minutes at 75°C, reannealed at 37°C for 1 hour, placed on the slide, and covered with a glass coverslip. The coverslip was sealed with rubber cement and the slides placed in a damp container in a 37°C incubator. After hybridizing overnight, the posthybridization washes were performed per manufacturer's instructions (Applied Spectral Imaging).

The metaphase images were captured using an SD 200 spectral bioimaging system (Applied Spectral Imaging Ltd, MigdalHaemek, Israel) attached to a Zeiss microscope (Axioplan 2, Oberkochen, Germany) and stored on a SKY image-capture workstation. The images were analyzed using the SKYView software version 1.2 (Applied Spectral Imaging), which resolves individual fluorochrome spectra by Fourier spectroscopy and distinguishes the spectral signatures for each chromosome to provide a unique pseudocolor for each chromosome (classified image). G-banding and SKY analyses were performed sequentially on each of the three cell lines with the same 10 metaphase images captured for G-banding also analyzed by SKY. Because of the presence of nonclonal changes in

DU145 and PC-3, composite karyotype descriptions were made for these two cell lines.

The determination of the position of translocation breakpoints was performed by aligning the G-banding pattern for each rearranged chromosome with its respective SKY pseudocolor classified image and mapping each translocation boundary with respect to the associated G-banded chromosomal interval and the International System for Human Cytogenetic Nomenclature designation [27] for the band locations where breakage and rearrangement has occurred.

Results

Sequential G-banding and SKY analysis of LNCaP cells on a metaphase-by-metaphase basis confirmed the bimodal diploid and tetraploid chromosome number [17]. Overall, LNCaP showed a consistent karyotype, with few nonclonal changes (incidental gains/losses and/or structural rearrangements not contributing to the karyotype) per metaphase (Table 1). Six of the seven previously reported marker chromosomes [17] were confirmed by G-banding and SKY analyses in 10 of 10 metaphases (Fig. 1). Marker 7 (an interstitial deletion of 13q21.1) was detected in 9 of 10 metaphases but was absent in the metaphase shown in Fig. 1. The level of resolution afforded by the current sensitivity of the SKY system enabled identification of a cryptic or hidden novel rearrangement in LNCaP. Markers 3 and 6, previously identified by G-banding to be involved in a nonreciprocal translocation of a fragment of 6p onto 16q [17], were instead found by SKY to be involved in a reciprocal $t(6;16)$. When normalized to a diploid chromosome number, LNCaP cells were found to have nine structural aberrations per metaphase. For example, the reciprocal $t(1;15)\times 2$ counted as four aberrations, the $der(6)t(4;6)\times 2$ as two aberrations, and the $del(2)$ as one aberration; numerical changes such as the loss of chromosome 2 were not included in the count. G-banding and SKY analysis of LNCaP metaphase cells showed few structural aberrations per metaphase, indicating that the karyotype was relatively simple.

As previously reported [18,21], DU145 was observed to have a hypotriploid chromosome number with more complex karyotypic changes than LNCaP, showing approximately 18 aberrations per diploid cell (Fig. 2). Chromosomal loss in DU145

Table 1. Karyotype Description of LNCaP (passage 23), DU145 (passage 83), and PC-3 (passage 38)

Cell Line	Chromosomal Rearrangements	Structural Aberrations/ Diploid Cell
LNCaP	86~90,XXYY,t(1;15)(p22;q24)×2,-2,del(2)(p13~23),der(4)t(4;6)(q21;q?15)t(6;10)(q?25;q11)×2,der(6)t(4;6)(q25;q15)×2,t(6;16)(p21.1;q22)×2,del(10)(q24)×2,del(13)(q21.1),[10]	18/2 = 9
DU145	57~62<3n>,X,-X,der(Y)t(Y;20)(q12;p11)[10],der(1;4)(q10;p10)[9],-2[10],-3[10],-4[9],der(4)t(4;6)(q31;?) [9],i(5)(p10)[10],+der(5)del(5)(p?13)del(5)(q?11)×2[8],+der(5)t(5;21)(p13;q11.2)[10],der(6;16)(p10;q10)[9],der(7;8)(p10;q10)[7],del(9)(p21)[10],+der(9)del(9)(p13)t(9;11)(q22;?) [8],der(10;19)(q10;p10)[9],del(11)(q23)[10],der(11;12)(q10;q10)[9],-13[10],der(13)t(2;13)(p11;q33)[10],der(13)t(11;13)(?q23;q33)[10],der(14)t(3;14)(q21;q31)[8],ider(14)(q10)t(3;14)(q21;q31)[2],der(15;20)(q10;q10)×2[10],-16[10],+18[8],der(18)t(14;18)(q13;q21)×2[10],-19[10],-20[10],-22[10],[cp10]	27*(2/3) = 18
PC-3	59~64,XX,-Y,+1[7],der(1)t(1;2)(q22;?)t(1;12)(p31;?)t(8;12)(q13;?) [8],der(1)t(1;15)(p22;q15)t(1;2)(q25;p21)[9],der(2)t(2;15)(p24;q22)t(15;17)(q11;q12)[10],der(2)t(2;8)(p24;q13)×2[10],-3[10],der(3)t(3;10)(q13;?)×2[10],der(4;6)(q10;p10)[9],der(4)t(4;10)(q21;?)×2[10],der(4;12)(q10;q10)[10],-5[10],i(5)(p10)[9],del(6)(q25~26)[10],+7[9],-8[9],del(8)(p21)[10],der(8)t(X;8)(q10;q10)[5],der(8)t(8;15)(q10;q10)t(15;?17)(q26;?)t(3;?17)(q25;?) [3],-9[9],-10[9],der(10)t(3;10)(p14.1;q21)t(4;10)(?;q25)t(4;10)(?;q21)t(4;10)(?;p12)t(4;10)(?;?)t(3;10)(q13.3;?)×2[10],+11[7],der(11)t(2;11)(?;p11)t(2;19)(?;?)t(5;19)(q13;?) [10],der(11;14)(q10;q10)[3],der(12)t(8;12)(q13;q24.3)×2[10],+14[7],+14[4],der(14)t(X;14)(?p22.1;q32)×2[6],der(14)dup(14)(?)t(14;15)(p12;?)t(15;17)(?;?)t(3;17);(q25;?) [2],-15[10],der(15)t(5;15)(q13;p13)[10],der(15)t(15;17)(?;?)t(15;17)(?;q21)t(3;17)(q25;?) [8],-16[10],-17[9],del(17)(p11.2)[10],-19[8],+20[6],+21[10],-22[10],[cp10]	51*(2/3) = 34

Karyotype description is by sequential G-banding and SKY, according to the International System for Human Cytogenetic Nomenclature convention [27]. LNCaP has a clonal karyotype (10 metaphases). In the composite karyotype descriptions for DU145 and PC-3, numbers in brackets refer to the frequency of occurrence of the directly preceding structural/numerical change (of 10 metaphases).

was more common than gain, with losses of whole chromosomes 2, 3, 4, 13, 16, 19, 20, 21, 22, and X and partial losses of 5q, 9p and 11q and gains of chromosome 18 and derivative chromosomes 5 and 9 (Table 1). Structural chromosomal changes of interest were the t(5;21) and t(4;6) translocations not detected by G-banding analyses but easily identified by SKY. Other translocations, such as the t(1;4), t(Y;20), t(2;13), t(6;16), and t(9;11), were recognized as abnormal derivative chromosomes 1, Y, 2, 6, and 9 by G-banding analysis, but required SKY analysis for identification of the involved partner chromosomes (Table 1). The previously unidentified minute chromosomes observed by Stone et al. [18] were determined by SKY analysis to be derived from chromosome 5. The sequential analysis of DU145 by G-banding and SKY allowed the identification of 27 structural breakpoints, of which 14 involved centromeric or pericentromeric regions. More than half the chromosomes in the DU145 genome showed rearrangements involving centromeric breaks. DU145 showed more nonclonal changes per metaphase than either LNCaP or PC-3.

PC-3 cells were also observed to be hypotriploid

and showed more karyotypic abnormalities than either LNCaP or DU145 cells, with approximately 34 aberrations per diploid cell. Almost every chromosome in this cell line had either structural or numerical abnormalities (Fig. 3), with chromosomal loss more prevalent than gain. PC-3 showed losses of whole chromosomes 3, 5, 8, 9, 10, 15, 16, 17, 19, and 22 and partial losses of chromosomes 6q, 8p, and 17p. In addition, whole chromosomal gains of 1, 7, 11, 14, 20, and 21 were observed, and an additional gain of chromosome 14 was observed in 4 of 10 metaphases (Table 1). Seven complex rearrangements involving more than two chromosome partners were characterized in this cell line. Sequential G-banding and SKY analysis of PC-3 allowed the identification of 37 structural breakpoints, of which eight involved centromeric or pericentromeric regions. Many of the structural rearrangements were paired, suggesting that these changes occurred in a diploid progenitor that subsequently underwent tetraploidization. The isochromosome 5p, previously reported by Bernadino et al. [21], was also identified by SKY in both DU145 and PC-3.

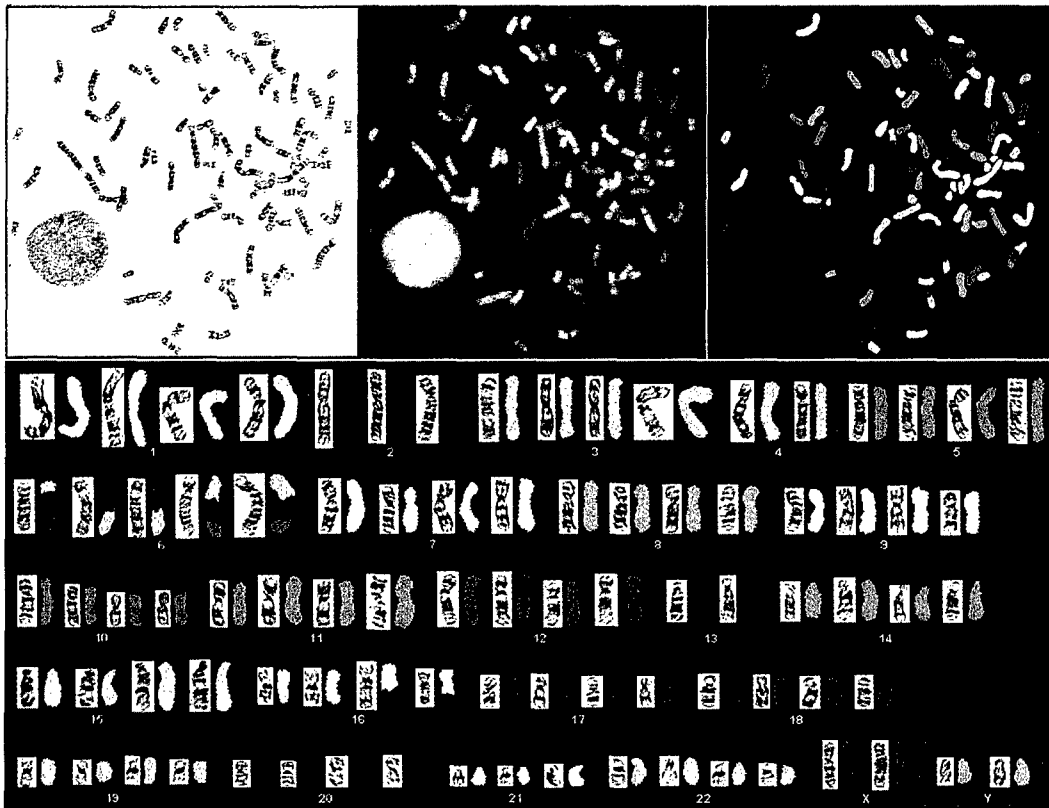


Fig. 1. G-banding and SKY composite karyogram of LNCaP (passage 23). G-banded metaphase (top left), spectral metaphase (top middle), pseudocolor classification (top right). There are 87 chromosomes in the metaphase spread. The karyogram (bottom) depicts each chromosome by aligning its G-banded (left chromosome) and classified (right chromosome) representations.

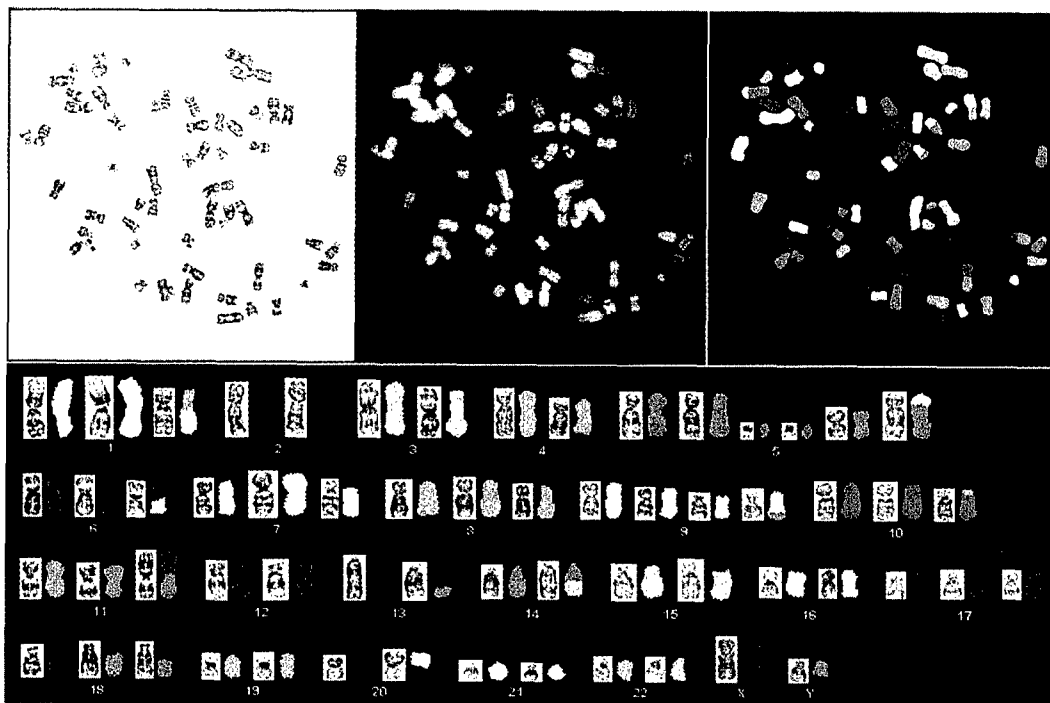


Fig. 2. G-banding and SKY composite karyogram of DU145 (passage 83). There are 60 chromosomes in the metaphase spread.

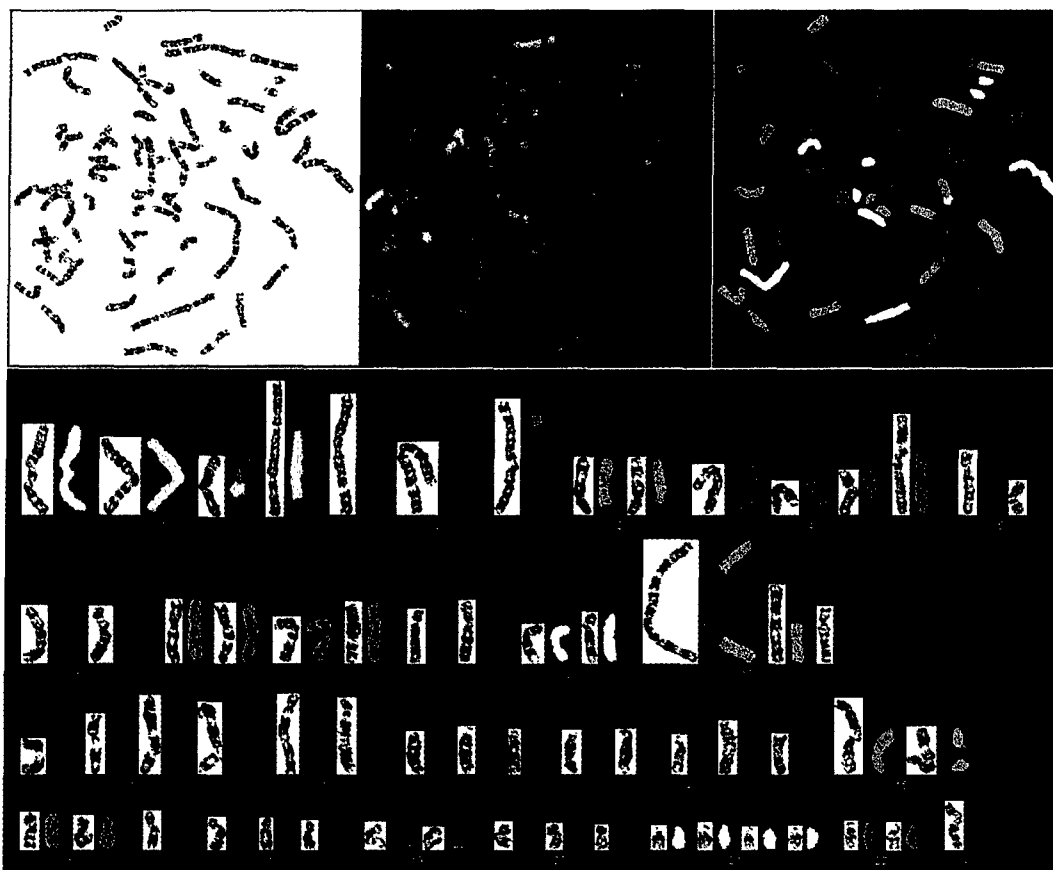


Fig. 3. G-banding and SKY composite karyogram of PC-3 (passage 38). There are 62 chromosomes in the metaphase spread.

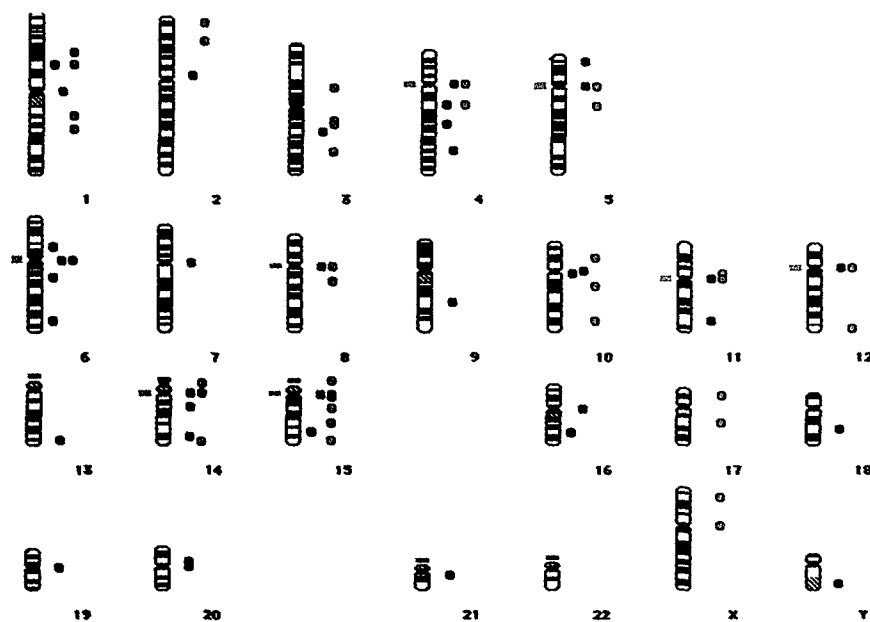


Fig. 4. Breakpoint analysis of the three CaP cell lines. Breakpoints found in the CaP cell lines (LNCaP, red; DU145, blue; PC-3, green) are designated as circles to the right of each chromosome ideogram in the center of the chromosomal interval in which the breakpoint occurs. Clustering of centromeric and pericentromeric breakpoints in DU145 and PC-3 are indicated as bars to the left of the ideograms (cyan).

Table 2. Examples of Chromosome Rearrangements Previously Identified by Chromosome Painting Experiments and Probable Identities Found by G-banding and SKY Analysis

Cell Line	Chromosome Painting Results	Identity by G-banding and SKY
DU145	add(13)(q33) add(13)(q33) add(5)(p13) 1–5 markers	der(13)t(2;13)(?p11;q33) der(13)t(11;13)(?q23;q33) der(5)t(5;21)(p13;q11.2) eg.: der(5)del(5)(p?13)del(5)(q?11)×2; der(14)t(3;14)(q21;q31)
PC-3	add(14)(q32) der(15)t(5;?;15)(q14;p12) der(11)t(5;10;11)(q14;p11) hsr(10)(1;3;10) der(2)t(2;?;8)(p25;p21)×2 add(2)(p25) 2–5 markers	der(14)t(X;14)(?p22.1;q32) der(15)t(5;15)(q13;p13) der(11)t(5;2;11;19)(q13;p11;?) der(10)t(3;10;4;10) der(2)t(2;8)(p24;q13)×2 der(2)t(2;15;17) eg.: der(8)t(X;8)(q10;q10);der(1)t(2;1;12;8)

See Table 1 for correct International System for Human Cytogenetic Nomenclature classification of listed results.

Data from [21].

In both DU145 and PC-3, marker chromosomes that had been partially characterized by classic banding and chromosome painting approaches were more fully characterized by sequential G-banding and SKY. Listed in Table 2 are several examples of marker chromosomes with identities previously reported by Bernardino et al. [21] that have been further defined by sequential G-banding and SKY analyses.

The composite G-banding and SKY results for the three CaP cell lines listed in Table 1 show an increasing complexity of chromosomal aberrations, with LNCaP having the simplest pattern of chromosomal change, followed by DU145 with intermediate complexity, and PC-3 as the more complex line. Whereas no consistent rearrangement or common chromosomal aberration was detected using the increased sensitivity afforded by SKY, examination of DU145 and PC-3 showed eight chromosomal rearrangements involving breakage within the centromeric regions of chromosomes 4, 5, 6, 8, 11, 12, 14, and 15 (Fig. 4). Furthermore, DU145 was found to have involvement of eight additional centromeric or pericentromeric rearrangements on chromosomes 1, 2, 7, 10, 16, 19, 20, and 21; PC-3 had only one additional involvement on chromosome X.

Discussion

Obtaining a detailed characterization of chromosomal abnormalities in solid tumors by classic cytogenetics has been limited by difficulties in both

culturing fresh tumor tissue and obtaining good-quality representative banded metaphase preparations. The use of tumor cell lines has provided an alternative resource for studying cytogenetic changes in greater depth, and the recent development of SKY has significantly enhanced the ability to detect and comprehensively identify the structural aberrations present in a cell line [28]. However, SKY analysis as a single method of chromosome identification has significant limitations. For example, the current SKY probe kit does not permit detection of intrachromosomal dosage changes or interstitial structural rearrangements. In addition, SKY classification does not provide information on the region of the abnormal chromosome involved in the rearrangement. We therefore used a sequential approach of G-banding followed by SKY to examine the identity of all chromosomal aberrations present in the three CaP cell lines, LNCaP, DU145, and PC-3. Similar sequential methods were recently reported to identify the origins of an unusual marker chromosome in a leukemia [29].

The advantages of the sequential approach of G-banding and SKY are evident in genomes showing increased karyotypic complexity, such as DU145 and PC-3. G-banding data for both these cell lines [18] were unable to fully characterize the observed chromosomal aberrations. The use of pairwise combinations of chromosome paints provided more information on the chromosomes involved in rearrangements [21]. For example, although Stone et al. [18] identified a marker Y chromosome by G-

banding, the partner chromosome was unidentifiable by this method. Bernardino et al. [21] used pairwise combinations of chromosome-painting FISH experiments to resolve the identity of this marker chromosome as a der(Y)t(Y;20)(q12;?). Despite these advantages, karyotyping by pairwise chromosome painting is cumbersome and limited by the number of potential combinations of chromosomal rearrangements found in derivative chromosomes. Combined G-banding and SKY has overcome these limitations and permits further characterization of novel rearrangements and more precise definition of previous rearrangements in DU145 and PC-3 (Table 2).

The chromosomal stability of the karyotypes present in each cell line is also a consideration when comparing cytogenetic findings ascertained using different sources of the same cell line and at different cell passage numbers. In our analysis, sequential G-banding and SKY showed a cryptic novel translocation of a small fragment of 16q onto 6p but did not show additional chromosomal changes in LNCaP in comparison to previous G-banding results [17]. However, a study by Ford et al. [30] using whole-chromosome paints detected the non-reciprocal translocation of 10q24 material to two sites on chromosome 5q, forming a derivative chromosome 5 that was not present in our analysis. Similarly, a recent SKY analysis of LNCaP cells reviewed by Brothman et al. [31] showed additional chromosomal rearrangements, such as t(15;22) and t(3;11), also not observed in our analysis. Whether these rearrangements in LNCaP are representative clonal changes is unclear. Previous studies have shown that the karyotype of DU145 also varies as a function of passage number. Both Stone et al. [18] and Bernardino et al. [21] found that the DU145 karyotype was stable through 90 passages, and at passage 73, the cells had a near-triploid chromosome number with extensive chromosomal rearrangements. By passage 153, however, DU145 was found to have a near-tetraploid karyotype with an increased number of rearrangements [18,21]. The karyotype for DU145 (passage 83) reported here is similar to that reported by Stone et al. [18] and Bernardino et al. [21] below passage 90. In contrast to DU145, PC-3 is believed to be a karyotypically stable cell line [19]. This is supported by the study of Camby et al. [32] that showed PC-3 to be more hormone sensitive and to maintain a greater degree of differentiation than DU145. Kaighn et al. [19]

described PC-3 as 100% aneuploid with complete losses of chromosomes 1, 2, 3, 5, 15, and Y and the presence of at least 10 marker chromosomes per metaphase spread, a finding confirmed by the present study. The prevalence of chromosomal losses over gains seen in both DU145 and PC-3 is supported by recent comparative genomic hybridization findings [33].

Our results for the CaP cell lines showed that in terms of the karyotypic complexity of rearrangements, LNCaP < DU145 < PC-3, with approximately 9, 18, and 34 structural aberrations per diploid cell, respectively (Table 1). This finding is in agreement with the suggestion by Nupponen et al. [33] that DU145 and PC-3 represent the more advanced, androgen-independent CaP disease state, whereas LNCaP resembles more closely primary CaP disease. This would support the concept that the stepwise progression to a more advanced disease state, modeled by DU145 and PC-3, involves an accumulation of chromosomal alterations that may confer selective growth advantages.

Sequential G-banding and SKY analyses showed there was no common chromosomal rearrangement or common translocation breakpoint present in all three CaP cell lines. When comparing breakpoint regions of DU145 and PC-3, the most common shared feature was involvement of the centromeric regions of chromosomes 4, 5, 6, 8, 11, 12, 14, and 15 in structural chromosomal aberrations. In contrast, LNCaP was observed to have only one centromeric rearrangement on chromosome 10. The high involvement of the centromeric regions in DU145 and PC-3 is of interest because the centromere has an essential role in maintaining diploidy [34]. The greater frequency of aberrations at centromeric and pericentromeric regions in DU145 than PC-3 may be of importance given the increased instability observed in DU145 through passaging [18,21]. Only monocentric chromosomes were observed in all three cell lines, suggesting orderly chromosome separation, which is not seen in cells containing ring, dicentric, and multicentric chromosome structures [34]. Normally, the centromere is the last chromosomal segment replicated in monocentric mammalian chromosomes during cell division [35]; however, premature centromere separation could lead to the type of aneuploidy [34] observed in DU145 and PC-3. The significant involvement of centromeric breakpoints may reflect the high degree of chromosomal misdivision and

sister-chromatid exchange or increased instability of the pericentromeric regions during mitosis [34,36]. There is an increasing interest in understanding the role of the kinetochore in normal and abnormal mitosis [37,38] and its relationship to the acquisition of centromeric aberrations and aneusomies in cancer cells [39,40].

Although the use of tumor cell lines has provided an alternative resource for studying cytogenetic changes in carcinomas that ordinarily would present difficulties in tissue culture, the question is raised as to whether the cytogenetics remain representative of primary tumors. Given the slow-onset pathological characteristics of CaP, however, it may be surmised that the initiating event(s) may not be a single genetic alteration, but instead caused by aberrations in cell division. In this regard, the accumulation of multiple genetic aberrations during CaP progression may be downstream effects that confer selective growth advantages. The observed alterations at the centromeric regions support this view and suggest that amid the other chromosomal aberrations within each cell line, the initial tumorigenic events are not lost in the cell lines studied.

In summary, sequential G-banding and SKY is an effective FISH-based whole-genome screening technique that significantly improves the ability to identify cryptic and complex chromosomal rearrangements in tumor cells. Using this approach, we have confirmed and more precisely defined the karyotypes of three CaP cell lines, identifying a cryptic novel rearrangement in LNCaP and resolving previously unknown marker chromosomes and complex rearrangements in the more complicated DU145 and PC-3 genomes. No consistent translocation breakpoint suggestive of a common structural rearrangement in all three cell lines was observed; however, centromeric breakpoints were shown to be the most frequent shared feature between DU145 and PC-3. Our results imply that karyotypically, LNCaP may be less advanced than DU145 and PC-3. This observation is in agreement with the multistep model of accumulated hits in CaP tumorigenesis and suggests an increasing importance in understanding the role of the centromere in CaP tumorigenesis.

Acknowledgment

The authors acknowledge the technical expertise of Jaudah Al-maghrabi, Jane Bayani, Shawn Bren-

nan, Paula Marrano, Ajay Pandita, Silvia Rogatto, and Zong Zhang.

References

1. Haas GP, Sakr WA: Epidemiology of prostate cancer. *CA Cancer J Clin* 1997;47:273-287
2. Weinberg R: How cancer arises. *Sci Am* 1996;275:62-70
3. Rowley JD: The critical role of chromosome translocations in human leukemias. *Annu Rev Genet* 1998;32:495-519
4. Ladanyi M: The emerging molecular genetics of sarcoma translocations. *Diagn Mol Pathol* 1995;4:162-173
5. Webb HD, Hawkins AL, Griffin CA: Cytogenetic abnormalities are frequent in uncultured prostate cancer cells. *Cancer Genet Cytogenet* 1996;88:126-132
6. Konig JJ, Teubel W, van Dongen JW, Hagemeijer A, Romijn JC, Schroder FH: Tissue culture loss of aneuploid cells from carcinomas of the prostate. *Genes Chromosomes Cancer* 1993;8:22-27
7. Ketter R, Zwergel T, Romanakis K, et al.: Selection toward diploid cells in prostatic carcinoma-derived cell cultures. *Prostate* 1996;28:364-371
8. Chopra DP, Sarkar FH, Grignon DJ, Sakr WA, Mohammed A, Waghray A: Growth of human nondiploid primary prostate tumor epithelial cells in vitro. *Cancer Res* 1997;57:3688-3692
9. Limon J, Lundgren R, Elfving P, et al.: An improved technique for short-term culturing of human prostatic adenocarcinoma tissue for cytogenetic analysis. *Cancer Genet Cytogenet* 1990;46:191-199
10. Peehl DM, Sellers RG, Wong ST: Defined medium for normal adult human prostatic stromal cells. *In Vitro Cell Dev Biol Anim* 1998;34:555-560
11. Szucs S, Zitzelsberger H, Breul J, Bauchinger M, Hofler H: Two-phase short-term culture method for cytogenetic investigations from human prostate carcinoma. *Prostate* 1994;25:225-235
12. Zwergel T, Kakirman H, Schorr H, Wullich B, Unteregger G: A new serial transfer explant cell culture system for human prostatic cancer tissues preventing selection toward diploid cells. *Cancer Genet Cytogenet* 1998;101:16-23
13. Arps S, Rodewald A, Schmalenberger B, Carl P, Bressel M, Kastendieck H: Cytogenetic survey of 32 cancers of the prostate. *Cancer Genet Cytogenet* 1993;66:93-99
14. Micale MA, Sanford JS, Powell IJ, Sakr WA, Wolman SR: Defining the extent and nature of cytogenetic events in prostatic adenocarcinoma: Paraffin

- FISH vs metaphase analysis. *Cancer Genet Cytogenet* 1993;69:7-12
15. Zitzelsberger H, Szucs S, Robens E, Weier HU, Hofler H, Bauchinger M: Combined cytogenetic and molecular genetic analyses of fifty-nine untreated human prostate carcinomas. *Cancer Genet Cytogenet* 1996;90:37-44
 16. Horoszewicz JS, Leong SS, Kawinski E, et al.: LNCaP model of human prostatic carcinoma. *Cancer Res* 1983;43:1809-1818
 17. Gibas Z, Becher R, Kawinski E, Horoszewicz J, Sandberg AA: A high-resolution study of chromosome changes in a human prostatic carcinoma cell line (LNCaP). *Cancer Genet Cytogenet* 1984;11:399-404
 18. Stone KR, Mickey DD, Wunderli H, Mickey GH, Paulson DF: Isolation of a human prostate carcinoma cell line (DU 145). *Int J Cancer* 1978;21:274-281
 19. Kaighn ME, Narayan KS, Ohnuki Y, Lechner JF, Jones LW: Establishment and characterization of a human prostatic carcinoma cell line (PC-3). *Invest Urol* 1979;17:16-23
 20. Veronese ML, Bullrich F, Negrini M, Croce CM: The t(6;16)(p21;q22) chromosome translocation in the LNCaP prostate carcinoma cell line results in a tpc/hpr fusion gene. *Cancer Res* 1996;56:728-732
 21. Bernardino J, Bourgeois CA, Muleris M, Dutrillaux AM, Malfoy B, Dutrillaux B: Characterization of chromosome changes in two human prostatic carcinoma cell lines (PC-3 and DU145) using chromosome painting and comparative genomic hybridization. *Cancer Genet Cytogenet* 1997;96:123-128
 22. Schrock E, du Manoir S, Veldman T, et al.: Multicolor spectral karyotyping of human chromosomes. *Science* 1996;273:494-497
 23. Horoszewicz JS, Leong SS, Chu TM, et al.: The LNCaP cell line—A new model for studies on human prostatic carcinoma. *Prog Clin Biol Res* 1980;37:115-132
 24. Gustashaw KM: Chromosome stains. In Barch MJ, Knutsen T, Spurbeck JL: *The AGT cytogenetics laboratory manual*, 3. Lippincott-Raven, Philadelphia, 1997, pp. 259-324
 25. Veldman T, Vignon C, Schrock E, Rowley JD, Ried T: Hidden chromosome abnormalities in haematological malignancies detected by multicolour spectral karyotyping. *Nat Genet* 1997;15:406-410
 26. Garini Y, Macville M, Manoir S, et al.: Spectral karyotyping. *Bioimaging* 1996;4:65-72
 27. Mitelman F: *ISCN (1995): International system for human cytogenetic nomenclature*. Karger, New York, 1995
 28. Padilla-Nash HM, Nash WG, Padilla GM, et al.: Molecular cytogenetic analysis of the bladder carcinoma cell line BK-10 by spectral karyotyping. *Genes Chromosomes Cancer* 1999;25:53-59
 29. Allen RJ, Smith SD, Moldwin RL, et al.: Establishment and characterization of a megakaryoblast cell line with amplification of MLL. *Leukemia* 1998;12:1119-1127
 30. Ford S, Gray IC, Spurr NK: Rearrangement of the long arm of chromosome 10 in the prostate adenocarcinoma cell line LNCaP. *Cancer Genet Cytogenet* 1998;102:6-11
 31. Brothman AR, Maxwell TM, Cui J, Deubler DA, Zhu XL: Chromosomal clues to the development of prostate tumors. *Prostate* 1999;38:303-312
 32. Camby I, Etievant C, Petein M, et al.: Influence of culture media on the morphological differentiation of the PC-3 and DU145 prostatic neoplastic cell lines. *Prostate* 1994;24:187-196
 33. Nupponen NN, Hyytinen ER, Kallioniemi AH, Visakorpi T: Genetic alterations in prostate cancer cell lines detected by comparative genomic hybridization. *Cancer Genet Cytogenet* 1998;101:53-57
 34. Vig BK, Sternes KL, Paweletz N: Centromere structure and function in neoplasia. *Cancer Genet Cytogenet* 1989;43:151-178
 35. Broccoli D, Paweletz N, Vig BK: Sequence of centromere separation: Characterization of multicentric chromosomes in a rat cell line. *Chromosoma* 1989;98:13-22
 36. Kaiser-Rogers K, Rao K: Structural chromosome rearrangements. In Gersen SL, Keagle MB: *The principles of clinical cytogenetics*, Humana Press, Totowa, 1999, pp. 191-228
 37. Chan GK, Schaar BT, Yen TJ: Characterization of the kinetochore binding domain of CENP-E reveals interactions with the kinetochore proteins CENP-F and hBUBR1. *J Cell Biol* 1998;143:49-63
 38. Faulkner NE, Vig B, Echeverri CJ, Wordeman L, Vallee RB: Localization of motor-related proteins and associated complexes to active, but not inactive, centromeres. *Hum Mol Genet* 1998;7:671-677
 39. Cahill DP, da Costa LT, Carson-Walter EB, Kinzler KW, Vogelstein B, Lengauer C: Characterization of MAD2B and other mitotic spindle checkpoint genes. *Genomics* 1999;58:181-187
 40. Sawyer JR, Tricot G, Mattox S, Jagannath S, Barlogie B: Jumping translocations of chromosome 1q in multiple myeloma: Evidence for a mechanism involving decondensation of pericentromeric heterochromatin. *Blood* 1998;91:1732-1741



Genetic Characterization of Immortalized Human Prostate Epithelial Cell Cultures: Evidence for Structural Rearrangements of Chromosome 8 and i(8q) Chromosome Formation in Primary Tumor-Derived Cells

Jill A. Macoska, Ben Beheshti, John S. Rhim, Bharati Hukku, Jeff Lehr, Kenneth J. Pienta, and Jeremy A. Squire

ABSTRACT: We have utilized a combination of conventional and spectral karyotyping (SKY) techniques and allelotype analysis to assess numerical and structural chromosome alterations in two cell lines derived from normal human prostatic epithelium, and three cell lines derived from human prostate primary tumor epithelium, immortalized with the E6 and E7 transforming genes of human papilloma virus (HPV) 16 or the large T-antigen gene of simian virus 40 (SV40). These studies revealed trisomy for chromosome 20 and rearrangements involving chromosomes 3, 4, 8, 9, 10, 16, 17, 18, 19, 21, or 22. In addition, the four HPV-immortalized cell lines exhibited extensive duplications or translocations involving the 11q chromosomal region. Interestingly, allelotyping data disclosed loss of 8p sequences in two of the three primary tumor-derived cell lines, and SKY data revealed that the loss of 8p sequences was directly due to i(8q) chromosome formation and/or other structural alterations of chromosome 8. This provides intriguing evidence that 8p loss in primary human prostate tumors may, in some cases, result from complex structural rearrangements involving chromosome 8. Moreover, the data reported here provide direct evidence that such complex structural rearrangements sometimes include i(8q) chromosome formation. © 2000 Elsevier Science Inc. All rights reserved.

INTRODUCTION

Many genetic and epigenetic events are likely involved in prostate tumorigenesis. In particular, several cytogenetic and molecular studies from our laboratory and others have suggested that deletion or rearrangement of se-

quences that map to the short arm of chromosome 8 (8p) may be critically permissive for tumorigenesis in the prostate gland [1–7].

Deletion of 8p sequences is observed at comparable frequencies in low- and high-grade tumors, as well as in localized and invasive regionally metastatic prostate cancers [3, 5, 7]. Moreover, the frequency of 8p loss is almost equivalent in prostate tumors and prostatic intraepithelial neoplasia (PIN), a putative premalignant lesion of the prostate [6, 8]. Taken together, these data suggest that 8p losses are frequent events during the initiation or early promotion of prostate tumorigenesis.

Other studies have also reported loss of 8p concurrent with gain of the long arm of chromosome 8 (8q) sequences in advanced prostatic cancer [9–13]. This combination of events occurring on the same chromosome—loss of 8p sequences and gain of 8q sequences—suggests formation of i(8q) chromosomes in advanced prostate tumors. Although i(8q) chromosomes have been detected in uncultured metastatic prostate tumors using conventional karyotypic analyses, no direct evidence for the existence of

From the Department of Surgery, Section of Urology (J. A. M.), the Department of Internal Medicine, Section of Hematology/Oncology (J. L., K. J. P.), and the Comprehensive Cancer Center, (J. A. M., K. J. P.), The University of Michigan, Ann Arbor, Michigan, USA; The Ontario Cancer Institute, Princess Margaret Hospital, University Health Network, and Department of Laboratory Medicine and Pathobiology, and Medical Biophysics, Faculty of Medicine, University of Toronto (B. B., J. A. S.), Toronto, Ontario, Canada; The Center for Prostate Disease Research, The Uniformed Services University of the Health Sciences (J. S. R.), Rockville, Maryland, USA; and the Cell Culture Laboratory of the Children's Hospital of Michigan (B. H.), Detroit, Michigan, USA.

Address reprint requests to: Jill A. Macoska, Ph.D., Department of Surgery, Section of Urology, The University of Michigan, 7306 CCGC, 1500 East Medical Center Drive, Ann Arbor, MI 48109-0946.

Received October 4, 1999; accepted November 30, 1999.

i(8q) chromosomes in primary prostate tumors has been obtained, possibly due to the inability of interphase fluorescence in situ hybridization (FISH) techniques used with clinical specimens to accurately and precisely identify these chromosomes [10–13]. Therefore, we have utilized a combination of conventional and spectral karyotyping (SKY) techniques and allelotyping analysis to assess numerical and structural alterations of chromosome 8 in two cell lines derived from normal human prostate epithelium, and three cell lines derived from primary human prostate tumors. The specific objective of these studies was to determine whether losses of 8p sequences previously reported for two of the cell lines, 1532T and 1542T [14], were directly due to i(8q) chromosome formation and/or other structural alterations of chromosome 8.

MATERIALS AND METHODS

Cell Lines and Culture

The 1535N, 1532T, 1535T, and 1542T cell lines were produced through immortalization of primary prostate epithelial cultures by transduction with a recombinant retrovirus encoding the E6 and E7 genes of HPV 16, as previously described [14]. The 1535N cells were produced from immortalization of normal prostatic epithelium, whereas the 1532T, 1535T, and 1542T cells were produced through immortalization of malignant epithelium from primary prostate tumors. The PrEC-T cells were produced through immortalization of normal human prostate epithelial cells (Clonetics, Inc.) by transfection with the pMT10D plasmid (Japanese Cancer Research Resources Bank, Tokyo) containing sequences encoding the simian virus 40 (SV40) Large T-antigen. All cell lines were grown in defined keratinocyte-SFM (GIBCO/BRL), 5% FBS, and 1% penicillin/streptomycin/fungizone antibiotic mixture (BioWhittaker) in a humidified incubator at 37°C with 5% CO₂.

G-Banding and Karyotypic Analysis

For the 1535N cells, chromosome counts, ploidy distributions, and GTG-banded karyotypes were prepared as previously described [15]. Briefly, exponentially growing cul-

tures were treated with 0.04 µg/mL Colcemid for 1–2 hours, trypsinized, treated with 0.0375 M KCl for 9 minutes, then fixed in 3:1 methanol: glacial acetic acid. The resulting cell nuclei were pelleted by centrifugation, dropped onto cold, wet slides, then air-dried and stained using a 4% Giemsa solution. Chromosomes were examined and counted to establish ploidy distribution and constitutional alterations. Specific numerical and structural chromosomal alterations were established after the slides were aged at 60°C on a slide warmer for 18 hours, immersed in 0.025% trypsin for 11 seconds, stained with 4% Gurr-Giemsa solution for 11 minutes, washed in buffer, then air-dried and mounted in permount. Well-banded metaphase spreads were photographed at 800× magnification with Technical Pan Film 2415 (Kodak) and printed on Rapidoprint FP 1-2 (Agfa-Gevaert), or studied on the AKSII image analysis system.

SKY Analysis

Spectral karyotyping analysis was carried out on the 1532T, 1535T, 1542T, and PrEC-T cells using previously G-banded slides. Images were captured and the microscope coordinates were noted. Residual oil was removed with xylenes followed by destaining with methanol. The slides were then rehydrated in a descending ethanol series and fixed with 1% formaldehyde in a 50 mM MgCl₂/phosphate buffer solution for 10 minutes. Slides were dehydrated and denatured for 30–45 seconds at 75°C in 70% formamide/2 × SSC (saline sodium citrate), followed by a final dehydration. The SKY paints (Applied Spectral Imaging, Carlsbad, CA, USA) were denatured for 7 minutes at 75°C, reannealed at 37°C for 1 hour, then placed on the slide and covered with a glass coverslip. The coverslip was sealed with rubber cement, and hybridization was carried out in a humidified chamber for 24 hours at 37°C. Post-hybridization washes were carried out using established techniques and according to the manufacturer's instructions [16]. Ten metaphase images were captured per preparation using an SD 200 spectral bioimaging system (ASI Ltd., MigdalHaemek, Israel) attached to a Zeiss microscope (Axioplan 2) and stored on a SKY image-capture workstation. The images were analyzed using the SKY-

Table 1 Karyotype analysis of immortalized normal and malignant prostate epithelial cells

Cell lines	Karyotype
1532T	44~47,XY,i(8)(q10),+20[2]/46~47,idem,dup(11)(q13q23)[3]/ 46~47,idem,dup(11)(p11.2p13),ins(17;11)(q21p11.2p13)[5]
1535T	46,XY,der(11)?qdp(q13q23)t(11;20)(q23;q11),der(20)t(11;20)(q13;q13.3)qdp(11)(q13q23)or hsr(11)[6] 46,idem,der(3)t(3;11)(p21;q13),del(18)(q21)[4]
1542T	46,XY,der(8;20)(q10;p10),der(11)qdp(q13q23)t(11;20)(q23;q11)[4]/46~47,idem,i(8)(q10)[2] 36~51,idem,der(22)t(11;22)(q14;p11)t(11;20)(q23;q11.2)[2] 45~47,idem,-der(8;20),der(8;21)(p10;q10)[2]
1535N	45~48,XY,der(18)[9]/45~48,idem,add(19)(q13)[8] 45~48,idem,der(11)dup(11)(q11q23)t(10;11)(q22;q23)[4]/45~48,idem,del(10)(q21)[3]
PrEC-T	44,XY,der(3;15)(q10;q10),der(4)t(4;?14)(q35;p10),der(8)dup(8)(q11.2q24.3)t(8;8)(q24.3;q24.3), del(10)(q24),der(14;17)(q10;q10),der(16)t(9;16)(q10;q10),del(18)(q21), der(22)dup(??)t(22;22)(p13;?)t(8;22)(?;?),der(22)t(17;22)(p11.2;q11.2)[10]

Nonclonal chromosomal changes were also noted in the cell lines.

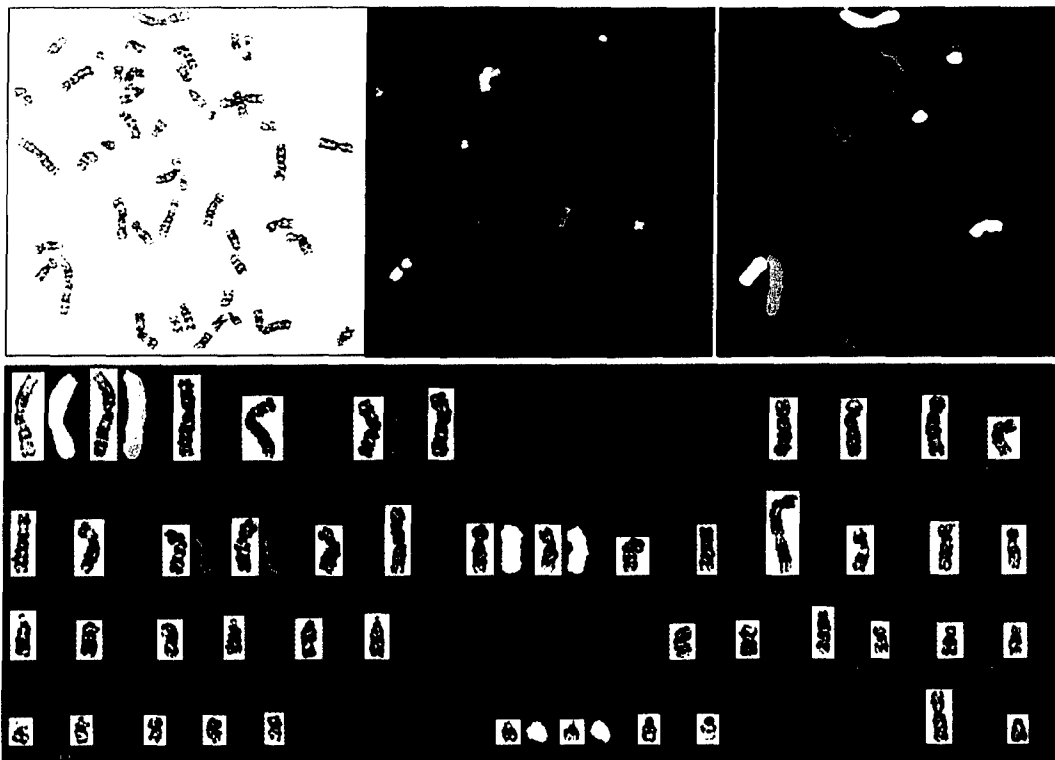
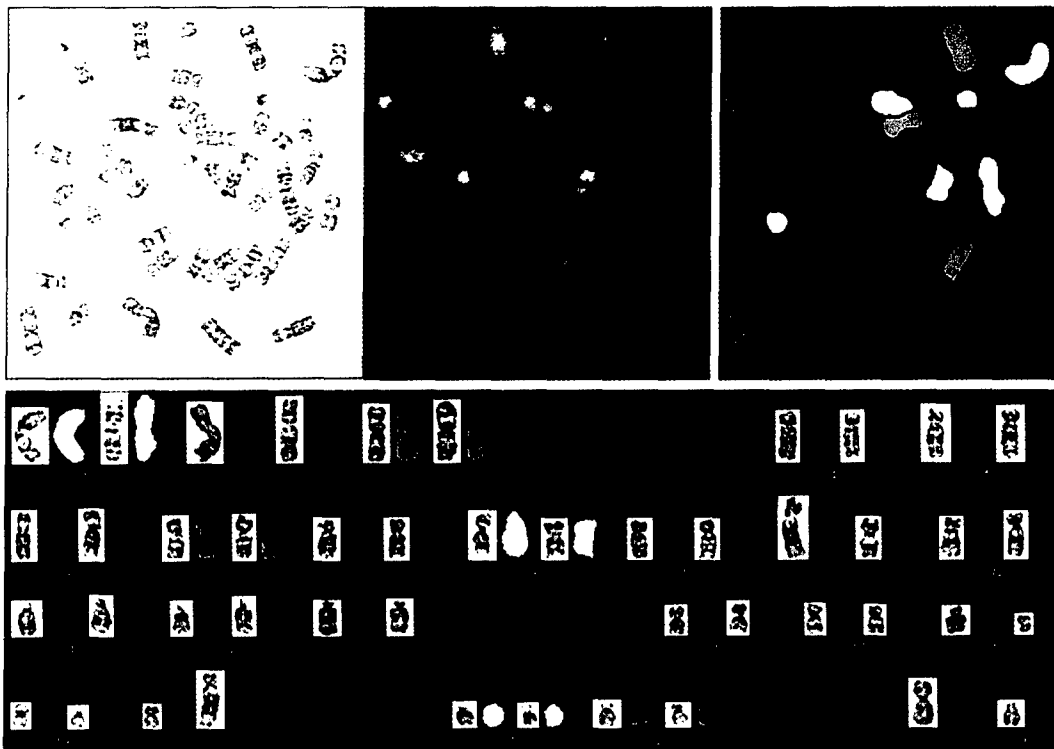


Figure 1 Spectral karyotype composite of the 1532T cell line. Upper panel: G-banded preparation of metaphase chromosomes from 1532T cells (left), hybridized to SKY paints (middle), and after pseudocolor application (right), as described in the text. Lower panel: Composite karyotype showing G-banded and pseudocolored chromosomes. The karyotype for the cell shown is: 47,XY,i(8)(q10),+20.

Figure 2 Spectral karyotype composite of the 1535T cell line. Upper panel: G-banded preparation of metaphase chromosomes from 1535T cells (left), hybridized to SKY paints (middle), and after pseudocolor application (right), as described in the text. Lower panel: Composite karyotype showing G-banded and pseudocolored chromosomes. The karyotype for the cell shown is: 46,XY,der(11)?qdp(q13q23)t(11;20)(q23;q11),der(20)t(11;20)(q13;q13),qdp(11)(q13q23),der(3)t(3;11)(p21;q13),del(18)(q21).



View software version 1.3. G-banding and SKY analyses were performed sequentially on each of the cell lines with the same ten metaphase images captured for G-banding also analyzed by SKY.

Allelotyping

Cells were trypsinized and DNA was purified using the Oncor (Gaithersburg, MD, USA) nonorganic DNA extraction kit according to the manufacturer's protocols. Polymerase chain reaction (PCR) reactions were performed as previously described [7]. The loci examined by PCR spanned 8p (12 loci) or localized to 8q12 (2 loci), and contained highly polymorphic microsatellite repeats. The linkage order of these markers has been reported as pter – D8S504 – D8S277 – D8S549 – D8S261 – NEFL – D8S540 – D8S513 – D8S535 – D8S505 – D8S87 – D8S1121 – D8S255 – D8S531 – D8S519 – qter (Table I). Primer sequences, additional linkage and contig information, and genetic mapping information were obtained from public databases maintained by the Center for Genome Research at the Whitehead Institute for Biomedical Research (<http://www-genome.wi.mit.edu/>), and the National Center for Biotechnology Information (<http://www.ncbi.nlm.nih.gov/>), as accessed through the Internet.

RESULTS

Cytogenetic Analysis

Metaphase analysis showed that the five prostate-derived cell lines were pseudodiploid, with modal numbers ranging from 43 to 49 chromosomes/cell. The karyotypes of each cell line are described below and in Table 1.

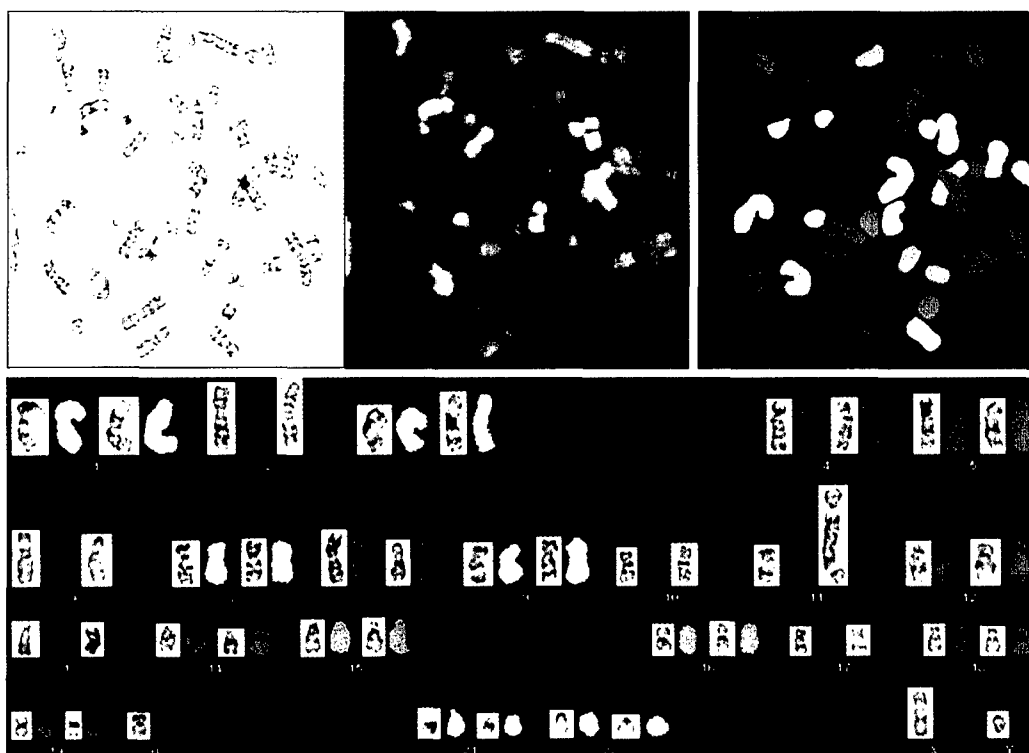
1532T

Ten karyotypes were analyzed from passage 44 of this cell line using SKY techniques. The consensus karyotype was 44~47,XY,i(8)(q10),+20. Eight cells also demonstrated duplication of the (q13–q23) region of chromosome 11, and five cells demonstrated a duplication of the p11.2–p13 region of chromosome 11 and insertion into the q21 region of chromosome 17. Figure 1 shows a representative karyotype for this cell line.

1535T

Ten karyotypes were analyzed from passage 12 of this cell line using SKY techniques. The consensus karyotype was 46,XY,der(11)?qdp(q13q23)t(11;20)(q23;q11)der(20)t(11;20)(q13;q13.3)qdp(11)(q13q23) or hsr(11), with four cells also demonstrating der(3)t(3;11)(p21;q13),del(18)(q21). Figure 2 shows a representative karyotype for this cell line.

Figure 3 Spectral karyotype composite of the 1542T cell line. Upper panel: G-banded preparation of metaphase chromosomes from 1542T cells (left), hybridized to SKY paints (middle), and after pseudocolor application (right), as described in the text. Lower panel: Composite karyotype showing G-banded and pseudocolored chromosomes. The karyotype for the cell shown is: 45,XY,i(8)(q10),der(11)qdp(q13q23)t(11;20)(q23;q11).



1542T

Ten karyotypes were analyzed from passage 44 of this cell line using SKY techniques. The consensus karyotype was 46,XY,der(8;20)(q10;p10),der(11)qdp(q13q23)t(11;20)(q23;q11). In addition, two cells also demonstrated an i(8)(q10); 2 cells demonstrated these changes as well as der(22)t(11;22)(q14;p11)t(11;20)(q23;q11.2), and 2 cells were characterized by these accumulated changes except that the der(8;20) was absent and a der(8;21)(p10;q10) was apparent instead. Figure 3 shows a representative karyotype for this cell line.

1535N

Nine karyotypes were analyzed from passage 13 of this cell line using G-banding techniques. The consensus karyotype was 45~48,XY,der(18), with eight cells also demonstrating an add(19)(q13) chromosome, and four cells demonstrating a complex derivative of chromosome 11 involving t(10;11). Three cells also displayed a deletion of chromosome 10 involving band q21. Figure 4 shows a representative karyotype for this cell line.

PrEC-T

Ten karyotypes were analyzed from passage 27 of this cell line using SKY techniques. The consensus karyotype was 44,XY,der(3;15)(q10;q10),der(4)t(4;?14)(q35;p10),der(8)dup(8)(q11.2;q24.3)t(8;8)(q24.3;q24.3),del(10)(q24),der(14;17)(q10;q10),der(16)t(9;16)(q10;q10),del(18)(q21),der(22)dup(??)t(22;22)(p13;?)t(8;22)(?;?),der(22)t(17;22)

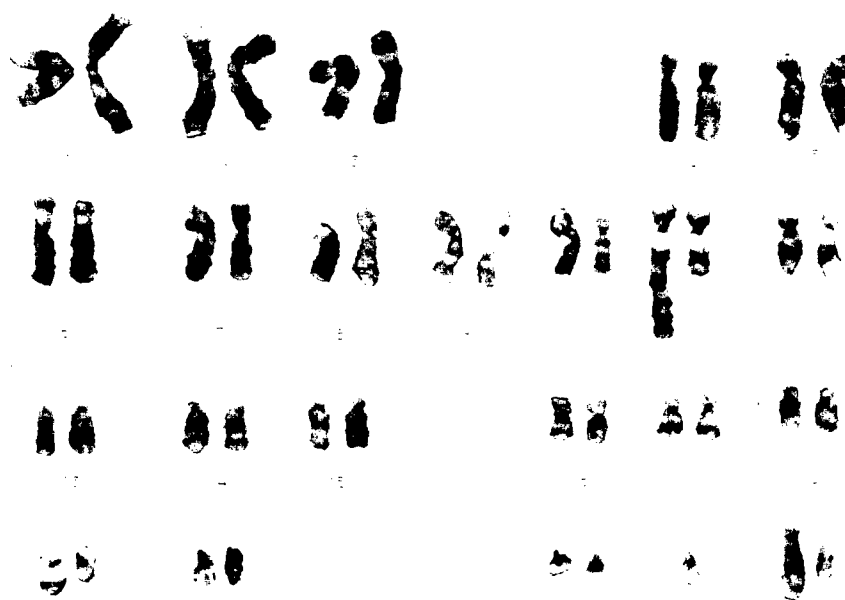
(p11.2;q11.2)[10]. Figure 5 shows a representative karyotype for this cell line.

Interestingly, duplications, translocations and other structural changes involving 11q13q22q23 were observed in all four HPV-immortalized cell lines. The 1542T cells exhibited a distinctive quadruplication (abbreviated as "qdp" using ISCN nomenclature), suggesting a low-level amplification of the q13 to q23 region in this cell line.

Allelotyping

The 1532T, 1535T, and 1542T cell lines were allelotyped at 14 chromosome 8 loci, 12 spanning 8p, and 2 mapping to the pericentromeric region of 8q. Table 2 summarizes these data. As shown in Table 2, the 1532T cell line was homozygous for all 8p loci examined, consistent with the cytogenetic data revealing one normal chromosome 8 and one i(8)(q10) chromosome in these cells (Fig. 6). The 1542T cell line demonstrated one allele for all 8p loci, but two alleles for each of the pericentromeric 8q loci, D8S531 and D8S519. These data were also consistent with the cytogenetic findings for one normal chromosome 8 accompanied by any of three different structural alterations of chromosome 8: i(8)(q10), der(8;20)(q10;p10), and der(8;21)(p10;q10) in these cells (Fig. 6). In contrast, the 1535T cell line demonstrated two alleles for 9 of 12 8p, and both 8q loci examined, with no evidence for extended regions of homozygosity by allelotyping. These results were consistent with the SKY data, which did not reveal clonal numerical or structural alterations of chromosomes 8 in these cells.

Figure 4 G-banded karyotype of the 1535N cell line. G-banded metaphase chromosomes from 1535N cells were prepared as described in the text. The karyotype for the cell shown is: 45,XY,der(11)dup(11)(q11q23)t(10;11)(q22;q23),der(18),add(19)(q13),-22.



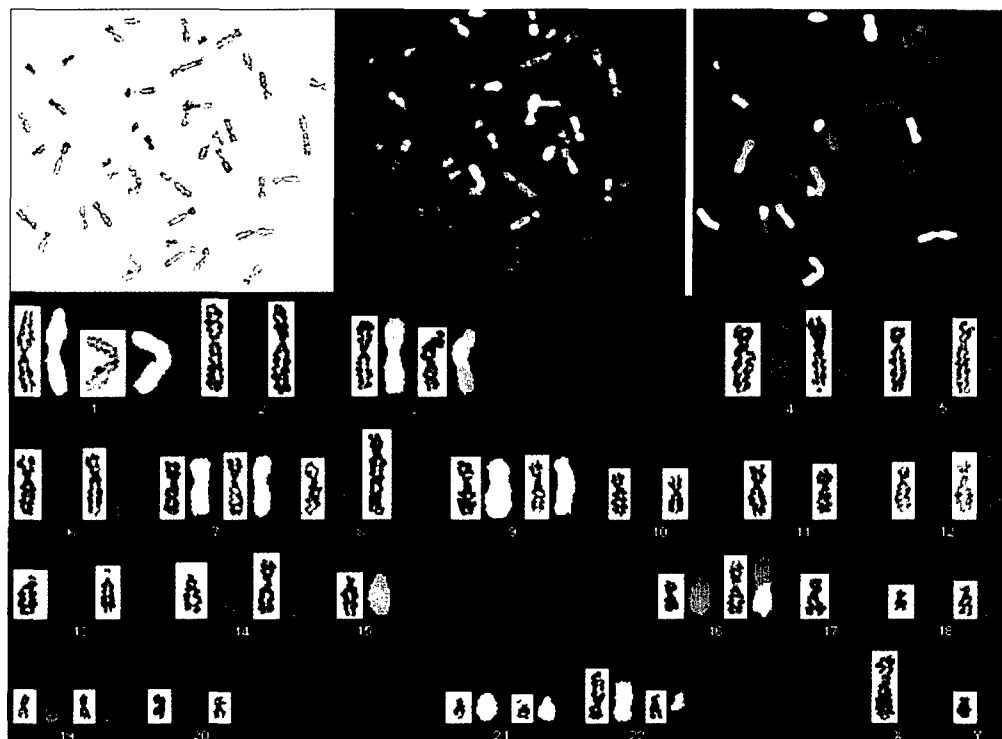


Figure 5 Spectral karyotype composite of the PrEC-T cells line. Upper panel: G-banded preparation of metaphase chromosomes from PrEC-T cells (left), hybridized to SKY paints (middle), and after pseudocolor application (right), as described in the text. Lower panel: Composite karyotype showing G-banded and pseudocolored chromosomes. The karyotype for the cell shown is: 44,XY,der(3;15)(q10;q10),der(4)t(4;?14)(q35;p10),der(8)dup(8)(q11.2;q24.3)t(8;8)(q24.3;q24.3),del(10)(q24),der(14;17)(q10;q10),der(16)t(9;16)(q10;q10),del(18)(q21),der(22)dup(??)t(22;22)(p13;?)t(8;22)(?;?),der(22)t(17;22)(p11.2;q11.2).

DISCUSSION

Cell lines provide a unique resource for the investigation of numerical and structural chromosomal alterations present in the tissues from which they were derived. However, the most intensively studied prostate-derived cell lines—PC3, DU145, and LNCaP—were all established from metastatic lesions. These cell lines possess highly aberrant karyotypes characterized by numerous structural and numerical chromosomal alterations [17]. As such, it is unlikely that these cell lines accurately recapitulate the genetic composition of human primary prostate tumors. Unfortunately, human prostate tissues, whether normal or malignant, survive only short term in culture, and rarely immortalize spontaneously. The use of viral transforming proteins to immortalize normal and primary tumor epithelium from human prostate has allowed the continual propagation of normal and malignant-derived cells in vitro [14]. The cell lines examined in the present study were created by Bright et al. through the transduction, and subsequent immortalization, of normal and primary tumor prostatic epithelium with the E6 and E7 transforming genes of HPV 16, or in our laboratory through the immortalization of normal prostatic epithelium with the large T-antigen gene of SV40 [14].

The cell lines demonstrated several numerical and structural chromosomal alterations, including trisomy for

chromosome 20 (1532T cells) and rearrangements involving 3p (1535T cells) or 3q (PrEC-T cells), chromosome 9 (PrEC-T cells), 10 (1535N and PrEC-T cells), 16 (PrEC-T cells), 17 (1532T and PrEC-T cells), 18 and 19 (1535N), 20 (1542T cells), or 21, and 22 (1542T and PrEC-T cells). The PrEC-T cells also exhibited structural alterations of chromosomes 4 and 14. All of these alterations have been reported for epithelial cells from diverse tissue types, including uroepithelial and prostate, immortalized through transduction with all or part of the HPV 16 or 18 genomes [18-21]. Some of these alterations, notably gain of chromo-

Figure 6 Structural alterations involving chromosome 8. Structural alterations of chromosome 8, including i(8q) chromosomes, are shown for 1542T cells (left), 1532T cells (middle), and PrEC-T cells (right).

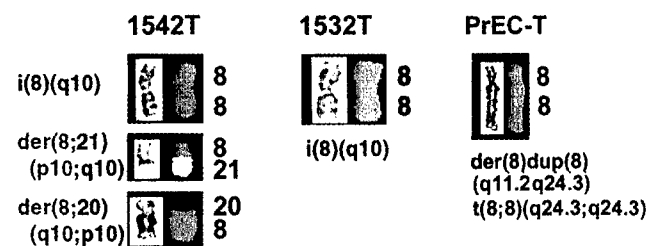


Table 2 Allelic status of chromosome 8 loci^a

Locus	D8S504	D8S277	D8S549	D8S261	NEFL	D8S540	D8S513	D8S535	D8S505	D8S87	D8S1121	D8S255	D8S531	D8S519
cM	0.0	8.4	30.7	35.8		60.0	60.0	60.0	60.0			64.0	65.7	65.8
Chromosome location	8pter	8p23	8p23	8p22	8p21	8p12				8p12			8c 8q12	8q12
1532T	1 ^b	1 ^b	1 ^b	1 ^b	1 ^b	1 ^b	1 ^b	1 ^b	1 ^b	1 ^b	1 ^b	1 ^b	1	1
1542T	1 ^b	1 ^b	1 ^b	1 ^b	1 ^b	1 ^b	1 ^b	1 ^b	1 ^b	1 ^b	1 ^b	1 ^b	2	2
1535T	1	1	2	2	2	2	2	2	1	2	2	2	2	2

^aThe allelic status of each locus is denoted by 1 (homozygous) or 2 (heterozygous). Where known, the genetic distance (cM) and cytogenetic localization are shown.

^bExtended regions of homozygosity defined as the observation of three or more adjacent homozygous loci.

some 20 and structural alterations involving chromosomes 3, 10, and 18, have also been observed through karyotypic analysis of short-term or uncultured primary prostate tumors [13]. It is therefore difficult to determine which genetic alterations were originally present in the prostatic tissues, and which arose subsequent to cellular immortalization. The presence of some of these genetic alterations in 1535N cells, however, suggests at least a subset of the observed karyotypic aberrations arose consequent to cellular immortalization. In particular, all four HPV-immortalized cell lines exhibited extensive duplications or translocations involving the 11q13q22;q23 chromosomal region. 11q+ alterations have been reported in cells immortalized with the HPV 16 or 18 genomes [22, 23], and the 11q23 region has been classified both as a fragile site and possible viral modification site [24, 25]. It appears that the 11q+ alteration observed in the cell lines examined comprises the common chromosomal aberration directly due to immortalization with the E6 and E7 genes of HPV 16.

Allelotype analysis demonstrated loss of 8p sequences in the 1532T and 1542T primary prostate tumor-derived cell lines. The four HPV-immortalized cell lines examined in the present study were partially allelotyped for 8p sequences by Bright et al., who reported loss for a limited number of markers mapping to 8p in the 1532T and 1542T, but not the 1535N or 1535T, cell lines [14]. Interestingly, the 8p loss pattern observed in the tumor tissues and resulting immortalized cell lines was concordant for the 1542T, but not 1532T or 1535T, cell lines. We have confirmed these results for the cell lines, and report a more precise allelotyping, with 12 markers spanning 8p and 2 markers pericentromeric to 8q (Table 2). Complete loss of one copy of 8p in the 1532T and 1542T cell lines was observed, with loss extending pericentromerically into 8q in 1532T cells. These findings are remarkably similar to those reported by others describing reduction to homozygosity for all or part of 8p in prostate tumor tissues [1–10]. Moreover, conventional G-banding and SKY data revealed that loss of 8p sequences in the 1532T and 1542T cell lines was associated with complex structural alterations of chromosome 8 (Fig. 6). The 1532T cells exhibited an i(8q) chromosome in all ten metaphases examined by spectral karyotyping. The 1542T cells also demonstrated an i(8q) chromosome, as well rearrangement of chromosome 8 material with either chromosome 20 or 21. The SKY data confirm reports of an i(8q) chromosome in

1542T cells demonstrated by CGH, FISH, and allelotyping data by Virgin et al., though other aspects of the 1542T karyotype—monosomy 4 and trisomy 11—reported by Virgin et al. differed from the SKY results reported here, possibly due to differences in the passage number and/or clones examined in these studies [26]. The PrEC-T cells, derived from normal prostatic epithelium immortalized after stable transfection with the large T-antigen gene of SV40, also exhibited extensive structural alterations of chromosome 8. These alterations included duplication of q arm material, from q11.2 to q24. In contrast to the 1532T and 1542T cells, the gain of 8q arm material observed in PrEC-T cells was not in the form of an i(8q) chromosome, although the net gain of 8q arm material was the same for all three cell lines.

In conclusion, the data presented here provide intriguing evidence that 8p loss in primary human prostate tumors may not result from simple deletion of all or part of the short arm, as has been previously inferred from allelotyping data [1–8]; rather, 8p loss may, in fact, result from complex structural rearrangements of chromosome 8, often resulting in gain of 8q material, which occurs during tumorigenesis. Moreover, the data reported here provide direct evidence that such complex structural rearrangements sometimes include i(8q) chromosome formation. These studies also suggest that gain of 8q sequences may occur as a consequence of i(8q) chromosome formation in some instances, but may also occur independently of either 8p loss or i(8q) chromosome formation.

The authors would like to thank Ms. Tanya Trybus and Ms. Jana Karaskova for their technical contributions to these studies. We would also like to thank Dr. Suzanne Topalian for her kind gift of the HPV-immortalized cell lines. This work was supported by grants R29 CA60948 from the National Institutes of Health, and RPG-98-338-01-MGO from The American Cancer Society (J. A. M.), the NIH/NCI 1P50 CA69568 SPORE in Prostate Cancer (K. J. P.), and by U.S. Army Medical Research and Materiel Command (USAMRMC) Prostate Cancer Research Program (PCRP) Grant PC970601 (J. A. S.).

REFERENCES

- Bergerheim USR, Kunimi K, Collins VP, Ekman P (1993): Deletion mapping of chromosomes 8, 10 and 16 in human prostatic carcinoma. *Genes Chromosom Cancer* 3:215–220.
- Bova GS, Carter BS, Bussemakers JG, Emi M, Fujiwara Y,

- Kyprianou N, Jacobs SC, Robinson JC, Epstein JI, Walsh PC, Isaacs WB, (1993): Homozygous deletion and frequent allelic loss of chromosome 8p22 loci in human prostate cancer. *Cancer Res* 53:3869-3873.
3. MacGrogan D, Levy A, Bostwick D, Wagner M, Wells D, Bookstein R (1994): Loss of chromosome arm 8p loci in prostate cancer: mapping by quantitative allelic imbalance. *Genes Chromosom Cancer* 10:151-159.
 4. Trapman J, Sleddens HFBM, van der Weiden MM, Dinjens WNM, Konig JJ, Schroder FH, Faber PW, Bosman FT (1994): Loss of heterozygosity of chromosome 8 microsatellite loci implicates a candidate tumor suppressor gene between the loci *D8S87* and *D8S133* in human prostate cancer. *Cancer Res* 54:6061-6064.
 5. Macoska JA, Trybus TM, Benson PD, Sakr WA, Grignon DJ, Wojno KD, Pietruk T, Powell IJ (1995): Evidence for three tumor suppressor gene loci on chromosome 8p in human prostate cancer. *Cancer Res* 55:5390-5395.
 6. Vocke C, Pozzatti RO, Bostwick DG, Florence CD, Jennings SB, Strup SE, Duray PH, Liotta LA, Emmert-Buck MR, Linehan WM (1996): Analysis of 99 microdissected prostate carcinomas reveals a high frequency of allelic loss on chromosome 8p12-21. *Cancer Res* 56:2411-2416.
 7. Prasad MA, Wojno KJ, Macoska JA (1998): Homozygous and frequent deletion of proximal 8p sequences in human prostate cancers: identification of a potential tumor suppressor gene site. *Genes Chromosom Cancer* 23:255-262.
 8. Sakr WA, Macoska JA, Benson PD, Grignon DJ, Wolman SR, Pontes JE, Crissman JD (1994): Allelic loss in locally metastatic, multisampled prostate cancer. *Cancer Res* 54:3273-3277.
 9. Macoska JA, Trybus TM, Sakr WA, Wolf MC, Benson PD, Powell IJ, Pontes JE (1994): Fluorescence in situ hybridization (FISH) analysis of 8p allelic loss and chromosome 8 instability in human prostate cancer. *Cancer Res* 54:3824-3830.
 10. Van Den Berg C, Guan X-Y, Von Hoff D, Jenkins R, Bittner M, Griffin C, Kallioniemi O, Visakorpi T, McGill J, Herath J, Epstein J, Sarosdy M, Meltzer P, Trent J (1995): DNA sequence amplification in human prostate cancer identified by chromosome microdissection: potential prognostic implications. *Clin Cancer Res* 1:11-18.
 11. Takahashi S, Alcaraz A, Brown JA, Borell TJ, Herath JF, Bergstralh EJ, Lieber MM, Jenkins RB (1996): Aneuploidies of chromosomes 8 and Y detected by fluorescence in situ hybridization are prognostic markers for pathological stage C (pT₃N₀M₀) prostate carcinoma. *Clin Cancer Res* 2:137-145.
 12. Jenkins RB, Qian J, Lieber MM, Bostwick DG (1997): Detection of c-myc oncogene amplification and chromosomal aneuploidies in metastatic prostatic carcinoma by fluorescence in situ hybridization. *Cancer Res* 57:524-531.
 13. Webb HD, Hawkins AL, Griffin CA (1996): Cytogenetic abnormalities are frequent in uncultured prostate cancer cells. *Cancer Genet Cytogenet* 88:126-132.
 14. Bright K, Vocke CD, Emmert-Buck MR, Duray PH, Solomon D, Fetsch P, Rhim JS, Linehan WM, Topalian SL (1997): Generation and genetic characterization of immortal human prostate epithelia cell lines derived from primary cancer specimens. *Cancer Res* 57:995-1002.
 15. Hukku B, Rhim JS (1993): Role of chromosome 5 in immortalization and tumorigenesis of human keratinocytes. *Cancer Genet Cytogenet* 68:22-31.
 16. Schrock E, du Manoir S, Veldman T, Schoell B, Wienberg J, Ferguson-Smith MA, Ning Y, Ledbetter DH, Bar-Am I, Soenksen D, Garini Y, Ried T (1996): Multicolor spectral karyotyping of human chromosomes. *Science* 273:494-497.
 17. Beheshti B, Karaskova J, Park PC, Squire J, Beatty BG (in press): Identification of a high frequency of chromosomal rearrangements in the centromeric regions of prostate cancer cell lines by sequential Giemsa-banding and spectral karyotyping. *Mol Diagn*.
 18. Coursen JD, Bennett WP, Gollahon L, Shay JW, Harris CC (1997): Genomic instability and telomerase activity in human bronchial epithelial cells during immortalization by human papillomavirus-16 E6 and E7 genes. *Exp Cell Res* 235:245-253.
 19. Weijerman PC, van Drunen E, Konig JJ, Teubel W, Romijn JC, Schroder FH, Hagemeijer A (1997): Specific cytogenetic aberrations in two novel prostatic cell lines immortalized by human papillomavirus type 18 DNA. *Cancer Genet Cytogenet* 99:108-115.
 20. Oda D, Bigler L, Mao EJ, Distech CM, (1996): Chromosomal abnormalities in HPV-16 immortalized oral epithelial cells. *Carcinogenesis* 17:2003-2008.
 21. Savelieva E, Belair CD, Newton MA, DeVries S, Gray JW, Waldman F, Reznikoff CA (1997): 20q gain associated with immortalization: 20q13.2 amplification correlates with genome instability in human papillomavirus 16 E7 transformed human uroepithelial cells. *Oncogene* 14:551-560.
 22. Sutherland GR, Baker E, Callen DF (1998): A BrdU-enhanceable fragile site or viral modification site at 11q23.1 in lymphoblastoid cultures. *Cytogenet Cell Genet* 47:201-203.
 23. Seki N, Tsuji H, Takahashi E, Yamauchi M, Saito T, Hashimoto T, Yanamoto K, Hori T (1992): Induction of a BrdU-enhanceable fragile-like lesion and sister chromatid exchanges at 11q23.1 in EBV-transformed lymphoblastoid cell lines. *Cytogenet Cell Genet* 61:95-98.
 24. Hoffschir F, Ricoul M, Dutrillaux B (1988): SV40-transformed human fibroblasts exhibit a characteristic chromosomal pattern. *Cytogenet Cell Genet* 49:264-268.
 25. Ray FA, Peabody DS, Cooper J, Scott-Cram L, Kraemer PM (1990): SV40 T antigen alone drives karyotype instability that precedes neoplastic transformation of human diploid fibroblasts. *J Cell Biochem* 42:13-31.
 26. Virgin JB, Hurley PM, Nahhas FA, Bechuk KG, Mohamed AN, Sakr WA, Bright RK, Cher ML (1999): Isochromosome 8q formation is associated with 8p loss of heterozygosity in a prostate cancer cell line. *Prostate* 41:49-57.

Evidence of Chromosomal Instability in Prostate Cancer Determined by Spectral Karyotyping (SKY) and Interphase FISH Analysis¹

Ben Beheshti*, Paul C. Park*, Joan M. Sweet†, John Trachtenberg†, Michael A.S. Jewett† and Jeremy A. Squire*‡

*Department of Laboratory Medicine and Pathobiology, University of Toronto, Toronto, ON, Canada;

†The University Health Network, Faculty of Medicine, University of Toronto, Toronto, ON, Canada and ‡Department of Medical Biophysics, University of Toronto, Toronto, ON, Canada

Abstract

The way in which cytogenetic aberrations develop in prostate cancer (CaP) is poorly understood. Spectral karyotype (SKY) analysis of CaP cell lines has shown that they have unstable karyotypes and also have features associated with chromosomal instability (CIN). To accurately determine the incidence of *de novo* structural and numerical aberrations *in vitro* in CaP, we performed SKY analysis of three independent clones derived from one representative cell line, DU145. The frequent generation of new chromosomal rearrangements and a wide variation in the number of structural aberrations within two to five passages suggested that this cell line exhibited some of the features associated with a CIN phenotype. To study numerical cell-to-cell variation, chromosome 8 aneusomy was assessed in the LNCaP, DU145, and PC-3 cell lines and a patient cohort of 15 CaP primary tumors by interphase fluorescence *in situ* hybridization (FISH). This analysis showed that a high frequency of numerical alteration affecting chromosome 8 was present in both *in vitro* and in CaP tissues. In comparison to normal controls, the patient cohort had a statistically significant ($P < .05$), greater frequency of cells with one and three centromere 8 copies. These data suggest that a CIN-like process may be contributing towards the generation of *de novo* numerical and structural chromosome abnormalities in CaP. *Neoplasia* (2001) 3, 62–69.

Keywords: karyotype evolution, translocation, aneuploidy, ploidy, molecular cytogenetics.

Introduction

Prostate cancer (CaP) has the highest cancer incidence in men and the second most common cause of male cancer mortality [1]. The tumorigenic process has slow onset pathology occurring over a few decades during the lifetime of the individual [2]. Our understanding of the disease process that underlies the progression of CaP has been complicated by both genotypic and phenotypic heterogeneity [3]. A model of CaP progression based on the well-established model of colon cancer progression [4,5] involves the accumulation of multiple genetic alterations. This model is

essentially descriptive and does not address the mechanism leading to the early steps of CaP tumorigenesis.

Recent spectral karyotyping (SKY) analyses of the three CaP cell lines (LNCaP, DU145, PC-3) have demonstrated aneuploid karyotypes with many chromosomal aberrations including complex chromosomal rearrangements and a high degree of karyotype instability [6,7]. In contrast, most early-stage CaP tumors appear to be karyotypically normal diploid with the most common chromosomal changes affecting chromosome 8 [8]. In a small but significant number of cases, the disease progresses to advanced stages, giving the transition from a diploid to aneuploid chromosomal constitution a greater degree of karyotype complexity [9,10].

Karyotype instability can be defined as a progressive alteration of the karyotype affecting a cell population, either *in vivo* or *in vitro* [11]. It implies the selective transmission of chromosomal alterations through cell generations, resulting in clonal cell populations derived from a single cell but not necessarily completely homogeneous. Karyotype instability is distinct from chromosomal instability (CIN) in which an excess of chromosome alterations occurs at each cell generation and, without selective force, these alterations need not necessarily be transmitted through each cell generation [12,13]. CIN is thought to arise as a result of aberrations in the mitotic machinery and/or structural integrity of the chromosome constitution, leading to excessive numerical and structural chromosomal changes [12–15]. The current model for CaP progression does not provide experimental approaches for understanding why *in vitro* CaP cell lines have such complex karyotypes in comparison to the relatively simple karyotypes observed by direct analysis of CaP [8] nor has the role of CIN in this tumor type been rigorously assessed.

Abbreviations: add, additional material to chromosome; CIN, chromosomal instability; del, deleted chromosome; der, derivative chromosome; ider, isochromosome derivative; SCC, single cell clone

Address all correspondence to: Dr. J. A. Squire PhD., Ontario Cancer Institute, The University Health Network, 610 University Avenue, Toronto, ON, Canada M5G 2M9. E-mail: jeremy.squire@utoronto.ca

¹Financial support for this project is funded by a research grant from the Concern Foundation. P.C.P. was supported by a grant from the AFUD/AUA Research Scholar Program and Imclone Systems.

Received 23 October 2000; Accepted 23 November 2000.

Copyright © 2001 Nature Publishing Group All rights reserved 1522-8002/01/\$17.00



In this study, we have employed a comprehensive molecular cytogenetic analysis of CaP including SKY [16] analysis of three DU145-derived single cell clones (SCCs) and fluorescence *in situ* hybridization (FISH) to assess numerical variation of chromosome 8 in 15 early-stage low-grade patient tumors. SKY is a "24-color" FISH approach that uniquely identifies each chromosome based on its specific spectral color composition [16], and allows for the unambiguous identification of the diversity of each chromosomal region present in aberrations and marker chromosomes on a cell-by-cell basis. Therefore, SKY is ideal for assessing both the qualitative and quantitative chromosomal changes associated with tumors expressing the CIN phenotype. Our findings suggest that a CIN-like process may be contributing significantly towards the generation of *de novo* numerical and structural chromosome abnormalities in CaP.

Materials and Methods

CaP Cell Lines and Clone Selection

LNCaP (CRL-1740), DU145 (HTB-81), and PC-3 (CRL-1435) were obtained from the American Type Culture Collection (ATCC, Rockville, MD). LNCaP, an androgen-dependent cell line originating from a lymph node metastasis [17], was grown in RPMI 1640 with 2 mM L-glutamine, 1.5 g/l sodium bicarbonate, 4.5 g/l glucose, 10 mM HEPES, 1.0 mM sodium pyruvate, and 10% fetal bovine serum. PC-3, an androgen-independent cell line originating from a brain metastasis [18], was grown in Ham's F12K with 2 mM L-glutamine, 1.5 g/l sodium bicarbonate, and 10% fetal bovine serum.

DU145, also an androgen-independent cell line and obtained from a metastasis to the bone [19], was grown in F15K Minimum Essential Medium with 1.5 g/l sodium bicarbonate and 10% fetal bovine serum. Three individual subclones were derived from single cells selected from the parental DU145 flask (passage 83). Briefly, the parental culture was incubated in trypsin (Gibco BRL, Gaithersburg, MD), washed in medium, and dissociated by gentle titration. Following microscopic examination to measure complete dissociation of cells, the cell suspension was serially diluted to the approximate concentration of 100 cells/ml. Ten microliters of the suspension was seeded into multiwell flasks and examined by phase contrast microscopy by two independent observers. Three wells containing a single cell were maintained as SCC1, SCC2, and SCC3. After a period of 2 weeks, the SCC cells were dissociated and reseeded into flasks, and maintained for three, two, and five passages (SCC1, SCC2, SCC3, respectively) prior to SKY and FISH analyses.

Tissue Accrual, Tissue Culture, and Cytogenetic Preparations

CaP patients who underwent radical prostatectomy at the University Health Network (Toronto, ON, Canada) and had no previous radiotherapy or chemotherapy were

evaluated for study eligibility based on tumor stage (pT1–T2), low tumor grade, prostate-specific antigen (PSA) levels, and past biopsy history. The surgeon dissected a small wedge (approximately 1–2 cm³) of tumor tissue from the excised prostate, and the resected prostatic capsule was analyzed for extracapsular tumor extension by the pathologist. The tissue wedge was quick-sectioned and hematoxylin- and eosin-stained, and the histopathology was assessed. Samples from 15 patients which showed high tumor content (>80%) were included in this study, and their apposing regions obtained for analysis.

The tissue was digested in 250 U/ml collagenase IV (Gibco BRL) in tissue culture media (RPMI 1640, 10% fetal bovine serum, antibiotics) for 2 to 3 hours. The resulting cell suspension was centrifuged gently and washed with phosphate buffer saline. The cells were then either directly harvested or harvested following a short-term culture (<1 week) for FISH analysis. Tissue sections from the tumor samples were not used since it is well established [20] that a large proportion of nuclei is bisected during preparation, leading to loss of FISH signals.

SKY

The SKY KIT probe cocktail from Applied Spectral Imaging (ASI, Carlsbad, CA) was hybridized to metaphase slides for the DU145 and DU145-derived subclones according to standard protocols [16] and the manufacturer's instructions (ASI).

Results in the figures were reported using an abbreviated format of the International System for Human Cytogenetic Nomenclature (ISCN) for chromosomal aberrations, omitting breakpoint information [21]. In keeping with ISCN conventions, irrespective of ploidy, an individual chromosomal aberration (structural or numerical change) is considered a clonal gain when it is observed at least twice, and clonal loss when missing in at least three cells [21]. The frequency of nonclonal changes were taken to reflect the propensity of aberration within the cell line. Clonal changes, however, indicate the perpetuation of aberrations through successive cell divisions.

FISH

Cytogenetic slides were prepared as previously described [22] from a total of 15 patients as well as the CaP cell lines using 1.5-hour colcemid treatment and 75 mM KCl hypotonic treatment. While metaphase and interphase nuclei were readily produced from the CaP cell lines, only interphase nuclei were obtained from the patient samples. Normal cytogenetic control slides bearing metaphases and interphase nuclei were made from phytohemagglutinin-stimulated normal male lymphoblasts. The centromere 8 *D8Z1* alphoid centromeric sequence genomic clone was obtained from the ATCC (#59904, Rockville, MD) and labeled with biotin-14-dATP (Gibco BRL). A minimum of 100 cells was evaluated in each cytogenetic sample for assessing the centromere 8 frequencies.

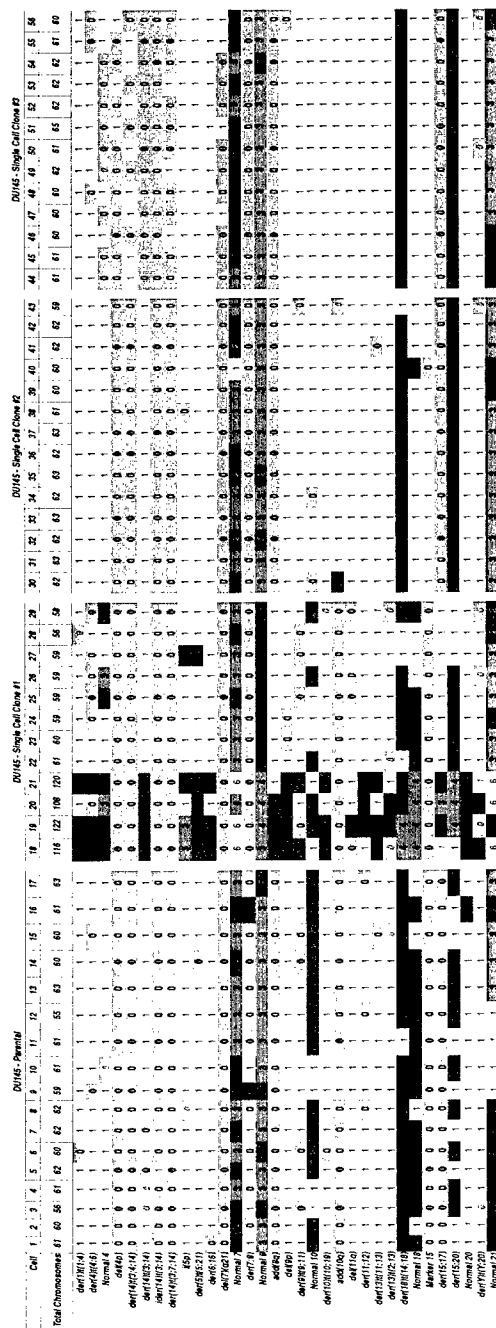


Figure 1. Overview of the frequency of numerical change of chromosomal aberrations in the three DU145 subclones. In this figure, a color grid has been used to depict numerical change of the various aberrations that are characteristic of DU145 and its three subclones. The leftmost panel is the parental DU145 culture obtained from the ATCC. The three panels to its right depict copy number change in each of the three independently derived DU145 subclones. Each cell studied is represented by a column and each one of the 33 chromosomal aberrations of DU145 is identified as separate row. Colors have been used to depict copy number (1 = yellow; 2 = green; 3 = light blue; etc.) so that it is easy to see that SCC2 and SCC3 exhibit a more homogeneous pattern of numerical change than SCC1 based on the more uniform appearance of the colored grid in the two rightmost panels. All cells in this analysis were hypotriploid except for cells 18 to 21 in SCC1, which had double the chromosome number. Copy numbers written in red text indicate that a nonclonal structural rearrangement of the chromosomal aberration was present in that particular cell.

Statistical Analysis

Statistical analysis using the chi-square test evaluated each of the patient samples *versus* the normal control, with 3 *df* ($\alpha=0.05$). A similar comparison was made between each of the DU145 subclones and the DU145 parental cell line (4 *df*, $\alpha=0.001$).

Results

Ploidy

As previously reported for this early passage number [6,7,19,23], our analysis by SKY demonstrated the DU145 parental cell line to have a range of 55 to 63 chromosomes per cell (Figure 1A). Because this range is less than three times the haploid chromosome count and most chromosomes were present in three copies, this cell line is probably derived from a hypotriploid stem line. The SCC2 and SCC3 cells were also observed to be hypotriploid, with ranges of 59 to 63 (Figure 1C) and 60 to 65 (Figure 1D), respectively. The SCC1 cells, however, had two distinct populations with different ploidy levels. In addition to the hypotriploid (56–61) cells, the SCC1 subclone had cells with double this ploidy (108–122) or hypohexaploid (Figure 1B). These results were corroborated by interphase and metaphase FISH on the DU145 cell lines (Table 1).

The LNCaP cell line was observed by interphase and metaphase FISH analysis to have two populations with diploid and tetraploid centromere 8 signals, reflecting previous data that demonstrated a mixed ploidy in this cell line [6,24]. The PC-3 cells were shown to have predominantly two copies of centromere 8 signals, which is in accordance with our previous data that showed it to be hypotriploid but with only two copies of chromosome 8 [6]. FISH results for LNCaP and PC-3 are also reported in Table 1.

Since the patient samples used in this study were derived from early-stage, low-grade primary tumors, it is probable that they have a diploid karyotype [25,26]. In keeping with this observation, our interphase FISH observations showed predominantly two centromere 8 copies in all the tumor samples (Table 2).

Table 1. Interphase and Metaphase FISH Analyses of the Centromere 8 Copy Number in the CaP Cell Lines and the Three DU145-Derived SCC Cells.

Cell Line	Centromere 8 Copy Number					
	1 (%)	2 (%)	3 (%)	4 (%)	5 (%)	≥6 (%)
LNCaP	3.0	67.0	6.0	20.5	1.5	2.0
PC-3	–	79.4	5.9	10.3	2.2	2.2
DU145 Parental	–	0.7	70.0	21.3	1.3	6.7
DU145 SCC1	–	5.1	79.2	2.0	2.5	11.2
DU145 SCC2	–	5.5	89.0	2.8	1.4	1.4
DU145 SCC3	–	1.9	88.3	0.6	3.1	6.2

In each cell line, the copy number with the highest observed frequency is in boldface. There is variability of the centromere 8 copy number around the modal values.

Table 2. Interphase FISH Analyses of the Centromere 8 Copy Number in the CaP Patients.

Patient	Centromere 8 copy number			
	1 (%)	2 (%)	3 (%)	≥4 (%)
Normal blood	1.0	96.0	–	3.0
1	5.4	79.6	8.2	6.8
2	4.9	84.2	4.9	6.1
3	2.7	90.3	6.0	1.1
4	0.8	86.3	7.3	5.7
5	1.5	85.1	10.5	3.0
6	0.7	89.8	7.5	2.0
7	2.5	91.5	5.9	–
8	3.6	48.7	44.1	3.6
9	10.2	83.2	4.4	2.2
10	7.2	75.5	5.0	12.2
11	4.9	76.1	18.6	0.4
12	3.0	92.3	2.7	1
13	9.7	80.2	6.9	3.2
14	7.6	69.6	14.3	8.5
15	5.0	86.1	7.5	1.5

In each patient, the copy number with the highest observed frequency is in boldface. There is variability of the centromere 8 copy number around the diploid modal value.

Aneusomy

Our SKY analysis of aneusomies drew attention to a number of consistent features associated with karyotype evolution in each of the subclones (Figure 1). With the exception of SCC1, all the cell lines had two copies of chromosome 4. In the parental DU145 and SCC2 cells, the two copies were comprised of the normal 4 and derivative 4 chromosomes. As outlined in Figure 1, in parental cells where these chromosomes were not present, for instance in cells 9 and 10, the der(4)t(4;6) was replaced with a der(4)t(4;15) and the normal 4 was replaced with a der(4)t(4;9), respectively, to maintain the total of two copies of chromosomes 4. Similarly, in SCC3, two copies of chromosome 4 or derivative 4 chromosomes were maintained by having any two combinations of der(4)t(4;6), normal 4, del(4p), or der(14)t(3;14). The exception to this was cell 49, where a der(4)t(4;7) was observed in place of the normal chromosome 4 (Figure 1D).

Several clonal rearrangements were observed by SKY analyses that were specific to the parental or subclone cell lines. These results are summarized in Figure 1. For example, the isochromosome derivative 14 chromosome, ider(14)t(3;14), was observed in 2/17 parental cells, but not in any of the subclones. The der(7;8), which was a centromeric fusion of the short arm of chromosome 7(7p) and long arm of chromosome 8(8q), was observed in the parental cells (7/17) but was absent in the subclones. The clonal addition of chromosome 10 material to 10q, add(10q), was present in 3/17 parental cells, absent in the SCC1 cells, and ubiquitous in the SCC2 and SCC3 cells. Several novel chromosomal rearrangements that were not previously observed in the parental cells were identified in the subclones. The der(15;17), and the clonal addition of chromosome 8 material to 8q, add(8q), were specific to the

SCC1 cells. A small derivative chromosome 15 rearranged with another minute indeterminable partner chromosome, designated Marker 15, was observed in only SCC2 and SCC3 cells. The $\text{del}(7)(p21)$, and the previously described $\text{der}(14)\text{t}(3;4;14)$, $\text{der}(14)\text{t}(3;7;14)$, and $\text{del}(4p)$ chromosomes were observed clonally and only in the SCC3 cells.

In addition to the observed structural changes, chromosomal aneusomy was also evident as numerical changes specific to the parental or subclone cell lines. As outlined in Figure 1, SKY analysis revealed that chromosome 10 was observed in one or two copies in the parental cells (4/17 and 13/17 cells, respectively), but SCC2 and SCC3 cells consistently had one copy. Similarly, while the parental cells had one, two, or three copies of chromosome 21 (4/17, 9/

17, and 4/17, respectively), trisomy was a more dominant feature than disomy in the SCC2 (12/14 and 2/14, respectively) and SCC3 cells (9/13 and 4/13, respectively). Furthermore, the variability of chromosome 18 copy number in the parental line (13/17 disomy, 4/17 monosomy) was eliminated in the SCC2 and SCC3 cells which consistently exhibited a single copy.

Structural Aberrations

SKY analysis of the DU145 cell lines was able to identify all the complex chromosomal rearrangements within the DU145 cell lines. Of interest was the $\text{der}(14)\text{t}(3;14)$, which was present in 13/17 cells of the DU145 parental cells (Figure 1). The evolution of the $\text{der}(14)\text{t}(3;14)$ is particu-

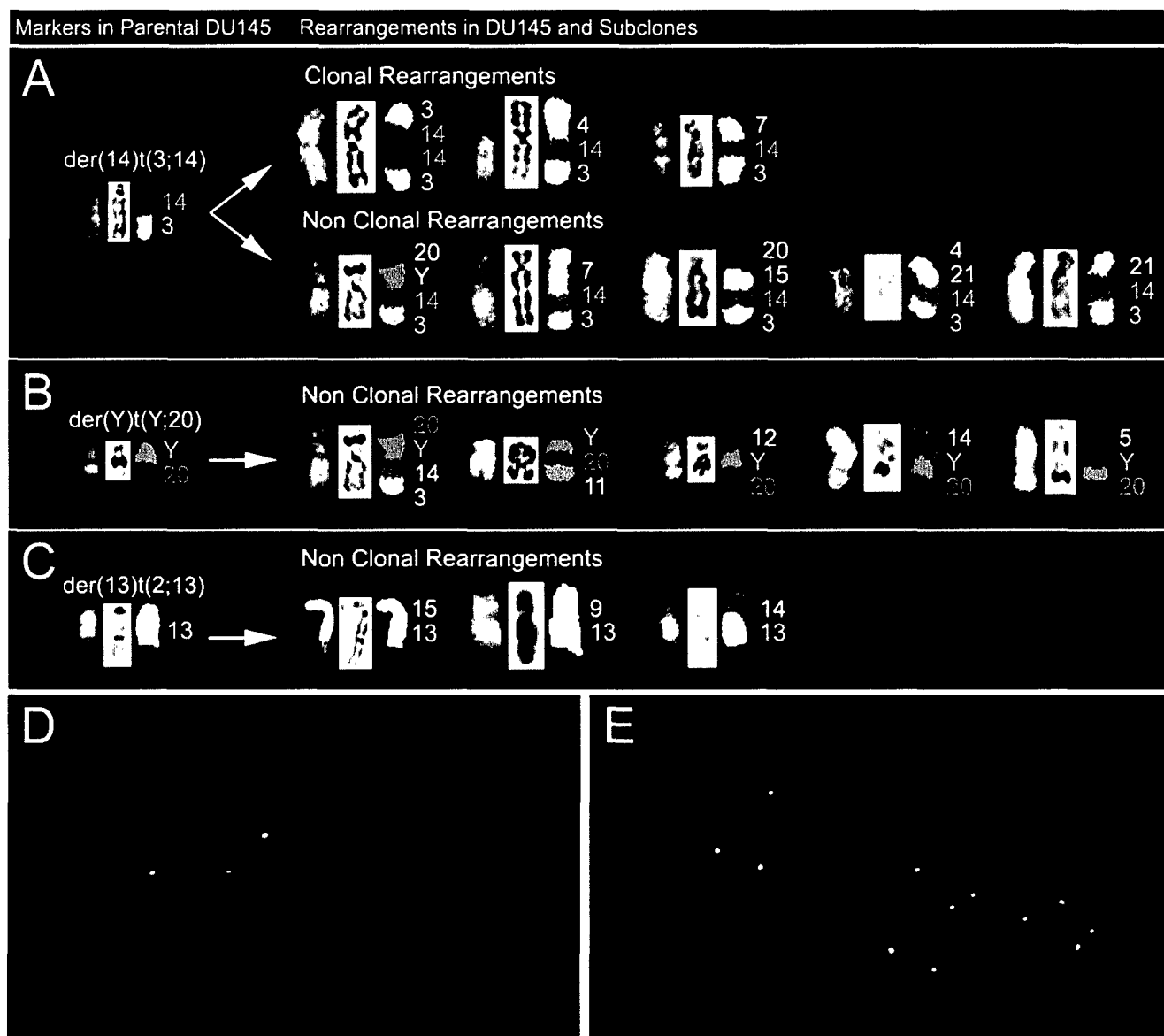


Figure 2. Evidence of a CIN-like process in DU145 cells as shown by structural and numerical aberrations. Panels A, B, C: Representative marker chromosomes observed in parental DU145 cell line [$\text{der}(14)\text{t}(3;14)$; $\text{der}(Y)\text{t}(Y;20)$; $\text{der}(13)\text{t}(2;13)$], and putative structural derivatives thereof (clonal and nonclonal) in the parental and subclone cell lines. Note the maintenance of the original marker chromosome in each of the structural derivatives and progression from a simple to a more complex rearrangement, suggestive of marker evolution. Panels D, E: Representative metaphase (Panel D) and interphase nuclei (Panel E) FISH image using centromere 8 probe (green) from the DU145 parental cell line. Analysis on a cell-by-cell basis revealed frequent chromosome 8 copy number change in a subpopulation of DU145 cells.

larly interesting (Figure 2A). Where this rearrangement was absent, rearrangements involving the derivative 14 chromosome were observed: e.g., der(Y)t(Y;3;14;20) (cell 3), der(14)t(3;14;21) (cell 4), and isoderivative chromosomes der(14)t(3;14) (cells 5 and 7). Interestingly, the der(14)t(3;14) was also present in SCC1 (12/12) and SCC2 (14/14), but absent in SCC3 (0/13). In SCC3 cells, the der(14)t(3;14) usually presented as der(14)t(3;4;14) (8/13) or der(14)t(3;7;14) (3/13) rearrangements; exceptions to this observation were cells 51 and 56, in which these chromosomes were lost. Neither the novel der(14)t(3;4;14) nor der(14)t(3;7;14) chromosomes were observed in the SCC1, SCC2, or the parental cell lines. The occurrence of this der(14)t(3;14) in several different rearrangements in DU145 and its subclones is remarkable and suggests that it may confer a selective advantage.

In Figure 2B, the der(Y)t(Y;20) was also observed to participate in five different nonclonal structural translocations, suggesting that the Y chromosome may be preferentially involved in rearrangement. Similarly, the distal part of the der(13)t(2;13) (Figure 2C) was involved in three different aberrations. It is noteworthy that the breakpoints involved in the marker evolution of der(14)t(3;14), der(13)t(2;13), and der(Y)t(Y;20) are all at regions of repetitive DNA.

The SCC1 cells demonstrated a greater number of nonclonal structural rearrangements and gains and losses of chromosomes than the other two subclones (Figure 1B). For instance, in cell 18, there were 11 novel, unique chromosomal rearrangements (not shown). Furthermore, while in the SCC2, SCC3, and DU145 parental cells there were consistent trends such as the total chromosome 4 and der(14)t(3;14) content reported above, this consistency was not as apparent in the SCC1 cells. Interestingly, more marked variation was observed even when comparing between the hypohexaploid cells (cells 18–21) of the SCC1 cell line. For instance, cell 18 had many more nonclonal structural and numerical aberrations than cell 21 (not shown).

By SKY analysis, it was apparent that dicentric chromosomes were present within the DU145 cell lines. As demonstrated in Figure 2C, the der(13)t(2;13) translocation, which is present in almost every cell of the DU145 cell lines, has two centromeres. Also depicted are other nonclonal dicentric chromosomes. There was no evidence of double minutes, ring chromosomes, or other chromosomal features associated with gross CIN in the DU145 cell lines.

Interphase FISH

Results for the FISH analysis of the CaP cell lines are given in Table 1, and representative metaphase and interphase FISH images of the DU145 parental cells are depicted in Figure 2D and E, respectively. The DU145 parental cells were observed to have a major population of cells with three copies of chromosome 8 (70%) and a smaller population with four copies (21%). SKY analysis of the DU145 parental cells demonstrated a similar frequency of cells having three copies of chromosome 8, and cells having four copies of chromosome 8 centromere when counted together with the additional der(7;8) chromosome. The

SCC2 and SCC3 cells demonstrated by FISH had less centromere 8 copy number variation than the parental DU145 cells, with the majority of cells having three copies (89% and 88%, respectively). While the SCC1 cells had similar frequencies of three and four centromere copy numbers (79% and 2%, respectively) as the other two subclones, it also had a relatively high frequency of cells with at least six copies (11%), suggesting more genomic variability than the other two subclones. The reduction in centromere 8 copy number variation in the DU145 subclones *versus* the DU145 parental cells was statistically significant ($P < .001$). It should be noted that in the DU145 parental, SCC1, and SCC3 cells, there were no greater than 8, 14, and 8 centromere 8 copies, respectively. Notably, although by FISH it appeared that the majority of cells in the DU145 cell lines had three copies of chromosome 8, SKY analysis distinguished that in SCC2 and SCC3 cells, these were all normal copies of chromosome 8, but that in DU145 parental cells one of the chromosome 8 copies may be involved in a der(7;8) translocation, and in the SCC1 cells there was additional chromosome 8 material at the qter in one of the copies.

FISH analysis of the LNCaP cells showed most cells to have two copies of centromere 8 signals (67%), and a smaller percentage of cells to have four copies (20%). The PC-3 cells had predominantly two copies of centromere 8 (79%), and a smaller percentage of cells with four copies (10%), most likely representing cells in G2 phase of the cell cycle. Interestingly, both cell lines were observed to have variation of centromere 8 copy number (Table 1).

Examination of the centromere 8 copy number by interphase FISH in the CaP patient cohort (Table 2) demonstrated that the majority of cells had predominantly two centromere 8 copies. Furthermore, as compared to the normal control, the patient cohort had a statistically significant ($P < .05$), greater frequency of cells with one and three centromere 8 copies. While many cells also had some frequency of four copies, it is indeterminate without further analysis if these cells are in the G2 phase of the cell cycle, similar to the normal control, or are truly aberrant. Of interest, four patients had a trisomy of centromere 8 of greater than 10%, with patient 10 having the greatest frequency of 44%. Also, one patient had a frequency of monosomy of the centromere 8 signal at 10%.

Discussion

Features expected of tumors expressing CIN include aneuploidy and random chromosomal alterations, including aneusomy and structural rearrangements [27,28]. CIN may be associated with aberrations in mitotic spindle checkpoints [29] and genes such as *hBUB1* and *MAD2* [14,15], aberrant sister chromatid exchange [30], DNA repair pathways [31], and abnormal centrosome copy numbers or amplification [32–35]. In a more recent study, breakage–fusion–bridge cycles have been implicated in generating CIN [36]. Interestingly, some tumors exhibit both microsatellite instability as well as CIN [15,37,38] as is the case for DU145 [39]. However, to date, there has been no direct evidence implicating CIN in CaP.

Giemsa banding and SKY analysis of DU145, reported previously [6,7], demonstrated that this cell line had a complex karyotype with some evidence of numerical variation suggestive that a CIN-like process may be operational. SKY analysis was performed on the DU145 parental cells, and as outlined in Figure 1, the pattern of chromosomal aberrations exhibits a high degree of cytogenetic heterogeneity. To investigate whether this karyotypic heterogeneity was due to the presence of multiple clones within the DU145 cell population, or had arisen *de novo* because of CIN, three DU145-derived subclones were studied by SKY analysis.

Since the three subclones were initially seeded as single cells derived from the parental cell population, it would be expected that they should maintain a high degree of karyotypic clonality and concordance with each other unless inherent instability was present. While it is possible that the high proliferation rate of *in vitro* growth may exaggerate inherent instability, it is clear that significant deviations between the subclones implicate a CIN-like process. As summarized in Figure 1, while these clones demonstrated an increased homogeneity of structural and numerical aberrations as compared to the DU145 parental cells, there were indications that *de novo* translocations occurred and that numerical aberrations were generated or lost within two to five passages following subclone generation. These include: del(4p), del(7)(q21), der(7;8) add(8q), der(10q), der(14)t(3;14), der(14)t(3;14), der(14)t(3;4;14), der(14)t(3;7;14), Marker 15, der(15;17), and copy number changes for chromosomes 4, 10, 18, and 21. Furthermore, from Figure 1, it is apparent that SCC1 demonstrated a more heterogeneous karyotype than the SCC2 and SCC3 cells, with a bimodal population of hypotriploid and hypohexaploid cells and a greater overall number of chromosomal aberrations (Table 3).

Detailed examination of the relative distribution of marker chromosomes in the three subclones also identified some preferred patterns of chromosomal aberration as the respective karyotypes evolved. For instance, while there

was copy number variation of chromosome 4 in all the DU145 cell lines, in general there were at least two copies of chromosome 4 present per cell either as normal copies or involved in a derivative chromosome 4 rearrangement. Similarly, although the der(14)t(3;14) was present in the SCC1, SCC2, and DU145 parental cells, it was involved in novel clonal rearrangements in SCC3 cells (Figure 2A), suggesting that selective forces favor acquisition of specific markers or combinations of certain chromosomal regions. In this regard, it is noteworthy that rearrangement often took place at sites rich in repetitive DNA such as distal Yp, 13p, and 14p. Overall, there appeared to be some consistent features associated with the chromosomal constitution within each subclone, but closer analysis of the aberrations by SKY indicated that chromosomal gain may be achieved by both simple numerical gain and/or unbalanced structural translocation. These results also draw attention to the potential limitations of comparative genomic hybridization (CGH) in the analysis of tumors exhibiting a high degree of complexity of rearrangements, since it is usually only possible to determine the average level of chromosomal imbalance with this method [40].

Our results suggested that intrinsic aneusomy would also be measurable by FISH analysis. Cell-by-cell analysis of numerical change as determined by FISH using the centromere 8 probe with LNCaP, DU145, PC-3, and DU145-derived subclones correlated well with the findings concerning chromosomal loss and gain identified by SKY (Table 1) [6]. Furthermore, it was apparent that there was variation in both the mean chromosome number and the range or spread of centromere 8 signals observed in all cell lines and subclones, suggesting that chromosomal segregation errors may be a general feature of CaP cell lines. Examination of the levels of aneusomy determined by centromere 8 FISH analysis of cells derived from primary tumor tissue revealed a modal distribution of frequencies with the majority of cells being close to diploid. Even if some bias towards diploidy — due to the unavoidable admixture of normal stromal and epithelial components with the tumor epithelial cells in these preparations — is considered, then the level of monosomy and trisomy is excessive in several tumor samples. Taken together, the levels of aneusomy for chromosome 8 present in cell line and primary tumor tissue are suggestive that CIN may be an early feature of the disease process in CaP.

In summary, the results suggest that 1) SKY is a valuable screening tool for the delineation of genomic instability in tumor cells; 2) a CIN-like process is an intrinsic feature of the DU145 cell line leading to excessive numerical and structural alterations to chromosomes; 3) there appears to be preferred sites of rearrangement at chromosomal regions rich in repetitive DNA; 4) the combination of such a CIN-like process and cell selection will lead to rapid acquisition of novel combinations of chromosomal aberrations within a given tumor cell population; 5) there may be different inherent rates of this CIN-like process, as demonstrated by the variation within the three subclones; and 6) excessive aneusomy of chromosome 8 in early-stage CaP tumors

Table 3. Quantification of Clonal and Nonclonal Changes Per DU145 Cell Line.

Cell Line		Clonal Changes	Nonclonal Changes
DU145 Parental	Total	11	40
	Normalised per cell	0.65	2.35
DU145 SCC1	Total	8	23
	Normalised per cell	0.67	1.92
DU145 SCC2	Total	1	13
	Normalised per cell	0.07	0.93
DU145 SCC3	Total	8	14
	Normalised per cell	0.62	1.08

For each cell line, the total numbers of clonal and nonclonal changes were determined and normalised by dividing by the total number of cells analyzed (17, 12, 14, and 13, respectively). These results objectively support that there is more homogenous pattern of numerical changes in SCC2 than in SCC3 and SCC1. Note that the rate of nonclonal changes approaches that of the parental DU145 cell line, indicating the presence of a CIN-like process.



suggests that a CIN-like process may initiate the numerical variation upon which selective forces subsequently operate. In this regard, the adaptive capacity of a tumor may be defined by its higher intrinsic rate of instability. Given that no specific tumor-suppressor genes or dominant oncogenes have been associated with CaP to date, the role of CIN in CaP tumorigenesis and perhaps other tumor systems in general may warrant further investigation as an alternate model of oncogenesis.

Acknowledgements

The authors gratefully acknowledge the technical expertise of Salomon Minkin and Jane Bayani.

References

- [1] Ekman P, Adolfsson J, and Gronberg H (1999). The natural history of prostate cancer. In *Textbook of Prostate Cancer Pathology, Diagnosis and Treatment*. Blackwell Sciences, London.
- [2] Bookstein R (1994). Tumor-suppressor genes in prostatic oncogenesis. *J Cell Biochem Suppl* 19, 217–223.
- [3] Macintosh CA, Stower M, Reid N, and Maitland NJ (1998). Precise microdissection of human prostate cancers reveals genotypic heterogeneity. *Cancer Res* 58, 23–28.
- [4] Fearon ER, Hamilton SR, and Vogelstein B (1987). Clonal analysis of human colorectal tumors. *Science* 238, 193–197.
- [5] Dong JT, Isaacs WB, and Isaacs JT (1997). Molecular advances in prostate cancer. *Curr Opin Oncol* 9, 101–107.
- [6] Beheshti B, Karaskova J, Park PC, Squire JA, and Beatty BG (2000). Identification of a high frequency of chromosomal rearrangements in the centromeric regions of prostate cancer cell lines by sequential Giemsa banding and spectral karyotyping. *Mol Diagn* 5, 23–32.
- [7] Pan Y, Kytola S, Farnebo F, Wang N, Lui WO, Nupponen N, Isola J, Visakorpi T, Bergerheim US, and Larsson C (1999). Characterization of chromosomal abnormalities in prostate cancer cell lines by spectral karyotyping. *Cytogenet Cell Genet* 87, 225–232.
- [8] Ozen M, and Pathak S (2000). Genetic alterations in human prostate cancer: a review of current literature. *Anticancer Res* 20, 1905–1912.
- [9] Oesterling J, Fuks Z, Lee CT, and Scher HI (1997). Cancer of the prostate. In *Cancer: Principles and Practice of Oncology*. Lippincott-Raven Publishers, Philadelphia. pp. 1322–1385.
- [10] Verma RS, Manikal M, Conte RA, and Godec CJ (1999). Chromosomal basis of adenocarcinoma of the prostate. *Cancer Invest* 17, 441–447.
- [11] Dutrillaux B (2000). Chromosome and karyotype instability in human cancers and cancer-predisposing syndromes. In *DNA Alterations in Cancer*. Eaton, Natwick, MA, USA. pp. 369–382.
- [12] Lengauer C, Kinzler KW, and Vogelstein B (1998). Genetic instabilities in human cancers. *Nature* 396, 643–649.
- [13] Cahill DP, Kinzler KW, Vogelstein B, and Lengauer C (1999). Genetic instability and Darwinian selection in tumours. *Trends Cell Biol* 9, M57–M60.
- [14] Pihan GA, and Doxsey SJ (1999). The mitotic machinery as a source of genetic instability in cancer. *Semin Cancer Biol* 9, 289–302.
- [15] Cahill DP, da Costa LT, Carson-Walter EB, Kinzler KW, Vogelstein B, and Lengauer C (1999). Characterization of MAD2B and other mitotic spindle checkpoint genes. *Genomics* 58, 181–187.
- [16] Schröck E, du Manoir S, Veldman T, Schoell B, Wienberg J, Ferguson-Smith MA, Ning Y, Ledbetter DH, Bar-Am I, Soenksen D, Garini Y, and Ried T (1996). Multicolor spectral karyotyping of human chromosomes. *Science* 273, 494–497.
- [17] Horoszewicz JS, Leong SS, Chu TM, Wajsman ZL, Friedman M, Papsidero L, Kim U, Chai LS, Kakati S, Arya SK, and Sandberg AA (1980). The LNCaP cell line — a new model for studies on human prostatic carcinoma. *Prog Clin Biol Res* 37, 115–132.
- [18] Kaighn ME, Narayan KS, Ohnuki Y, Lechner JF, and Jones LW (1979). Establishment and characterization of a human prostatic carcinoma cell line (PC-3). *Invest Urol* 17, 16–23.
- [19] Stone KR, Mickey DD, Wunderli H, Mickey GH, and Paulson DF (1978). Isolation of a human prostate carcinoma cell line (DU 145). *Int J Cancer* 21, 274–281.
- [20] Aubele M, Zitzelsberger H, Szucs S, Werner M, Braselmann H, Hutzler P, Rodenacker K, Lehmann L, Minkus G, and Hofer H (1997). Comparative FISH analysis of numerical chromosome 7 abnormalities in 5-micron and 15-micron paraffin-embedded tissue sections from prostatic carcinoma. *Histochem Cell Biol* 107, 121–126.
- [21] Mitelman F (1995). *ISCN (1995): International System for Human Cytogenetic Nomenclature*. S. Karger, New York.
- [22] Dracopoli NC (2000). *Current Protocols in Human Genetics*. John Wiley and Sons, New York, USA.
- [23] Bernardino J, Bourgeois CA, Muleris M, Dutrillaux AM, Malfroy B, and Dutrillaux B (1997). Characterization of chromosome changes in two human prostatic carcinoma cell lines (PC-3 and DU145) using chromosome painting and comparative genomic hybridization. *Cancer Genet Cytogenet* 96, 123–128.
- [24] Gibas Z, Becher R, Kawinski E, Horoszewicz J, and Sandberg AA (1984). A high-resolution study of chromosome changes in a human prostatic carcinoma cell line (LNCaP). *Cancer Genet Cytogenet* 11, 399–404.
- [25] Micale MA, Mohamed A, Sakr W, Powell IJ, and Wolman SR (1992). Cytogenetics of primary prostatic adenocarcinoma. Clonality and chromosome instability. *Cancer Genet Cytogenet* 61, 165–173.
- [26] Lieber MM (1992). DNA ploidy: early malignant lesions. *J Cell Biochem Suppl* 16H, 44–46.
- [27] Duesberg P, Rausch C, Rasnick D, and Hehlmann R (1998). Genetic instability of cancer cells is proportional to their degree of aneuploidy. *Proc Natl Acad Sci USA* 95, 13692–13697.
- [28] Duesberg P, Rasnick D, Li R, Winters L, Rausch C, and Hehlmann R (1999). How aneuploidy may cause cancer and genetic instability. *Anticancer Res* 19, 4887–4906.
- [29] Skibbens RV, and Hieter P (1998). Kinetochore and the checkpoint mechanism that monitors for defects in the chromosome segregation machinery. *Annu Rev Genet* 32, 307–337.
- [30] Dhillon VS, and Dhillon IK (1998). Chromosome aberrations and sister chromatid exchange studies in patients with prostate cancer: possible evidence of chromosome instability. *Cancer Genet Cytogenet* 100, 143–147.
- [31] Difilippantonio MJ, Zhu J, Chen HT, Meffre E, Nussenzweig MC, Max EE, Ried T, and Nussenzweig A (2000). DNA repair protein Ku80 suppresses chromosomal aberrations and malignant transformation. *Nature* 404, 510–514.
- [32] Salisbury JL, Whitehead CM, Lingle WL, and Barrett SL (1999). Centrosomes and cancer. *Biol Cell* 91, 451–460.
- [33] Ghadimi BM, Sackett DL, Difilippantonio MJ, Schrock E, Neumann T, Jauho A, Auer G, and Ried T (2000). Centrosome amplification and instability occurs exclusively in aneuploid, but not in diploid colorectal cancer cell lines, and correlates with numerical chromosomal aberrations. *Genes, Chromosomes Cancer* 27, 183–190.
- [34] Whitehead CM, and Salisbury JL (1999). Regulation and regulatory activities of centrosomes. *J Cell Biochem Suppl* 32–33, 192–199.
- [35] Zhou H, Kuang J, Zhong L, Kuo WL, Gray JW, Sahin A, Brinkley BR, and Sen S (1998). Tumour-amplified kinase STK15/BTAK induces centrosome amplification, aneuploidy and transformation. *Nat Genet* 20, 189–193.
- [36] Saunders WS, Shuster M, Huang X, Gharaibeh B, Enyenihi AH, Petersen I, and Gollin SM (2000). Chromosomal instability and cytoskeletal defects in oral cancer cells. *Proc Natl Acad Sci USA* 97, 303–308.
- [37] Leung SY, Yuen ST, Chan TL, Chan AS, Ho JW, Kwan K, Fan YW, Hung KN, Chung LP, and Wyllie AH (2000). Chromosomal instability and p53 inactivation are required for genesis of glioblastoma but not for colorectal cancer in patients with germline mismatch repair gene mutation. *Oncogene* 19, 4079–4083.
- [38] Ohshima K, Haraoka S, Yoshioka S, Hamasaki M, Fujiki T, Suzumiya J, Kawasaki C, Kanda M, and Kikuchi M (2000). Mutation analysis of mitotic checkpoint genes (hBUB1 and hBUBR1) and microsatellite instability in adult T-cell leukemia/lymphoma. *Cancer Lett* 158, 141–150.
- [39] Boyer JC, Umar A, Risinger JI, Lipford JR, Kane M, Yin S, Barrett JC, Kolodner RD, and Kunkel TA (1995). Microsatellite instability, mismatch repair deficiency, and genetic defects in human cancer cell lines. *Cancer Res* 55, 6063–6070.
- [40] Kallioniemi OP, Kallioniemi A, Piper J, Isola J, Waldman FM, Gray JW, and Pinkel D (1994). Optimizing comparative genomic hybridization for analysis of DNA sequence copy number changes in solid tumors. *Genes, Chromosomes Cancer* 10, 231–243.

Identification of numerical chromosomal changes detected by interphase FISH in high-grade prostrate intraepithelial neoplasia (HPIN) as a predictor of carcinoma.

Jaudah Al-Maghrabi MD FRCPC^{1,2,4,5,7}, Lada Vorobyova MD^{1,2,4,5}, A. Toi MD FRCPC,⁷ William Chapman MD FRCPC^{1,2,4,5}, Maria Zielenska PhD⁸, Jeremy A. Squire PhD¹⁻⁶

Ontario Cancer Institute¹, Princess Margaret Hospital², Toronto General Hospital³, University Health Network⁴, Department of Laboratory Medicine and Pathobiology⁵, Medical Biophysics⁶, and Radiology⁷, Department of Pathology, Hospital for Sick Children⁸, Faculty of Medicine, University of Toronto, Toronto, Ontario, Canada

Address for correspondence:

J.A. Squire Ph.D.

Division of Cellular and Molecular Biology

Ontario Cancer Institute

Princess Margaret Hospital

610 University Avenue

Room 9-721

Toronto, Ontario

M5G 2M9

tel. 416-946-4509

fax 416-920-5413

e-mail: jeremy.squire@utoronto

Corresponding Author: -

J.A. Squire Ph.D.

Division of Cellular and Molecular Biology

Ontario Cancer Institute

Princess Margaret Hospital

610 University Avenue

Room 9-721

Toronto, Ontario

M5G 2M9

tel. 416-946-4509

fax 416-920-5413

e-mail: jeremy.squire@utoronto.ca

ABSTRACT:

p53 mutation has been shown to be associated with chromosomal instability (CIN) in many human dysplastic and neoplastic lesions. However the precise role of p53 in the pathogenesis of Pca is unknown. Topographic analysis of p53 alteration using Immunohistochemistry (IHC) was performed on 35 archived prostatectomy specimens containing Pca foci, HPIN foci intermingled with cancer (HPINI) and situated away (HPINA). A subset of specimens was topographically genotyped using Laser capture microdissection, PCR amplification and direct sequencing of p53 exons 5-9. CIN was evaluated in the same tissue foci by interphase *in situ* hybridization (IFISH) using centromere probes for chromosome 7, 8 and Y. p53 immunoreactivity was found in 20%, 17%, 0%, and 0% in Pca, HPINI, HPINA, and benign epithelium respectively. p53 molecular analysis showed complete concordance with IHC. IFISH revealed numerical chromosomal alterations in keeping with CIN in 71% and 25% of p53+ve and p53-ve Pca respectively ($P=0.0.1$), 67% and 0% of p53+ve and p53-ve HPIN respectively ($P<0.02$) and in 27% and 0% of HPINI and HPINA respectively. We concluded that p53 mutation is an early change in at least a subset of Pca. HPINI foci tend to have higher overall p53 immunoreactivity and CIN than HPINA. The presence of p53 mutation in HPIN was associated with the presence of chromosomal instability as determined by IFISH. Also our study provided additional evidence in support of the concept that HPIN is the earliest precursor of cancer. Furthermore our studies identify genomic similarities in HPINI and Pca, implying that carcinoma may arise from progression of certain HPIN foci that most likely harbor p53 mutation and/or more CIN.

Key words: Chromosomal instability, *in situ* hybridization, prostate intraepithelial neoplasia, Prostate carcinoma, p53 sequencing, Immunohistochemistry,

BACKGROUND:

The reported frequency of mutation of the p53 tumor suppressor gene in Pca has varied widely, ranging from 3% to 72% in carcinomas of the prostate and 0% to 68% in HPIN (1-7) (8). In the literature there is controversy about the question of whether p53 alteration is an early or late genetic change (1, 6, 7, 9-13). Striking heterogeneity of p53 mutation in prostate cancer has been reported (14) and different mutated alleles were found among multiple tumor foci in single glands (14, 15). p53 has been found to be associated with genomic instability leading to chromosomal rearrangement which in turn has been demonstrated as a feature of many neoplastic and preneoplastic (dysplastic) human epithelia (16-28). The transition from preinvasive disease to invasive carcinoma was shown to be associated with changes in the number of chromosome copy and that coincide with the loss of *TP53* function. Whether there is a role of chromosomal instability in the progression of HPIN foci to invasive cancer and whether is that influenced by heterogeneity in the p53 expression between different HPIN foci is still unknown.

The objectives of this project are: firstly to study the p53 mutation pattern in HPIN foci which are intermingled with cancer and to compare them with different isolated HPIN foci situated in the same gland but away from any cancer foci and secondly, to study the relation between p53 mutation and chromosomal instability in precancerous and malignant prostate epithelium. We have found that HPINI foci tend to have higher incidence of p53 immunoreactivity and CIN than HPINA. We concluded that p53 impaired function at the transition from prostate premalignant stages to invasive

carcinomas is an important cellular event in a subset of Pca that coincides with the acquisition of chromosomal instability known to play a role in the carcinogenesis of Pca.

MATERIAL AND METHODS:

Patients accrual

Tissue samples were obtained from prostate carcinoma resected at Toronto General Hospital and Sunnybrook and Women's College Health Science Center, Toronto, Ontario, Canada. A total of 35 cases were selected based on the presence of HPIN foci intermingled with cancer and HPIN foci separated from cancer with no other cancer foci in the serial blocks superior and inferior to that particular foci.

Immunohistochemistry staining:

Immunohistochemistry was performed on archival formalin fixed paraffin embedded sections (5µm) from prostatectomy specimens containing both prostate carcinoma and HPIN foci. The appropriate control was used. Monoclonal antibody to p53 (DO7 clone; Novocastra Laboratories Ltd., Newcastle, England) was applied using avidin-biotin peroxidase complex (Elite kit; Vector Laboratories, Burlingame, CA). The positive control for p53 immunoreactivity consisted of formalin-fixed sections from an adenocarcinoma of breast and bladder transitional cell carcinoma. Negative internal controls were stromal cells. Immunoreactivity (IR) was categorized semi-quantitatively from 0 to 4+ (0 = no IR, 1+ = 1 % to 10%, 2+ = 11% to 40%, 3+ = 41 % to 70%, 4+ = 71 % to 100%). Staining was defined as positive whenever any specific nuclear brown staining is detected. Any

disagreement in quantification was reviewed by both observers, and a consensus score was agreed upon.

Interphase FISH analysis

Interphase FISH has been performed on 5 micron unstained tissue sections of the same blocks used for the p53 study, using adjacent H&E stained sections as guidance. Directly labeled VYSIS CEP probes for chromosomes 7, 8, X and Y have been used. Paraffin pretreatment and FISH procedure has been performed according to the company instruction (Vysis, Inc., Downers Grove). Dual-probe hybridization has been performed. For each probe 100 nuclei has been counted by each observer. Chromosome X was used as an internal hybridization control for chromosome Y to determine whether any apparent loss of Y was due to inadequate hybridization. The chromosome X signals were not enumerated.

Criteria of Scoring and evaluation of numerical chromosomal anomalies

In preliminary experiments the hybridization efficiency of every probe has been tested on prostate tissues. Slides were evaluated according to the accepted criteria (29). Briefly only sections with hybridization in at least 80% of cells were evaluated. For each probe two independent investigators have counted the number of FISH signals in 200 non-overlapped intact (spherical) interphase nuclei from foci of HPIN. The number of signals per nucleus has been scored as (0,1, 2, 3, 4, and >4) signal per nucleus. Nuclei from stromal element have not been enumerated. Normal and hyperplastic glandular

epithelium present in the biopsies was counted as internal control. Due to truncation of the nuclei, artifact loss of signals is expected; however we have applied very conservative criteria to detect any significant true numeric changes. Our criteria to evaluate numeric chromosomal abnormality is as follows:

- 1) Chromosomal gains have been diagnosed when more than 8% of the nuclei exhibit more than two signals (or one for chromosome Y).
- 2) Chromosomal losses have been diagnosed when more than 50% of the nuclei exhibit a reduction of signal number.
- 3) Tetraploidy has been suspected when the percentage of nuclei with 3 and 4 signals (or 2 for Y chromosome) was similar for both chromosomes 7 and 8. These cutoff values were adopted from the available literature (30-34). In our study as in others, no BPH specimens or normal prostate epithelium contained values that exceeded these criteria.

p53 sequencing

Laser capture microdissection (LCM) and Genomic DNA extraction

LCM has been performed with a Pixcell II Laser Capture Microscope (Arcturus Engineering, Mountain View, CA) in the Ontario Cancer Institute. Tissue (4-5 μ thickness) have been used and foci of choice have been dissected as described (35, 36).

DNA was extracted as previously described (37). DNA has been analyzed for p53 mutation by p53 sequencing method. DNA sequences of p53 (exons 5-9) have been amplified by PCR. sequencing analysis has been done using p53 Mutation Detection GeneKit™ (VISIBLE GENETICS INC, <http://www.visgen.com>) . Each exon has been

sequenced separately using 3 prime primer and those with any abnormality the other 5 prime direction was done to confirm the findings.

STATISTICAL ANALYSIS:

McNemar test was used to examine the difference between HPINA and HPINI in the same gland regarding p53 positivity and numeric chromosomal changes (CIN). Z test was used to analyze the difference between p53+ve and p53-ve HPIN regarding CIN. The same test was used to examine also the difference between p53+ve and p53-ve Pca regarding CIN.

RESULTS:

We identified 35 prostatectomy specimens that have Pca with intermingled HPIN foci and at the same time have HPIN foci that are completely separated from the cancer foci and admixed with benign epithelium (Figure 1). We have performed p53 analyses using immunohistochemistry (DO7) on representative sections of these specimens. Tables 1 summarizes the overall p53 and chromosomal anomalies in Pca, HPINI, HPINA and benign prostate epithelium. Seven cases (20 %) stained positively for p53 in Pca foci (Figure 2A-C). Immunoreactivity in those positive cases was categorized semi-quantitatively as follows: 3 cases as 1+, 2 cases as 2+, and 2 cases as 3+. There was a remarkable similarity between HPINI and Pca in the p53 immunoreactivity since six of those seven cases (86%) also stained positively in the HPINI (Figure 2A-D). None of those 7 cases showed immunoreactivity in the HPINA in the same glands (Figure 2E). None of p53 negative cancers showed positively in the HPIN foci. The normal, atrophic

and hyperplastic tissue situated in the same sections showed negative staining in all the cases (Figure 2F). When this results were compared to pathological findings there was no statistically significant difference between the p53 positive and p53 negative cases regarding Gleason grade, volume of the tumor, perineural invasion, seminal vesicle involvement and lymph nodes metastasis. In 5 out of 7 p53+ve cases, pathological examination showed extraprostatic extension and that finding was seen in 10 patients out of 28 of the p53 negative cases ($P=0.1$). Focal cytoplasmic staining was seen in 4 cases (pt 3,5,11 and 20) in the Pca and HPIN foci and was counted as negative. Focal p53 basal staining has also been seen in about 30% of the cases in the hyperplastic foci but that finding has been found very rarely in HPIN foci. p53 sequencing analysis has been performed for exons 5-9 using a laser captured microdissected specimens from Pca, HPIN foci and benign epithelium (figure 3) from 2 selected patients (one positive and one negative for p53 by IHC). In the patient with p53 immunoreactivity (pt 34), sequencing analysis revealed that the tumor foci harbored point mutation TGT at codon 273 instead of wild-type TGC in the highly conserved transcript region at exon 8 substituting the encoded amino acid from arginine to cystine (Figure 4). The mutation has been confirmed using primers from both 3' and 5' direction. . The other patient (pt 9) with a negative p53 by Immunohistochemistry showed chromosomal instability in cancer foci, so p53 sequencing analysis has been performed on normal foci, HPIN and cancer from that patient to see whether cancer foci harbor termination mutation in p53 which might be missed by Immunohistochemistry. The analysis, however, revealed that all those foci harbor a wild type p53. Our results showed complete concordance between molecular and IHC in all the samples examined. IFISH analysis for chromosomes 7, 8 and Y was

performed to assess chromosomal instability in sections from the same blocks used for IHC analysis. Numeric chromosomal aberrations were found in 27% of HPINI and 47% of Pca (figure 5-6). There were no statistical significant differences in the frequency of chromosomal anomalies between HPINI and Pca and the overall frequencies of numeric chromosomal anomalies between them were similar. Numeric chromosomal aberrations were found in 5/7 and 4/6 of the p53 +ve Pca and p53 +ve HPIN respectively. On the other hand numeric chromosomal abnormality has been seen only in 2/8 of p53-ve Pca and in none of the p53-ve HPIN including both HPIN which intermingled with cancer and those situated away. Gain of chromosome 8 was the most frequent change in both HPIN and Pca followed by gain of chromosome 7. Chromosome Y aneusomy was seen in 2 cases of Pca (Pt 6 as Y chromosome gain and Pt 26 as chromosome Y loss) and in both cases the intermingled HPIN foci showed similar changes. No CIN has been detected in the normal, hyperplastic, or atrophic epithelium. It was interesting to notice occasionally that early stromal invasion, the earliest morphologic indication of carcinomas, occurs at sites of acinar outpouching and basal cell disruption in acini with HPIN

DISCUSSION:

In agreement with other studies (6, 7, 38-42) our result showed that p53 mutation occurs relatively infrequently in Pca (20%) compared to other human cancers like colon, esophagus and lung cancer. P53 mutation was seen more commonly in Pca than HPIN. However, the presence of HPIN foci with positive staining for p53 indicated that in a subset of Pca, the mutation could occur at earlier stage of cancer pathogenesis. Our study

showed heterogeneity of p53 positivity in the HPIN foci in the same gland where foci of HPIN intermingled with p53 positive cancer foci tend to have higher incidence of p53 alteration than isolated HPIN situated away from cancer and admixed with benign epithelium. While 86% of HPINI in p53+ve Pca showed p53 positivity, none of HPINA was positive ($P < 0.05$). That may explain some of the controversy in the literature regarding the incidence of p53 mutation in HPIN. Our study did not show positive nuclear staining in the adjacent normal, hyperplastic or atrophic foci including those tissues adjacent or intermingled with cancer foci in any of the cases. This finding is not in favor of the recently proposed ideas that atrophy may give rise to carcinoma (43).. More than 98% of all p53 mutations are located in exons 5-9 (44, 45). We have performed p53 sequencing analysis for exons 5-9. Sequencing analysis has been performed using a laser captured microdissected specimen from Pca, HPIN foci and benign epithelium. It has been done on a subset of cases (samples from 2 patients) to confirm the IHC finding and the correlation was 100% between the two techniques. We have applied a laser capture microdissection technique which enabled us to dissect very pure Pca and HPIN foci with no contamination. The discrepancies between IHC and PCR-SSCP that has been reported by some reviewer in Pca could be due to contamination by normal tissue or foci without an apparent mutation because of the heterogeneity of Pca. Still, IHC does not detect all alteration that may affect p53 function such as LOH at the p53 locus, nonsense or splice site mutations or amplification of the MDM-2 gene, but all of these are very rare in prostate cancer. Generally a good correlation between p53 alteration detected by IHC and molecular studies has been noted in prostate cancer (4, 7, 42, 46, 47). Hall et al found complete agreement between IHC

and TP53 SSCP analysis. Wertz et al (46) reported 85% overall agreement between the two methods while the concordance was 76.7% by Salem et al (7). In one of our cases a point mutation has been seen at codon 273 changing the amino acid from arginine to cystine. p53 mutation at codon 273 has been described in Pca (10, 48-50). G:C-to-A:T transitions were the most common point mutations (64%) in prostate cancer (10). Six (55%) of 11 G:C-to-A:T transitions occurred at CpG dinucleotides in five hot-spot codons (175, 245, 248, 273, and 282) and it was suggested that specific p53 mutations participate in the progression of human prostate cancer and may be predictive of metastasis (10).

Our study as well as some other recent studies (both *in-vitro* and *in-vivo*) have demonstrated such correlation between loss or mutation of p53 and chromosomal instability (51-61). More recently centrosome hyperamplification was found to be the major mechanism responsible for chromosomal instability *in-vitro* and *in-vivo* (56, 57, 62-64). Centrosome is the major microtubule-organizing center and required for spindle bipolarity, spindle microtubule assembly and balanced segregation of the chromosomes (65). A very strong correlation has been found between p53 loss or mutation and centrosome hyperamplification (25, 53, 57, 65). Breast carcinoma and squamous cell carcinoma of the head and neck with either p53 deletion or mutation, show centrosome hyperamplification (56, 62, 63).

IFISH analysis for chromosomes 7, 8 and Y was performed to assess chromosomal instability. We used these chromosomes to assess CIN because they are the most frequently affected chromosomes in prostate cancer pathogenesis. Although CIN represents generalized changes in the cellular chromosomes, it is selective for certain

chromosomes in carcinogenesis of different organs. Our finding revealed numeric chromosomal aberrations in 5/7 and 2/8 of p53 positive and p53 negatives Pca respectively ($P=0.1$). On the other hand the presence of any numeric chromosomal abnormality has been seen in 4/6 and 0/9 of p53 positive and p53 negative HPIN ($P<0.02$). Generally none of the p53-ve intermingled and away HPIN foci showed any chromosomal abnormality. So generally HPINI tend to have more CIN than those situated away (4/15 vs. 0/15) with statistically significance difference ($P<0.05$). No CIN has been detected in the normal, hyperplastic, or atrophic epithelium and those areas showed no p53 alteration either. This suggest that those HPINI foci may represent the source of the adjacent invasive component while the other isolated HPINA foci which admixed with benign epithelium may still be in the early stages of the carcinogenesis pathway and probably require more CIN to progress to invasive cancer. This also suggested that p53 mutation may play a role in the progression of HPIN to invasive cancer and this could happen through induction of chromosomal instability.

We applied IFISH on sections from the same blocks that have been used for p53 IHC and that enabled us to compare the findings of the two assays in the same foci of tissue.

IFISH has higher sensitivity than other methods used for this purposes such as CGH, which detects copy number changes if they are present in more than 50% of the cell population (19). IFISH can identify CIN in a small subpopulations of interphase cells (66), allowing the detection of infrequent, possibly random changes before they lead to clonal expansion (18). Using IFISH on pretreatment and post anti-androgen therapy prostate cancer specimens, Karashima et al found a remarkable reduction in the number of cells with extra copies of chromosome 7 and 8 (67).

Our IFISH results showed that gain of chromosome 8 is the most frequent finding in both HPIN and Pca. c-Myc gene is located in the 8q arm and gain of chromosome 8 indicated an extra copy of that important oncogene. The role of c-Myc in the mechanism of CIN has been recently described. Extra copies of the c-Myc gene were identified in 52 and 44% of the high-grade PIN and carcinoma foci, respectively (68), and by Mark et al in 31% of Pca [Mark, 2000 #21. In some cancers displaying CIN, the loss of checkpoint was associated with the mutational inactivation of a human homologue of the yeast BUB1 gene. BUB1 controls mitotic checkpoints and chromosome segregation in yeast (69). Disruption of the mitotic spindle checkpoint is one of the underlying mechanisms leading to aneuploidy and alterations of hsMAD2 and hBUB1. This mechanism, assumed to take part in the spindle checkpoint in human cells, has been found to be associated with chromosomal instability in some tumor cell lines (8). However there is no study on these genes in prostate tumors. Other possible mechanisms may be involved in the causation of CIN such as shortened telomeres, hypomethylation, activation of certain genes or inactivation of tumor suppressor genes.

CONCLUSION

We demonstrated that p53 mutation is an early change in at least a subset of Pca. HPINI foci tend to have higher overall p53 immunoreactivity and CIN than HPINA. The presence of p53 mutation in HPIN was associated with the presence of chromosomal instability as determined by IFISH. Also our study provided additional evidence in support of the concept that HPIN is the earliest precursor of cancer. Furthermore our studies identify genomic similarities in HPINI and Pca, implying that carcinoma may arise from progression of certain HPIN foci that most likely harbor p53 mutation and/or more CIN.

ACKNOWLEDGEMENTS

We would like to thank our lab members; Khladoun Alromaih, Ben Beheshti, Zong Zhang, Bisera Vukovic, Paula Marrano, Jana Karaskova, Paul Park, Elena Kolomietz and Jane Bayani for their contribution to achieve this work. We would like to acknowledge also VISIBLE GENETICS INC for providing the reagents for p53 sequencing. Financial support for this project is funded by the U.S. Army Medical Research and Material Command (USAMRMC) Prostate Cancer Research Program (PCRP).

References

1. Tamboli P, Amin MB, Xu HJ, Linden MD. Immunohistochemical expression of retinoblastoma and p53 tumor suppressor genes in prostatic intraepithelial neoplasia: comparison with prostatic adenocarcinoma and benign prostate. *Mod Pathol* 1998;11(3):247-52.
2. Gumerlock PH, Chi SG, Shi XB, Voeller HJ, Jacobson JW, Gelmann EP, et al. p53 abnormalities in primary prostate cancer: single-strand conformation polymorphism analysis of complementary DNA in comparison with genomic DNA. The Cooperative Prostate Network. *J Natl Cancer Inst* 1997;89(1):66-71.
3. Heidenberg HB, Bauer JJ, McLeod DG, Moul JW, Srivastava S. The role of the p53 tumor suppressor gene in prostate cancer: a possible biomarker? *Urology* 1996;48(6):971-9.
4. Navone NM, Troncoso P, Pisters LL, Goodrow TL, Palmer JL, Nichols WW, et al. p53 protein accumulation and gene mutation in the progression of human prostate carcinoma. *J Natl Cancer Inst* 1993;85(20):1657-69.
5. Thomas DJ, Robinson M, King P, Hasan T, Charlton R, Martin J, et al. p53 expression and clinical outcome in prostate cancer. *Br J Urol* 1993;72(5 Pt 2):778-81.
6. Yasunaga Y, Shin M, Fujita MQ, Nonomura N, Miki T, Okuyama A, et al. Different patterns of p53 mutations in prostatic intraepithelial neoplasia and concurrent carcinoma: analysis of microdissected specimens. *Lab Invest* 1998;78(10):1275-9.

7. Salem CE, Tomasic NA, Elmajian DA, Esrig D, Nichols PW, Taylor CR, et al. p53 protein and gene alterations in pathological stage C prostate carcinoma [see comments]. *J Urol* 1997;158(2):510-4.
8. Imai Y, Shiratori Y, Kato N, Inoue T, Omata M. Mutational inactivation of mitotic checkpoint genes, hSMAD2 and hBUB1, is rare in sporadic digestive tract cancers. *Jpn J Cancer Res* 1999;90(8):837-40.
9. Massenkeil G, Oberhuber H, Hailemariam S, Sulser T, Diener PA, Bannwart F, et al. P53 mutations and loss of heterozygosity on chromosomes 8p, 16q, 17p, and 18q are confined to advanced prostate cancer. *Anticancer Res* 1994;14(6B):2785-90.
10. Navone NM, Labate ME, Troncoso P, Pisters LL, Conti CJ, von Eschenbach AC, et al. p53 mutations in prostate cancer bone metastases suggest that selected p53 mutants in the primary site define foci with metastatic potential. *J Urol* 1999;161(1):304-8.
11. Stricker HJ, Jay JK, Linden MD, Tamboli P, Amin MB. Determining prognosis of clinically localized prostate cancer by immunohistochemical detection of mutant p53. *Urology* 1996;47(3):366-9.
12. Cheng L, Leibovich BC, Bergstralh EJ, Scherer BG, Pacelli A, Ramnani DM, et al. p53 alteration in regional lymph node metastases from prostate carcinoma: a marker for progression? *Cancer* 1999;85(11):2455-9.
13. Meyers FJ, Gumerlock PH, Chi SG, Borchers H, Deitch AD, deVere White RW. Very frequent p53 mutations in metastatic prostate carcinoma and in matched primary tumors. *Cancer* 1998;83(12):2534-9.

14. Mirchandani D, Zheng J, Miller GJ, Ghosh AK, Shibata DK, Cote RJ, et al. Heterogeneity in intratumor distribution of p53 mutations in human prostate cancer. *Am J Pathol* 1995;147(1):92-101.
15. MacGrogan D, Bookstein R. Tumour suppressor genes in prostate cancer. *Semin Cancer Biol* 1997;8(1):11-9.
16. Veltman JA, Hopman AH, van der Vlies SA, Bot FJ, Ramaekers FC, Manni JJ. Double-target fluorescence in situ hybridization distinguishes multiple genetically aberrant clones in head and neck squamous cell carcinoma. *Cytometry* 1998;34(3):113-20.
17. Veltman JA, Bot FJ, Huynen FC, Ramaekers FC, Manni JJ, Hopman AH. Chromosome instability as an indicator of malignant progression in laryngeal mucosa. *J Clin Oncol* 2000;18(8):1644-51.
18. Rabinovitch PS, Dziadon S, Brentnall TA, Emond MJ, Crispin DA, Haggitt RC, et al. Pancolonic chromosomal instability precedes dysplasia and cancer in ulcerative colitis. *Cancer Res* 1999;59(20):5148-53.
19. Ried T, Heselmeyer-Haddad K, Blegen H, Schrock E, Auer G. Genomic changes defining the genesis, progression, and malignancy potential in solid human tumors: a phenotype/genotype correlation. *Genes Chromosomes Cancer* 1999;25(3):195-204.
20. Burt EC, James LA, Greaves MJ, Birch JM, Boyle JM, Varley JM. Genomic alterations associated with loss of heterozygosity for TP53 in Li-Fraumeni syndrome fibroblasts. *Br J Cancer* 2000;83(4):467-72.

21. Hawkins NJ, Gorman P, Tomlinson IP, Bullpitt P, Ward RL. Colorectal carcinomas arising in the hyperplastic polyposis syndrome progress through the chromosomal instability pathway. *Am J Pathol* 2000;157(2):385-92.
22. Shackney SE, Shankey TV. Common patterns of genetic evolution in human solid tumors. *Cytometry* 1997;29(1):1-27.
23. Williams AC, Miller JC, Collard T, Browne SJ, Newbold RF, Paraskeva C. The effect of different TP53 mutations on the chromosomal stability of a human colonic adenoma derived cell line with endogenous wild type TP53 activity, before and after DNA damage. *Genes Chromosomes Cancer* 1997;20(1):44-52.
24. Yasui W, Yokozaki H, Fujimoto J, Naka K, Kuniyasu H, Tahara E. Genetic and epigenetic alterations in multistep carcinogenesis of the stomach. *J Gastroenterol* 2000;35(Suppl 12):111-5.
25. Tarapore P, Fukasawa K. p53 mutation and mitotic infidelity. *Cancer Invest* 2000;18(2):148-55.
26. Kirchhoff M, Rose H, Petersen BL, Maahr J, Gerdes T, Lundsteen C, et al. Comparative genomic hybridization reveals a recurrent pattern of chromosomal aberrations in severe dysplasia/carcinoma in situ of the cervix and in advanced-stage cervical carcinoma. *Genes Chromosomes Cancer* 1999;24(2):144-50.
27. Mian C, Bancher D, Kohlberger P, Kainz C, Haitel A, Czerwenka K, et al. Fluorescence in situ hybridization in cervical smears: detection of numerical aberrations of chromosomes 7, 3, and X and relationship to HPV infection. *Gynecol Oncol* 1999;75(1):41-6.

28. Aubele M, Zitzelsberger H, Schenck U, Walch A, Hofler H, Werner M. Distinct cytogenetic alterations in squamous intraepithelial lesions of the cervix revealed by laser-assisted microdissection and comparative genomic hybridization. *Cancer* 1998;84(6):375-9.
29. Henke RP, Kruger E, Ayhan N, Hubner D, Hammerer P. Frequency and distribution of numerical chromosomal aberrations in prostatic cancer. *Hum Pathol* 1994;25(5):476-84.
30. Qian J, Bostwick DG, Takahashi S, Borell TJ, Brown JA, Lieber MM, et al. Comparison of fluorescence in situ hybridization analysis of isolated nuclei and routine histological sections from paraffin-embedded prostatic adenocarcinoma specimens. *Am J Pathol* 1996;149(4):1193-9.
31. Erbersdobler A, Bardenhagen P, Henke RP. Numerical chromosomal anomalies in latent adenocarcinomas of the prostate. *Prostate* 1999;38(2):92-9.
32. Erbersdobler A, Gurses N, Henke RP. Numerical chromosomal changes in high-grade prostatic intraepithelial neoplasia (PIN) and concomitant invasive carcinoma. *Pathol Res Pract* 1996;192(5):418-27.
33. Aubele M, Zitzelsberger H, Szucs S, Werner M, Braselmann H, Hutzler P, et al. Comparative FISH analysis of numerical chromosome 7 abnormalities in 5- micron and 15-micron paraffin-embedded tissue sections from prostatic carcinoma. *Histochem Cell Biol* 1997;107(2):121-6.
34. Qian J, Bostwick DG, Takahashi S, Borell TJ, Herath JF, Lieber MM, et al. Chromosomal anomalies in prostatic intraepithelial neoplasia and carcinoma detected by fluorescence in situ hybridization. *Cancer Res* 1995;55(22):5408-14.

35. Ornstein DK, Englert C, Gillespie JW, Paweletz CP, Linehan WM, Emmert-Buck MR, et al. Characterization of intracellular prostate-specific antigen from laser capture microdissected benign and malignant prostatic epithelium. *Clin Cancer Res* 2000;6(2):353-6.
36. Emmert-Buck MR, Bonner RF, Smith PD, Chuaqui RF, Zhuang Z, Goldstein SR, et al. Laser capture microdissection [see comments]. *Science* 1996;274(5289):998-1001.
37. Ehrig T, Abdulkadir SA, Dintzis SM, Milbrandt J, Watson MA. Quantitative amplification of genomic DNA from histological tissue sections after staining with nuclear dyes and laser capture microdissection. *J Mol Diagn* 2001;3(1):22-5.
38. Yang G, Stapleton AM, Wheeler TM, Truong LD, Timme TL, Scardino PT, et al. Clustered p53 immunostaining: a novel pattern associated with prostate cancer progression. *Clin Cancer Res* 1996;2(2):399-401.
39. Ruijter E, van de Kaa C, Aalders T, Ruiter D, Miller G, Debruyne F, et al. Heterogeneous expression of E-cadherin and p53 in prostate cancer: clinical implications. BIOMED-II Markers for Prostate Cancer Study Group. *Mod Pathol* 1998;11(3):276-81.
40. Schlechte HH, Schnorr D, Loning T, Rudolph BD, Pohrt UM, Loening SA. Mutation of the tumor suppressor gene p53 in human prostate and bladder cancers-- investigation by temperature gradient gel electrophoresis (TGGE). *J Urol* 1997;157(3):1049-53.
41. Stattin P, Bergh A, Karlberg L, Nordgren H, Damber JE. p53 immunoreactivity as prognostic marker for cancer-specific survival in prostate cancer. *Eur Urol* 1996;30(1):65-72.

42. Hall MC, Navone NM, Troncoso P, Pollack A, Zagars GK, von Eschenbach AC, et al. Frequency and characterization of p53 mutations in clinically localized prostate cancer. *Urology* 1995;45(3):470-5.
43. De Marzo AM, Marchi VL, Epstein JI, Nelson WG. Proliferative inflammatory atrophy of the prostate: implications for prostatic carcinogenesis. *Am J Pathol* 1999;155(6):1985-92.
44. Levine AJ, Momand J, Finlay CA. The p53 tumour suppressor gene. *Nature* 1991;351(6326):453-6.
45. Hollstein M, Sidransky D, Vogelstein B, Harris CC. p53 mutations in human cancers. *Science* 1991;253(5015):49-53.
46. Wertz IE, Deitch AD, Gumerlock PH, Gandour-Edwards R, Chi SG, de Vere White RW. Correlation of genetic and immunodetection of TP53 mutations in malignant and benign prostate tissues. *Hum Pathol* 1996;27(6):573-80.
47. Jacquemier J, Moles JP, Penault-Llorca F, Adelaide J, Torrente M, Viens P, et al. p53 immunohistochemical analysis in breast cancer with four monoclonal antibodies: comparison of staining and PCR-SSCP results. *Br J Cancer* 1994;69(5):846-52.
48. Carroll AG, Voeller HJ, Sugars L, Gelmann EP. p53 oncogene mutations in three human prostate cancer cell lines. *Prostate* 1993;23(2):123-34.
49. Dinjens WN, van der Weiden MM, Schroeder FH, Bosman FT, Trapman J. Frequency and characterization of p53 mutations in primary and metastatic human prostate cancer. *Int J Cancer* 1994;56(5):630-3.
50. Kunimi K, Amano T, Uchibayashi T. Point mutation of the p53 gene is an infrequent event in untreated prostate cancer. *Cancer Detect Prev* 1996;20(3):218-22.

51. Yin XY, Grove L, Datta NS, Long MW, Prochownik EV. C-myc overexpression and p53 loss cooperate to promote genomic instability. *Oncogene* 1999;18(5):1177-84.
52. Kanekawa A, Tsuji T, Oga A, Sasaki K, Shinozaki F. Chromosome 17 abnormalities in squamous cell carcinoma of the oral cavity, and its relationship with p53 and Bcl-2 expression. *Anticancer Res* 1999;19(1A):81-6.
53. Eshleman JR, Casey G, Kochera ME, Sedwick WD, Swinler SE, Veigl ML, et al. Chromosome number and structure both are markedly stable in RER colorectal cancers and are not destabilized by mutation of p53. *Oncogene* 1998;17(6):719-25.
54. Kohno H, Hiroshima K, Toyozaki T, Fujisawa T, Ohwada H. p53 mutation and allelic loss of chromosome 3p, 9p of preneoplastic lesions in patients with nonsmall cell lung carcinoma. *Cancer* 1999;85(2):341-7.
55. Albertoni M, Daub DM, Arden KC, Viars CS, Powell C, Van Meir EG. Genetic instability leads to loss of both p53 alleles in a human glioblastoma. *Oncogene* 1998;16(3):321-6.
56. Carroll PE, Okuda M, Horn HF, Biddinger P, Stambrook PJ, Gleich LL, et al. Centrosome hyperamplification in human cancer: chromosome instability induced by p53 mutation and/or Mdm2 overexpression. *Oncogene* 1999;18(11):1935-44.
57. Fukasawa K, Wiener F, Vande Woude GF, Mai S. Genomic instability and apoptosis are frequent in p53 deficient young mice. *Oncogene* 1997;15(11):1295-302.
58. Agapova LS, Ilyinskaya GV, Turovets NA, Ivanov AV, Chumakov PM, Kopnin BP. Chromosome changes caused by alterations of p53 expression. *Mutat Res* 1996;354(1):129-38.

59. Smith ML, Fornace AJ, Jr. Genomic instability and the role of p53 mutations in cancer cells. *Curr Opin Oncol* 1995;7(1):69-75.
60. Donehower LA, Godley LA, Aldaz CM, Pyle R, Shi YP, Pinkel D, et al. Deficiency of p53 accelerates mammary tumorigenesis in Wnt-1 transgenic mice and promotes chromosomal instability. *Genes Dev* 1995;9(7):882-95.
61. Bouffler SD, Kemp CJ, Balmain A, Cox R. Spontaneous and ionizing radiation-induced chromosomal abnormalities in p53-deficient mice. *Cancer Res* 1995;55(17):3883-9.
62. Lingle WL, Lutz WH, Ingle JN, Maihle NJ, Salisbury JL. Centrosome hypertrophy in human breast tumors: implications for genomic stability and cell polarity. *Proc Natl Acad Sci U S A* 1998;95(6):2950-5.
63. Pihan GA, Purohit A, Wallace J, Knecht H, Woda B, Quesenberry P, et al. Centrosome defects and genetic instability in malignant tumors. *Cancer Res* 1998;58(17):3974-85.
64. Ghadimi BM, Sackett DL, Difilippantonio MJ, Schrock E, Neumann T, Jauho A, et al. Centrosome amplification and instability occurs exclusively in aneuploid, but not in diploid colorectal cancer cell lines, and correlates with numerical chromosomal aberrations. *Genes Chromosomes Cancer* 2000;27(2):183-90.
65. Fukasawa K, Choi T, Kuriyama R, Rulong S, Vande Woude GF. Abnormal centrosome amplification in the absence of p53. *Science* 1996;271(5256):1744-7.
66. Lengauer C, Kinzler KW, Vogelstein B. Genetic instability in colorectal cancers. *Nature* 1997;386(6625):623-7.

67. Karashima T, Taguchi T, Yoshikawa C, Kamada M, Kasahara K, Yuri K, et al. Numerical chromosomal changes in metastatic prostate cancer following anti-androgen therapy: fluorescence in situ hybridization analysis of 5 Japanese cases. *Cancer Genet Cytogenet* 2000;120(2):148-54.
68. Qian J, Jenkins RB, Bostwick DG. Detection of chromosomal anomalies and c-myc gene amplification in the cribriform pattern of prostatic intraepithelial neoplasia and carcinoma by fluorescence in situ hybridization. *Mod Pathol* 1997;10(11):1113-9.
69. Cahill DP, Lengauer C, Yu J, Riggins GJ, Willson JK, Markowitz SD, et al. Mutations of mitotic checkpoint genes in human cancers [see comments]. *Nature* 1998;392(6673):300-3.

	Pca (%)	HPINI	HPINA	NORMAL
TOTAL	35	35	35	35
P53+ (n:35)	7(20)	6(17.1)	0(0)	0(0)
CIN+ (n:15)	7(47)	4(27)	0(0)	0(0)
P53+/CIN+	5	4	0	0
P53+/CIN-	2	2	0	0
P53-/CIN+	2	0	0	0
P53-/CIN-	6	9	15	15

Table 1: Summary of the p53 and interphase FISH results
on prostatectomy specimens.

Legends

Figure 1:A-D: H&E sections show foci of HPIN (blue arrow) intermingled with invasive cancer (green arrow), E: H&E section of HPIN surrounded by benign epithelium. F: is a higher power, HPIN foci (blue arrow) and benign epithelium in the lower part of the image

Figure 2: p53 immunohistochemistry (DO7). A: show positive nuclear staining in invasive cancer (green arrow) and in the adjacent HPIN (yellow arrow). B shows positivity in cancer gland. C shows another case with the same features. The blue arrow show vessels used as a negative control. D: is a high power. E: show HPIN away from cancer with negative staining in the same gland A. F: Negative staining in a hyperplastic epithelium

Figure 3: p53 sequencing analysis show in the top picture a normal sequence of exon 8, the middle picture show a wild type p53 (pt9), the bottom picture show a mutated p53 with a change in codon 273, changing the wild type TGC to TGT and changing the amino acid from arginine to cystine.

Figure 4: H&E sections show an example of laser capture microdissection (LCM). Dissection of benign epithelium on the left side and of HPIN on the right side. The top pictures represent the tissue before dissection, the middle pictures are after dissection and

the bottom pictures are the cap tissues, which were used for p53, automated sequencing analysis.

Figure 5: Interphase FISH on a focus of invasive prostate carcinoma using dual centromere probes. Some cells (white arrow heads) show more than 2 green and more than 2 red signals consistent with a gain of chromosome 7 and 8. The yellow arrowhead show cells with 2 green and 1 red signals.

Figure 6: Interphase FISH on a focus of invasive prostate carcinoma using dual probes. Some cells (white arrow heads) show 3 green signals and 4 red signals consist with a gain of chromosome 7 and 8. Other cells (yellow arrow head) show only one red and one green signal.

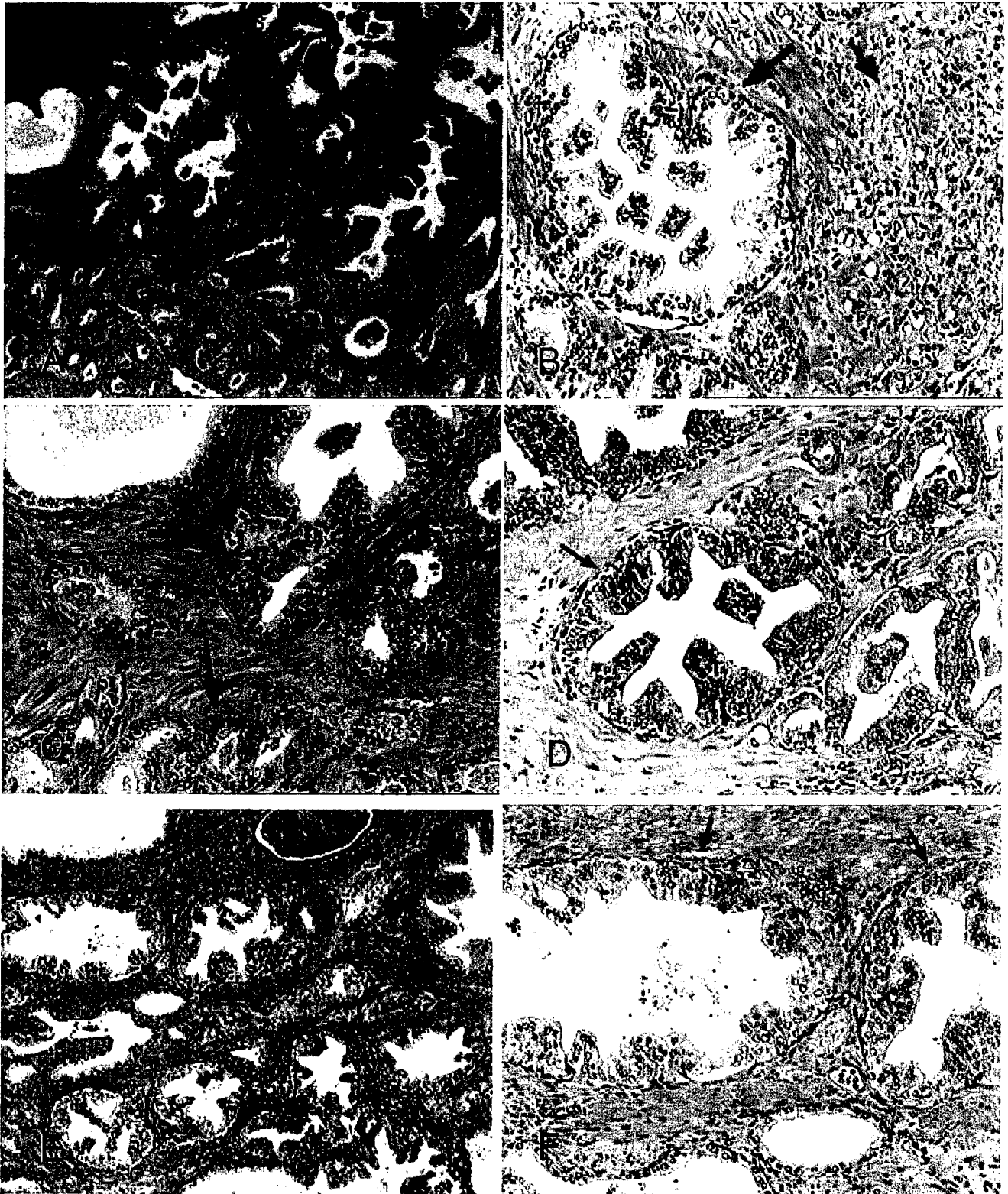


Figure 1:A-D: H&E sections show foci of HPIN (blue arrow) intermingled with invasive cancer (green arrow), E: H&E section of HPIN surrounded by benign epithelium. F: is a higher power, HPIN foci (blue arrow) and benign epithelium in the lower part of the image

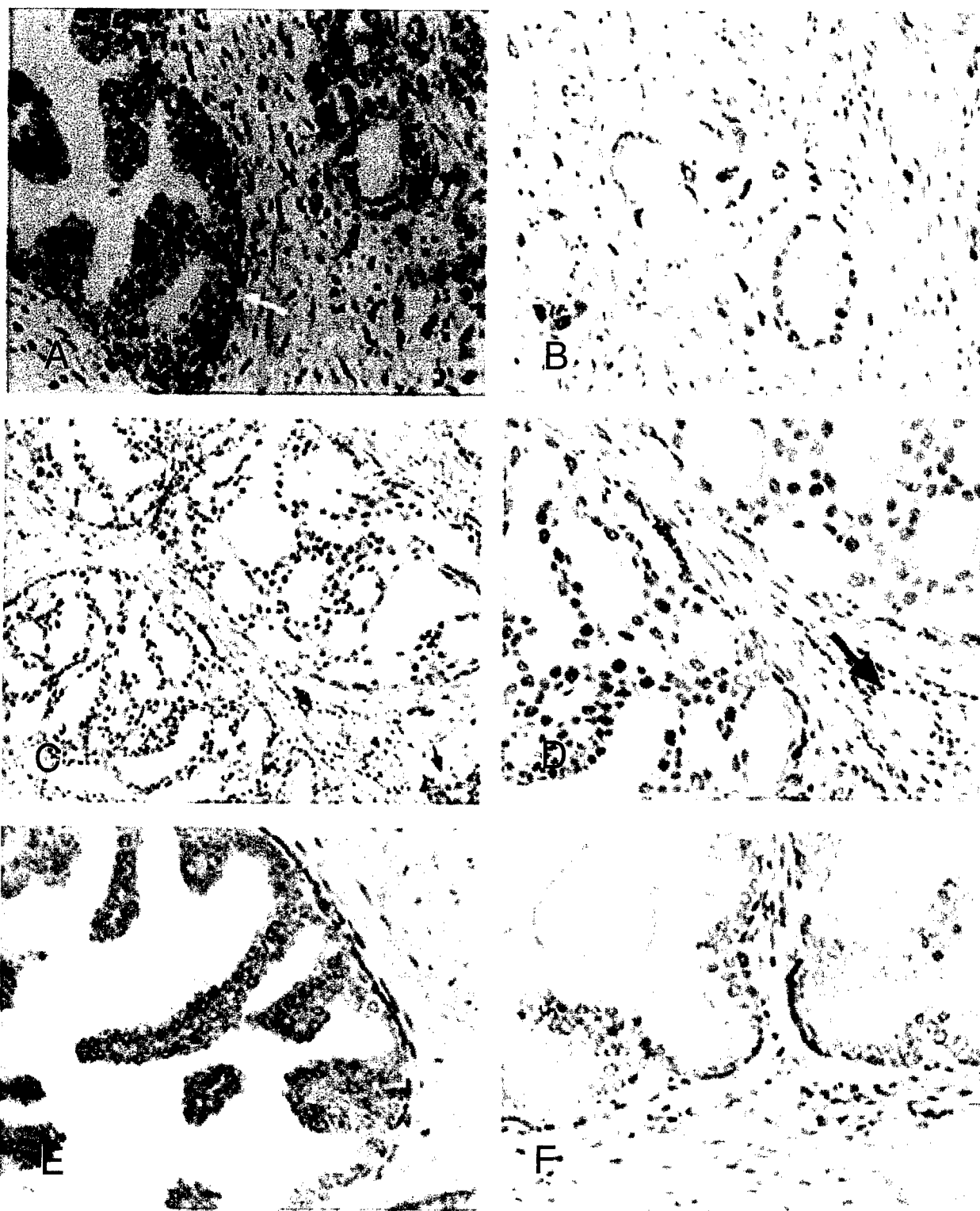


Figure 2: p53 immunohistochemistry (DO7). A: show positive nuclear staining in invasive cancer (green arrow) and in the adjacent HPIN (yellow arrow). B shows positivity in cancer gland. C shows another case with the same features. The blue arrow show vessels used as a negative control. D: is a high power. E: show HPIN away from cancer with negative staining in the same gland A. F: Negative staining in a hyperplastic epithelium

Normal exon 8
sequence

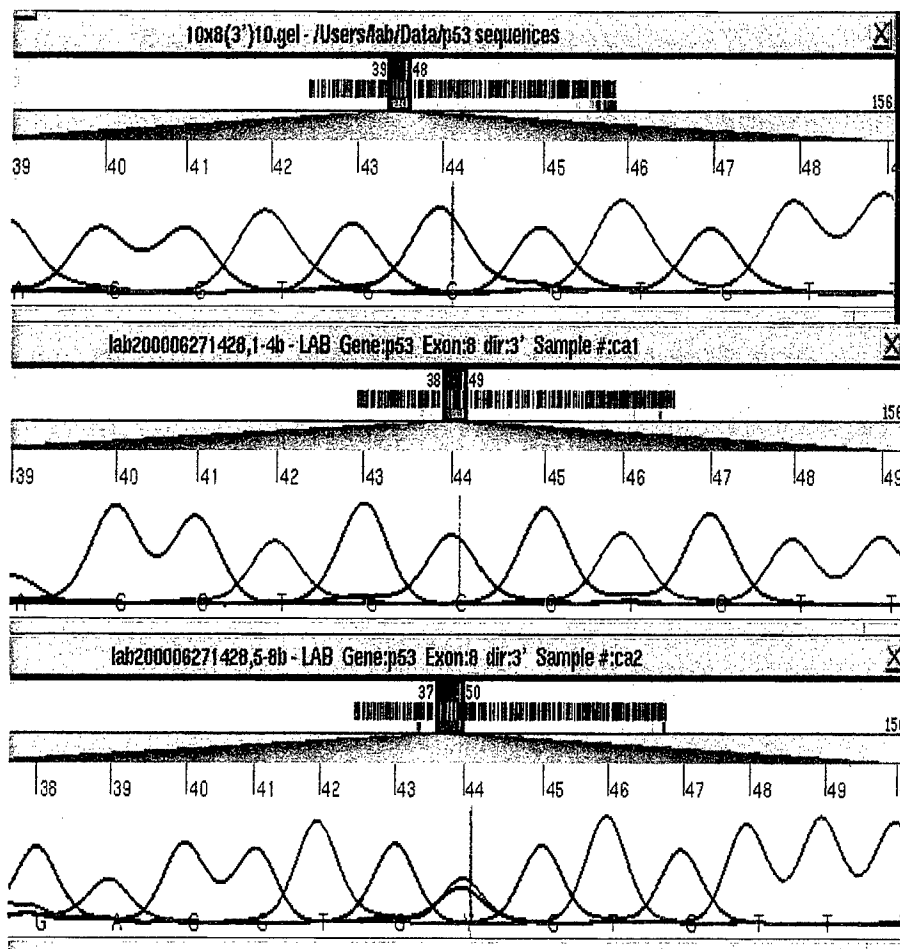


Figure 3: p53 sequencing analysis show in the top picture a normal sequence of exon 8, the middle picture show a wild type p53 (pt9), the bottom picture show a mutated p53 with a change in codon 273, changing the wild type TGC to TGT and changing the amino acid from arginine to cystine. The corresponding immunohistochemistry for p53 is on the left side.

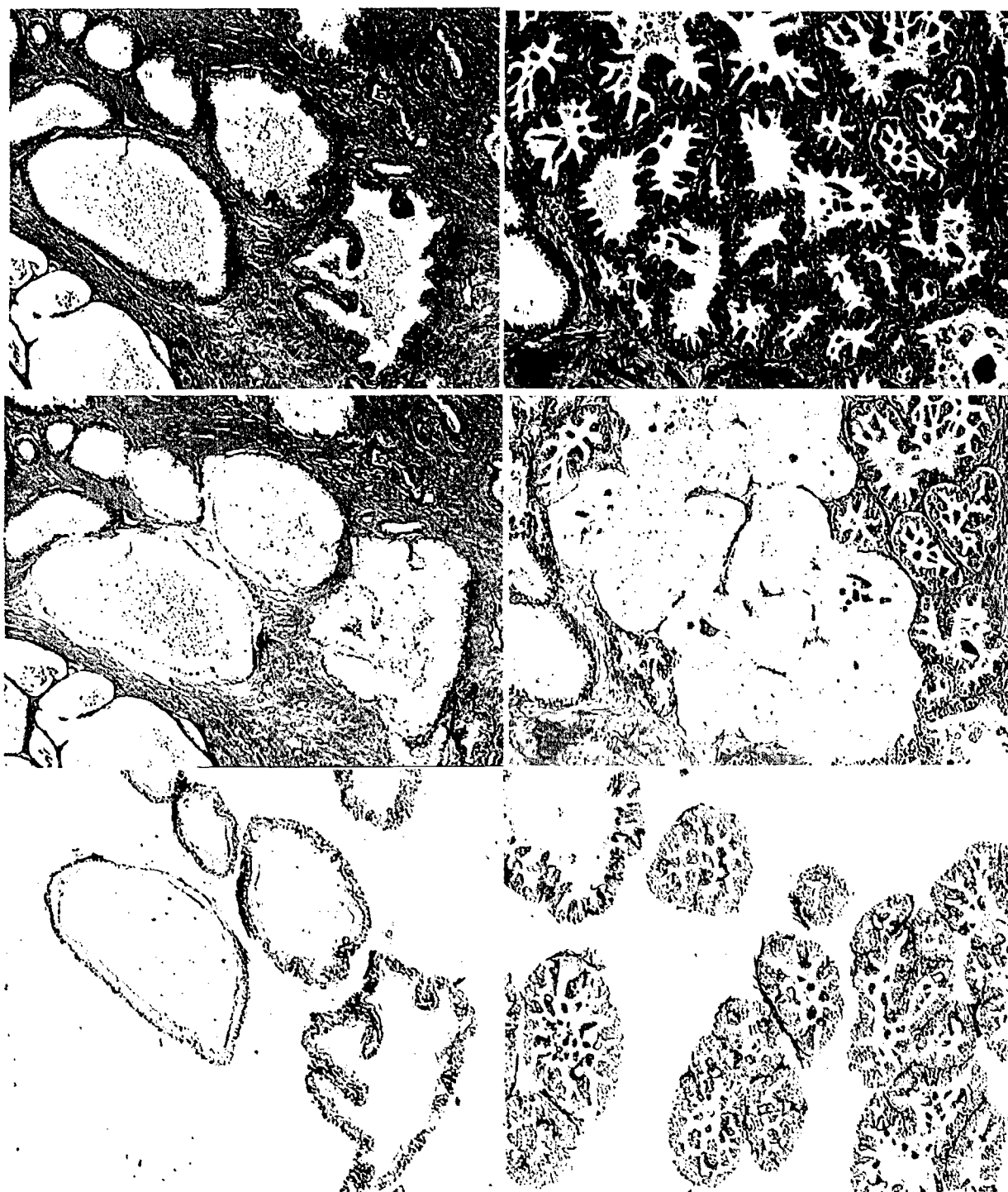


Figure 4: H&E sections show an example of laser capture microdissection (LCM). Dissection of benign epithelium on the left side and of HPIN on the right side. The top pictures represent the tissue before dissection, the middle pictures are after dissection and the bottom pictures are the cap tissues, which were used for p53, automated sequencing analysis.

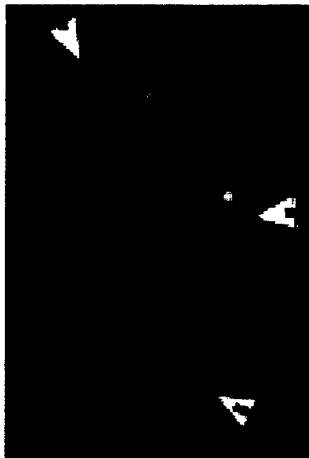
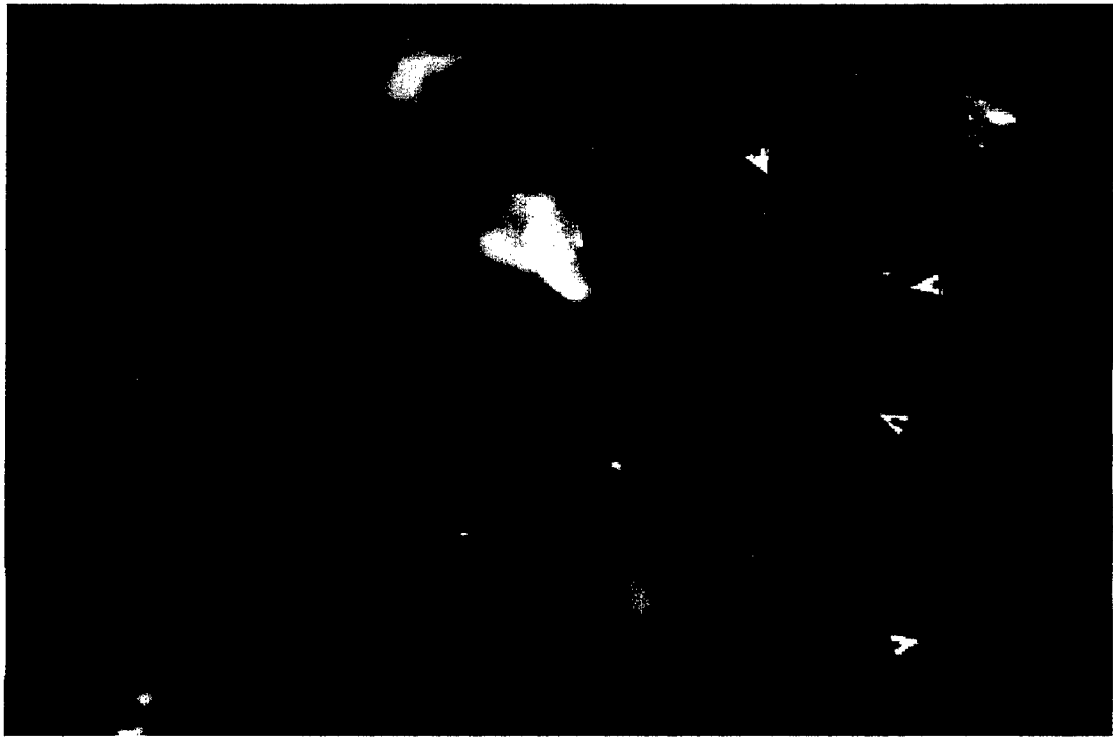


Figure 5: Interphase FISH on a focus of invasive prostate carcinoma using dual centromere probes. Some cells (white arrow heads) show more than 2 green and more than 2 red signals consistent with a gain of chromosome 7 and 8. The yellow arrowhead show cells with 2 green and 1 red signals.

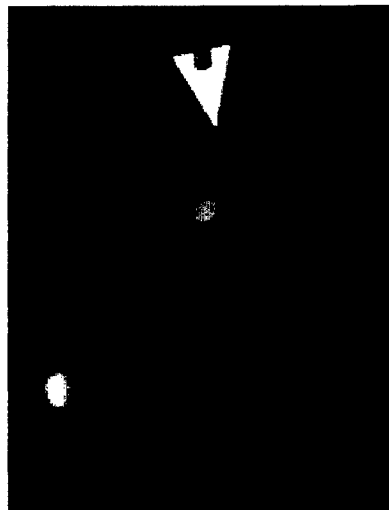


Figure 6: Interphase FISH on a focus of invasive prostate carcinoma using dual probes. Some cells (white arrow heads) show 3 green signals and 4 red signals consist with a gain of chromosome 7 and 8. Other cells (yellow arrow head) show only one red and one green signal.

Identification of numerical chromosomal changes detected by interphase FISH in high-grade prostrate intraepithelial neoplasia (HPIN) as a predictor of carcinoma.

Jaudah Al-Maghrabi MD FRCPC^{1,2,4,5,7}, Lada Vorobyova MD^{1,2,4,5}, A. Toi MD FRCPC,⁷ William Chapman MD FRCPC^{1,2,4,5}, Maria Zielenska PhD⁸, Jeremy A. Squire PhD¹⁻⁶

Ontario Cancer Institute¹, Princess Margaret Hospital², Toronto General Hospital³, University Health Network⁴, Department of Laboratory Medicine and Pathobiology⁵, Medical Biophysics⁶, and Radiology⁷, Department of Pathology, Hospital for Sick Children⁸, Faculty of Medicine, University of Toronto, Toronto, Ontario, Canada

Address for correspondence:

J.A. Squire Ph.D.

Division of Cellular and Molecular Biology

Ontario Cancer Institute

Princess Margaret Hospital

610 University Avenue

Room 9-721

Toronto, Ontario

M5G 2M9

tel. 416-946-4509

fax 416-920-5413

e-mail: jeremy.squire@utoronto

ABSTRACT

Context: HPIN is the most likely precursor of prostate cancer. Many patients with a diagnosis of HPIN in prostate needle core biopsy could, if left untreated, progress to invasive cancer. Currently there is no available clinical, immunohistochemical or morphological criteria that are predictive of this progression.

Objective: To determine whether chromosomal instability in these precursor lesions could increase its predictive value for cancer detection.

Design: Dual-color interphase *in situ* hybridization (IFISH) analysis was performed on archived prostate needle core biopsies from 54 patients with initial diagnosis of isolated HPIN and follow-up of 3 years or more. We utilized commercially available centromere probes for chromosomes 4, 7, 8, 10. We had interpretable results in 44 patents as follows: 1) group A: 24 HPIN patients with persistent HPIN and/or benign lesions in the follow-up biopsies, and 2) group B: 20 HPIN patients with progression to prostate carcinoma.

Results: Twenty five percent of the patients in group B displayed numerical chromosomal aberrations. Only 8.3 % of the patients from group A had chromosomal abnormalities ($P=0.1$). The overall chromosomal changes in HPIN were higher than normal or hyperplastic epithelium with statistically significant difference ($P<0.05$). All aberrations were detected in the form of chromosomal gain. Overall, the commonest aberration was gain of chromosome 8, followed by gains of chromosomes 7 and 10.

Conclusion: These results indicated that while no single numeric chromosomal abnormality could be assigned as a predictor of HPIN progression to carcinoma, the

overall level of numeric chromosomal abnormalities show a trend of elevation in HPIN patients that subsequently progressed to carcinoma.

Key words: Chromosomal instability, *in situ* hybridization, prostate intraepithelial neoplasia, Prostate carcinoma.

BACKGROUND

Prostatic intraepithelial neoplasia (PIN) is characterized by intraluminal proliferation of epithelial cells and can be divided into high-grade (HPIN) and low-grade (LPIN) lesions. HPIN is the earliest accepted stage in prostatic carcinogenesis. HPIN is regarded as the most likely precursor for Pca¹. The greatest value of PIN is high predictive value as a marker for Pca. This is particularly true for high grade PIN (HPIN). If this lesion is identified, close surveillance and follow-up biopsy are indicated². HPIN diagnosed in a prostate needle core biopsies of many patients, if left untreated could progress to invasive carcinoma. HPIN, when diagnosed in needle biopsy, is a powerful predictor of carcinoma in subsequent needle biopsy. No clinical or pathological parameter has been found to be helpful for distinguishing patients who had carcinoma on the next biopsy from those who did not. Chromosomal instability (CIN) is a high frequency of chromosomal loss and gain. It is a type of genomic instability, which has been introduced recently to the field of human cancer biology^{3, 4}. Recently CIN has been described in many human dysplastic lesions and that was proposed as a marker of progression to cancer and considered as a primary event in neoplastic transformation⁵⁻¹⁵. Whether chromosomal instability in HPIN can provide additional predictive information for early cancer progression is still unknown. The objective of this project was to examine if CIN can increase the predictive value of HPIN diagnosis by using interphase FISH applied on prostate biopsies with a diagnosis of HPIN only.

MATERIAL AND METHOD

Patient accrual

Between 1995-1997 in the record of The University Health Network, we had identified 123 patients with HPIN as the primary diagnosis in prostate needle core biopsies and we compared them with 100 patients with HPIN associated with invasive cancer simultaneously. HPIN associated with cancer was designated as (1st group) and isolated HPIN designated as (2nd group). The 2nd group has been divided as follows:

A) Group A: patients with HPIN as a primary diagnosis in prostatic biopsies and did not show evidence of carcinoma on subsequent follow-up biopsies.

B) Group B: patients with HPIN as a primary diagnosis in prostatic biopsies and did show invasive carcinoma on subsequent biopsies.

The clinical was reviewed for all the patients including age, PSA level, digital rectal examination (DRE) and transrectal ultrasound examination (TRUS). For the interphase FISH, 30 patents from group A and 24 patents from group B have been matched for age, PSA level (table2) IFISH has been performed only on the initial biopsies.

Materials and methods

All the H&E slides of the cases diagnosed as HPIN were reviewed by 2 pathologists to confirm the diagnosis and to determine the adequacy of the specimen for FISH analysis. Only those with sufficient material were included in the study. Interphase FISH was performed on 5 micron unstained tissue sections using adjacent H&E stained sections as guidance. The appropriate section was chosen. Directly labeled VYSIS CEP probes for chromosomes 4, 7, 8, and 10 were used. Paraffin pretreatment and FISH procedure was

performed according to the company instruction (Vysis, Inc., Downers Grove). Dual-probe hybridization was performed. For each probe 100 nuclei were counted by each observer. Ten of the cases could not be interpreted either due to poor hybridization, fluorescence background, or the decrease in size and subsequent disappearance of the HPIN foci on the deeper sections. In 10 cases only 75-99 nuclei have been counted at least by one observer.

Criteria of scoring and evaluation of numerical chromosomal anomalies

In preliminary experiments the hybridization efficiency of every probe was tested on prostate tissues. Slides were evaluated according to the accepted criteria ¹⁶. Briefly only sections with hybridization in at least 80% of cells were evaluated. For each probe two independent investigators counted the number of FISH signals in 100 non-overlapped intact (spherical) interphase nuclei from foci of HPIN. The number of signals per nucleus were scored as (0,1, 2, 3, 4, and >4) signal per nucleus. Nuclei from stromal element were not enumerated. FISH by using a centromere probe for chromosome 4 was used as a negative control. Normal and hyperplastic glandular epithelium present in the biopsies was counted as an internal control. Due to truncation of the nuclei, artifactual loss of signals is expected; however we applied very conservative criteria to detect any significant true numeric changes. For the control cases using chromosome 8centromere probe, the mean + 3 SD percentage of nuclei with 3 or more signals was 4.6 % and the mean + 3 SD percentage of nuclei with zero or 1 signals was 44.5%. Our criteria to evaluate numeric chromosomal abnormality was as follows:

- 1) Chromosomal gains were diagnosed when more than 4.6% of the nuclei exhibited

more than two signals.

2) Chromosomal loss was been diagnosed when more than 44.6% of the nuclei exhibited a reduction of signal number.

3) Tetraploidy was assumed when all chromosomes investigated showed signal gains up to four. These cutoff values were close to others¹⁷⁻²⁰.

STATISTICAL ANALYSIS:

Fisher's exact test was used to examine the difference between group A and group B regarding the presence of numeric chromosomal changes. The same test was used to analyze the difference between group1 and group2 as well as between group A and group B regarding PSA level, digital rectal examination and ultrasound examination. Student's t-test was used to compare the age between the different groups.

RESULTS

Clinicopathological findings:

Between 1995-1997 in the record of The University Health Network, we identified 123 patients with HPIN as the primary diagnosis in prostate needle core biopsies and we compared them with 100 patients with HPIN associated with invasive cancer simultaneously. HPIN associated with cancer designated as (1st group) and isolated HPIN designated as (2nd group). The mean age was 67 year and 64 for the 1st and 2nd group

respectively ($P < 0.05$). The PSA levels were 9.9 and 8 (ng/ml) for the 1st and 2nd groups respectively ($P < 0.05$). The US and DRE examinations were positive in 50%, 44% in the 1st group and 30 %, 23% in the 2nd groups respectively which was statistically significant ($P < 0.05$ for DRE and < 0.01 for US). The patients with isolated HPIN as the primary diagnosis (n:123) had at least one follow-up biopsy. Pca was identified in 33 cases (27%) in the follow-up biopsies with range of follow-up time between 2 and 36 months. The carcinoma was identified in the same side of the HPIN in 55% of the cases and in 33% and 12% in both sides and in the opposite sides respectively. Gleason score was predominantly 6 and 7. When we divided those patients to group A (did not progress to cancer) and group B (progressed to cancer) we found that the mean age was 64 and 62 years ($P = 0.2$) and the mean PSA value were 8 and 7.8 ng/ml ($P = 0.4$) respectively. US was positive in 11/33 and 18/90 in group A and B respectively ($P = 0.1$). DRE was positive in 11/33 and 26/90 in group A and B respectively ($P = 0.5$). Pathological review showed similarity between the two groups where the presence of cribriform, tufting, micropapillary and flat microscopic subtypes (figure 1A-D) present in 7%, 55%, 50%, and 11% in group A and 6%, 60%, 55% and 12% in group B respectively. The commonest morphological HPIN subtypes was the tufting and the micropapillary patterns. No statistical significant difference was between the group A and B in any of the clinical parameters examined including age, PSA level, rectal examination, rectal ultrasound or morphologic subtypes.

Interphase FISH findings

We had interpretable results in 44 cases (24 from group A and 20 from group B) for chromosomes 4,7,8 and 10. Our findings indicated the presence of different chromosomal anomalies in 5/20 (25%) cases of group B and in 2/24 (8.3%) cases of group A respectively ($P=0.1$). Patients with chromosomal anomalies are shown in table 2. All the chromosomal changes were in the form of a gain (figure 2 and 3). No chromosomal losses were identified in any case. Gain of chromosome 8 has been seen in 5 cases, gain of chromosome 7 in 3 case, gain of chromosome 10 in 2 cases. No numeric chromosomal changes were detected in chromosome 4. No numeric chromosomal anomalies were noticed in the adjacent hyperplastic or normal prostate glandular epithelium, which was counted in 30 cases. By applying the same cytogenetic technique on 5-micron paraffin-embedded sections from TURP specimens from patients with nodular hyperplasia (BPH) using probe for chromosome 8, there were no chromosomal numeric anomalies in any of the 14 specimens that have been examined. We had a total of 7/44 (16%) of HPIN, which showed chromosomal anomalies in at least one chromosome. At the time of the diagnosis, 3 of the 7 patients were below the age 60 years (all of them had a cancer in the follow-up biopsies) and only 2 of those 7 patients were abnormal US and none of them had abnormal DRE. Six out of seven had PSA above 4ng/ml.

DISCUSSION

HPIN is the earliest accepted stage in prostatic carcinogenesis. HPIN is regarded as the most likely precursor for Pca¹. The greatest value of PIN is high predictive value as a marker for Pca. This is particularly true for high grade PIN (HPIN). If this lesion is identified, close surveillance and follow-up biopsy are indicated². No clinical or pathological parameter has been found to be helpful for distinguishing patients who had carcinoma on the next biopsy from those who did not. In our study, we identified 123 patients with isolated HPIN as the primary diagnosis who had a subsequent follow-up biopsy. Pca was identified in 27% in the first follow-up with range of follow-up period between 2 and 36 months. That is consistent with the incidence described in the literature (27-100%). Davidson et al found that the likelihood of finding cancer was greater in patients with PIN undergoing more than one follow-up biopsy (44%) than in those with only one biopsy (32%)²¹. The carcinoma has been identified in the same side of the HPIN in 55% of the cases and in 33% and 12% in both sides and in the opposite sides respectively. Gleason score was predominantly 6 and 7. The mean age was 64 and 62 years and the mean PSA value were 8 and 7.8 ng/mL for group A and group B respectively. No statistically significant difference was identified between these two groups in any of the clinical parameter examined including age, PSA level, digital rectal examination (DRE) or rectal ultrasound which is consistent with other authors²², however many others indicated that age, PSA positivity and DRE increase the risk of the later cancer^{21, 23-25}. This indicated that HPIN is not detectable by elevated serum PSA or transrectal ultrasound or digital rectal examination. Pathological review showed that the most common morphological HPIN subtypes were the tufting and micropapillary

patterns and no statistically significant difference was found between the two groups regarding the morphologic subtypes which is consistent with other findings²¹. The underlying mechanism of progression of PIN to Pca is not clear. However the progression might be due to severe genetic instability, resulting in a clone that has the ability to invade²⁶. CIN may be defined as an excess of chromosome alterations occurring at each cell generation^{3, 4}. CIN is thought to arise as a result of aberrations in mitotic machinery of chromosome constitution leading to excessive numerical chromosomal changes.^{3, 4, 27}. CIN can be manifested in a form of numeric chromosomal changes of one or more chromosomes. To investigate if certain chromosomal abnormalities detected in the HPIN foci could be predictive of subsequent carcinoma or could increase the predictive value of HPIN, we examined prostate needle core biopsy with HPIN diagnosis for the presence of numeric chromosomal anomalies.

We performed a retrospective study using interphase FISH analysis on HPIN slides from 54 patients and had interpretable results in 44 cases (24 from group A and 20 from group B) for chromosomes 4,7,8 and 10. Our findings indicated the presence of different chromosomal anomalies in 5/20 (25%) cases of group B and in 2/24 (8.3%) cases of group A (P=0.1). This difference was not statistically significant, however, it is highly suggestive that HPIN with CIN have higher chance of progression to invasive cancer. No numeric chromosomal anomalies have been noticed in the adjacent hyperplastic or normal prostate glandular epithelium present in the same biopsies. The overall chromosomal changes in HPIN was higher than the normal or hyperplastic epithelium with statistically significant difference (P<0.05). The advantage of FISH when applied to histologic sections is that the tumor cells can be precisely evaluated and normal and

dysplastic foci can be evaluated for CIN even in small biopsies. FISH has been used in PIN to determine chromosomal anomalies in a few studies ^{19, 28-33}. However in those studies it has been performed on prostatectomy specimens which already contain Pca foci. Using centromere FISH probes, the commonest numeric changes in PIN and Pca include gain of chromosome 7,8,10 and loss of chromosome Y. The overall frequency of numeric chromosomal anomalies in PIN and Pca is remarkably similar which suggests that PIN is a precursor of carcinoma ³⁰. The overall incidence of any numeric chromosomal anomaly was seen in 7/44 (16%) in our study. The presence of any anomaly in PIN ranged in the literature between 12-62%. Our relatively lower incidence of chromosomal changes in HPIN foci can be explained by the small foci of tissue in biopsies, which might not be well representative of the whole HPIN foci. In our study all the chromosomal changes were in a form of a gain with no chromosomal losses being identified in any case. Gain of chromosome 8 was the commonest finding in our study which is consistent with the previous studies ^{19, 30, 31}. Gain of chromosome 7 has been shown to be frequent in Pca and associated with higher tumor grade, advanced stage and early patient death of Pca ^{29, 34, 35}, however, it could occur in early stage of Pca tumorigenesis as shown in our study. No numeric chromosomal changes have been seen in chromosome 4. Although chromosomal instability has been described recently in many premalignant lesions as a risk of progression to cancer, our current study although highly suggestive, does not confirm that in prostate.

The heterogeneity and the multifocality of prostate cancer which has been suggested and demonstrated recently by many investigators ³⁶⁻³⁸ in the same gland may not be restricted to cancer foci, but most likely applied on different HPIN foci in the same

prostate. The heterogeneity of the prostate neoplastic and epithelium make it relatively difficult to be studied and explains not only the wide range results but sometime conflicting data in the literature regarding many prognostic molecular markers. Chromosome instability can contribute to tumor progression by several possible mechanisms: loss of chromosomes that harbor genes encoding negative regulators of cell cycle progression and proteins involved in apoptosis or senescence; gain of extra chromosomes that harbor genes encoding positive regulators of cell cycle progression(oncogenes), antiapoptotic proteins and proteins that suppress senescence ¹². Although CIN has been described as a common feature of dysplastic and neoplastic lesions, its mechanism is still unclear. Many candidates have been incriminated in causing CIN through inducing unequal segregation of chromosomes due to multiple spindle poles during mitosis or through other mechanisms. Centrosome hyperamplification was found to be the major mechanism responsible for chromosomal instability *in-vitro* and *in-vivo* ^{27, 39-42}. Centrosome is the major microtubule-organizing center and required for spindle bipolarity, spindle microtubule assembly and balanced segregation of the chromosomes ⁴³. Tumor suppressor genes (such as p53, Rb, BRAC1 have been incriminated in controlling centrosome duplication ^{27, 39, 40, 44}. Other possible mechanisms may be involved in the causation of CIN such as shortened telomeres, hypomethylation and activation of certain genes. The detection of the HPIN which most likely will progress will be of great interest, especially since PIN is an excellent candidate for chemoprevention ¹.

We conclude that although no single numeric chromosomal abnormality could be assigned as a predictor of HPIN progression to carcinoma, the overall level of numeric

chromosomal abnormalities show a trend of elevation in HPIN patients who progressed to carcinoma, but the difference was not statistically significant. Although HPIN is by itself a powerful predictor of cancer, the presence of CIN increases that predictive value. All patients with diagnosis of HPIN in needle biopsies should be followed clinically and repeat biopsies should be performed, with increased frequency for those with CIN.

ACKNOWLEDGEMENTS

We would like to thank Dr Waleed A Milaat from Department of Community Medicine and primary Health Care, King Abdul-Aziz university Hospital, Jeddah, Saudi Arabia.

We would like also to thank our lab members; Khladoun Alromaih, Ben Beheshti, Zong Zhang, Bisera Vukovic, Paula Marrano, Jana Karaskova, Paul Park, Elena Kolomietz and Jane Bayani for their contribution to achieve this work. Financial support for this project is funded by the U.S. Army Medical Research and Material Command (USAMRMC) Prostate Cancer Research Program (PCRP).

References

1. van der Kwast TH, Labrie F, Tetu B. Prostatic intraepithelial neoplasia and endocrine manipulation. *Eur Urol.* 1999;35:508-10.
2. Bostwick DG. Progression of prostatic intraepithelial neoplasia to early invasive adenocarcinoma. *Eur Urol.* 1996;30:145-52.
3. Lengauer C, Kinzler KW, Vogelstein B. Genetic instabilities in human cancers. *Nature.* 1998;396:643-9.
4. Cahill DP, Lengauer C, Yu J et al. Mutations of mitotic checkpoint genes in human cancers [see comments]. *Nature.* 1998;392:300-3.
5. Rabinovitch PS, Dziadon S, Brentnall TA et al. Pancolonic chromosomal instability precedes dysplasia and cancer in ulcerative colitis. *Cancer Res.* 1999;59:5148-53.
6. Ried T, Heselmeyer-Haddad K, Blegen H, Schrock E, Auer G. Genomic changes defining the genesis, progression, and malignancy potential in solid human tumors: a phenotype/genotype correlation. *Genes Chromosomes Cancer.* 1999;25:195-204.
7. Burt EC, James LA, Greaves MJ, Birch JM, Boyle JM, Varley JM. Genomic alterations associated with loss of heterozygosity for TP53 in Li-Fraumeni syndrome fibroblasts. *Br J Cancer.* 2000;83:467-72.
8. Hawkins NJ, Gorman P, Tomlinson IP, Bullpitt P, Ward RL. Colorectal carcinomas arising in the hyperplastic polyposis syndrome progress through the chromosomal instability pathway. *Am J Pathol.* 2000;157:385-92.

9. Shackney SE, Shankey TV. Common patterns of genetic evolution in human solid tumors. *Cytometry*. 1997;29:1-27.
10. Williams AC, Miller JC, Collard T, Browne SJ, Newbold RF, Paraskeva C. The effect of different TP53 mutations on the chromosomal stability of a human colonic adenoma derived cell line with endogenous wild type TP53 activity, before and after DNA damage. *Genes Chromosomes Cancer*. 1997;20:44-52.
11. Yasui W, Yokozaki H, Fujimoto J, Naka K, Kuniyasu H, Tahara E. Genetic and epigenetic alterations in multistep carcinogenesis of the stomach. *J Gastroenterol*. 2000;35:111-5.
12. Tarapore P, Fukasawa K. p53 mutation and mitotic infidelity. *Cancer Invest*. 2000;18:148-55.
13. Kirchhoff M, Rose H, Petersen BL et al. Comparative genomic hybridization reveals a recurrent pattern of chromosomal aberrations in severe dysplasia/carcinoma in situ of the cervix and in advanced-stage cervical carcinoma. *Genes Chromosomes Cancer*. 1999;24:144-50.
14. Mian C, Bancher D, Kohlberger P et al. Fluorescence in situ hybridization in cervical smears: detection of numerical aberrations of chromosomes 7, 3, and X and relationship to HPV infection. *Gynecol Oncol*. 1999;75:41-6.
15. Aubele M, Zitzelsberger H, Schenck U, Walch A, Hofler H, Werner M. Distinct cytogenetic alterations in squamous intraepithelial lesions of the cervix revealed by laser-assisted microdissection and comparative genomic hybridization. *Cancer*. 1998;84:375-9.

16. Henke RP, Kruger E, Ayhan N, Hubner D, Hammerer P. Frequency and distribution of numerical chromosomal aberrations in prostatic cancer. *Hum Pathol.* 1994;25:476-84.
17. Qian J, Bostwick DG, Takahashi S et al. Comparison of fluorescence in situ hybridization analysis of isolated nuclei and routine histological sections from paraffin-embedded prostatic adenocarcinoma specimens. *Am J Pathol.* 1996;149:1193-9.
18. Erbersdobler A, Bardenhagen P, Henke RP. Numerical chromosomal anomalies in latent adenocarcinomas of the prostate. *Prostate.* 1999;38:92-9.
19. Erbersdobler A, Gurses N, Henke RP. Numerical chromosomal changes in high-grade prostatic intraepithelial neoplasia (PIN) and concomitant invasive carcinoma. *Pathol Res Pract.* 1996;192:418-27.
20. Aubele M, Zitzelsberger H, Szucs S et al. Comparative FISH analysis of numerical chromosome 7 abnormalities in 5- micron and 15-micron paraffin-embedded tissue sections from prostatic carcinoma. *Histochem Cell Biol.* 1997;107:121-6.
21. Davidson D, Bostwick DG, Qian J et al. Prostatic intraepithelial neoplasia is a risk factor for adenocarcinoma: predictive accuracy in needle biopsies. *J Urol.* 1995;154:1295-9.
22. Langer JE, Rovner ES, Coleman BG et al. Strategy for repeat biopsy of patients with prostatic intraepithelial neoplasia detected by prostate needle biopsy [see comments] [published erratum appears in J Urol 1996 Jul;156(1):185]. *J Urol.* 1996;155:228-31.

23. Raviv G, Janssen T, Zlotta AR et al. [High-grade intraepithelial prostatic neoplasms: diagnosis and association with prostate cancer]. *Acta Urol Belg.* 1996;64:11-5.
24. Raviv G, Zlotta AR, Janssen T et al. Do prostate specific antigen and prostate specific antigen density enhance the detection of prostate carcinoma after initial diagnosis of prostatic intraepithelial neoplasia without concurrent carcinoma? *Cancer.* 1996;77:2103-8.
25. Raviv G, Janssen T, Zlotta AR, Descamps F, Verhest A, Schulman CC. Prostatic intraepithelial neoplasia: influence of clinical and pathological data on the detection of prostate cancer. *J Urol.* 1996;156:1050-4; discussion 1054-5.
26. Montironi R, Hamilton PW, Scarpelli M, Thompson D, Bartels PH. Subtle morphological and molecular changes in normal-looking epithelium in prostates with prostatic intraepithelial neoplasia or cancer. *Eur Urol.* 1999;35:468-73.
27. Pihan GA, Purohit A, Wallace J et al. Centrosome defects and genetic instability in malignant tumors. *Cancer Res.* 1998;58:3974-85.
28. Macoska JA, Micale MA, Sakr WA, Benson PD, Wolman SR. Extensive genetic alterations in prostate cancer revealed by dual PCR and FISH analysis. *Genes Chromosomes Cancer.* 1993;8:88-97.
29. Takahashi S, Qian J, Brown JA et al. Potential markers of prostate cancer aggressiveness detected by fluorescence in situ hybridization in needle biopsies. *Cancer Res.* 1994;54:3574-9.

30. Qian J, Bostwick DG, Takahashi S et al. Chromosomal anomalies in prostatic intraepithelial neoplasia and carcinoma detected by fluorescence in situ hybridization. *Cancer Res.* 1995;55:5408-14.
31. Jenkins RB, Qian J, Lieber MM, Bostwick DG. Detection of c-myc oncogene amplification and chromosomal anomalies in metastatic prostatic carcinoma by fluorescence in situ hybridization. *Cancer Res.* 1997;57:524-31.
32. Alers JC, Krijtenburg PJ, Vissers KJ, Bosman FT, van der Kwast TH, van Dekken H. Interphase cytogenetics of prostatic adenocarcinoma and precursor lesions: analysis of 25 radical prostatectomies and 17 adjacent prostatic intraepithelial neoplasias. *Genes Chromosomes Cancer.* 1995;12:241-50.
33. Qian J, Jenkins RB, Bostwick DG. Genetic and chromosomal alterations in prostatic intraepithelial neoplasia and carcinoma detected by fluorescence in situ hybridization [In Process Citation]. *Eur Urol.* 1999;35:479-83.
34. Alcaraz A, Takahashi S, Brown JA et al. Aneuploidy and aneusomy of chromosome 7 detected by fluorescence in situ hybridization are markers of poor prognosis in prostate cancer. *Cancer Res.* 1994;54:3998-4002.
35. Bandyk MG, Zhao L, Troncoso P et al. Trisomy 7: a potential cytogenetic marker of human prostate cancer progression. *Genes Chromosomes Cancer.* 1994;9:19-27.
36. Bostwick DG, Shan A, Qian J et al. Independent origin of multiple foci of prostatic intraepithelial neoplasia: comparison with matched foci of prostate carcinoma. *Cancer.* 1998;83:1995-2002.

37. Zitzelsberger H, Kulka U, Lehmann L et al. Genetic heterogeneity in a prostatic carcinoma and associated prostatic intraepithelial neoplasia as demonstrated by combined use of laser- microdissection, degenerate oligonucleotide primed PCR and comparative genomic hybridization. *Virchows Arch.* 1998;433:297-304.
38. Yasunaga Y, Shin M, Fujita MQ et al. Different patterns of p53 mutations in prostatic intraepithelial neoplasia and concurrent carcinoma: analysis of microdissected specimens. *Lab Invest.* 1998;78:1275-9.
39. Lingle WL, Lutz WH, Ingle JN, Maihle NJ, Salisbury JL. Centrosome hypertrophy in human breast tumors: implications for genomic stability and cell polarity. *Proc Natl Acad Sci U S A.* 1998;95:2950-5.
40. Carroll PE, Okuda M, Horn HF et al. Centrosome hyperamplification in human cancer: chromosome instability induced by p53 mutation and/or Mdm2 overexpression. *Oncogene.* 1999;18:1935-44.
41. Ghadimi BM, Sackett DL, Difilippantonio MJ et al. Centrosome amplification and instability occurs exclusively in aneuploid, but not in diploid colorectal cancer cell lines, and correlates with numerical chromosomal aberrations. *Genes Chromosomes Cancer.* 2000;27:183-90.
42. Fukasawa K, Wiener F, Vande Woude GF, Mai S. Genomic instability and apoptosis are frequent in p53 deficient young mice. *Oncogene.* 1997;15:1295-302.
43. Fukasawa K, Choi T, Kuriyama R, Rulong S, Vande Woude GF. Abnormal centrosome amplification in the absence of p53. *Science.* 1996;271:1744-7.

44. Xu X, Weaver Z, Linke SP et al. Centrosome amplification and a defective G2-M cell cycle checkpoint induce genetic instability in BRCA1 exon 11 isoform-deficient cells. *Mol Cell*. 1999;3:389-95.

Legends

Figure 1: Hematoxylin and eosin sections of the four morphological subtypes of high-grade intraepithelial neoplasia (HPIN). 1A is a focus of micropapillary pattern, 1B; is a focus of cribriform pattern, 1C; is a focus of tufting pattern, 1D; is a focus of flat pattern, In all those foci there are the general features of HPIN including hyperchromasia, prominent nucleoli, nuclear enlargement and stratification

Figure 2: Interphase FISH on a focus of cribriform HPIN using dual centromere probes (red signal for chromosome 7 and green signal for chromosome 8. Many cells (arrow heads) show more than 2 signals for both probes.

Figure 3: Interphase FISH on a focus of cribriform HPIN using dual probes. Some cells (arrow heads) show 3 green signals consist with a gain of chromosome 8. The arrow show signals in stromal cells, which have been, used as internal control

Table 1: Age and PSA levels in patients used for FISH studies.

Group	Age (mean)	PSA mean(ng/ml)	P value
A	8.7	65.1	>0.05
B	7.9	62	>0.05

Table 2: Summary of the clinical and interphase FISH results for chromosome 4,7,8 and 10 on the needle core prostatic biopsies from patients with chromosomal abnormalities

Patient	Age (Years)	CH7	CH8	CH10	CH4	F-biop	PSA (ng/ml)
1	63	N	G	G	N	PIN	10.1
3	62	G	N	N	N	PIN	7.9
7	60	G	N	N	N	CA	4.7
11	53	N	G	N	N	CA	11.4
14	65	G	G	N	N	CA	1.8
16	52	N	G	G	N	CA	8.4
41	55	N	G	N	N	CA	8.4

N: Normal

CA: Carcinoma

B: Benign

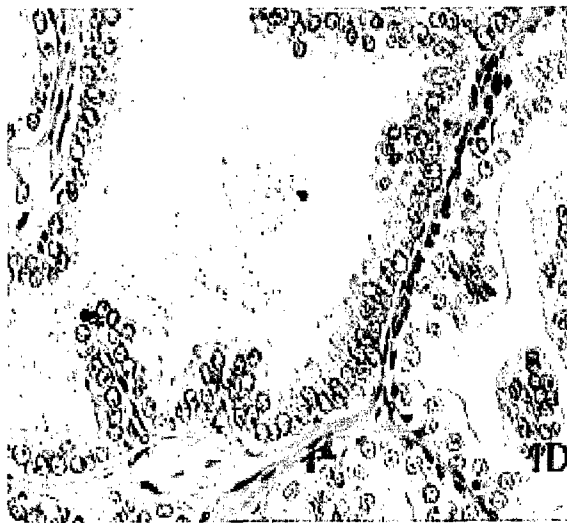
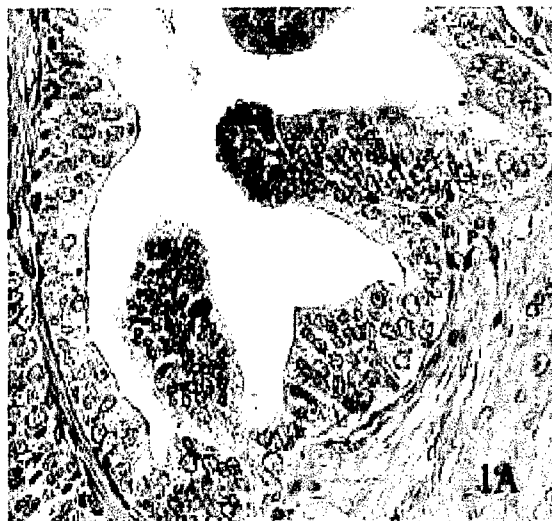
G: Gain

RE: Rectal exam

US: Ultrasound

PIN: Prostate intraepithelial neoplasia

F.biop: Follow-up biopsy







In Press – Urology

Prostatic Intraepithelial Neoplasia: Molecular Considerations

John Trachtenberg*, Jeremy Squire*, Joan Sweet*, Theodore J. Brown

University Health Network*
Mount Sinai Hospital+
And
University of Toronto
Toronto, Ontario, Canada

Address all correspondence to:
John Trachtenberg MD
Princess Margaret Hospital
University Health Network
620 University Avenue
Toronto, Ontario M5G 2C9
Canada
E-mail: john.trachtenberg@utoronto.ca

Financial support for this project is funded by the U.S. Army Medical Research and Materiel Command (USAMRMC) Prostate Cancer Research Program (PCRP).

Abstract

Prostatic intraepithelial neoplasia (PIN) is felt by many to be a premalignant entity. It is defined by histologic appearance. It seems reasonable that there are an orderly series of molecular changes that occur in prostate cells as they transit from normal to PIN to frank cancer. These changes likely determine the phenotypic appearance. Knowledge of these changes may predict the natural history of PIN and suggest means to prevent the development of cancer from PIN. We have developed a clinical trial to address these issues. Patients with histologically defined PIN will be randomly assigned to either androgen ablation with the potent antiandrogen bicalutamide or placebo in a controlled, blinded pilot study. They will be clinically assessed every 3 months and received transrectal ultrasound guided biopsies of the prostate every six months for 2 years. They then will be followed at three month intervals and be rebiopsied at 36 months after start of the trial. Clinical end points will be the percentage of patients in each arm at the end of the two-year with PIN or cancer. Secondary end points will be the development of PIN or cancer at 3 years. The collected tissue will be assayed by standard histology, immunohistochemistry of multiple markers felt integral to cancer progression, and investigated further using large-scale cDNA microarrays.

Introduction

Prostate cancer is the most common internal malignancy in man. It is the second most common cause of death due to malignancy in man, second only to lung cancer. The incidence of prostate cancer has increased dramatically over the last decade probably due to PSA screening but also because of a real increase in the development of the disease. Little is known of the etiology of the disease (1,2). While early detection strategies are probably finding more men who are curable by conventional methods such as surgery or radiation therapy, these treatments have significant associated life long morbidity. The natural history of the development of prostate cancer has only recently been elucidated. Most students of this disease believe that adenocarcinoma of the prostate probably passes through a premalignant phase termed prostatic intraepithelial neoplasia (PIN). This entity has only recently been characterized in the human prostate (3,4). PIN has been identified in 2 to 16% of men undergoing transrectal ultrasound guided biopsies. Histologically, high-grade prostatic intraepithelial neoplasia is characterized by a distinctive architectural arrangement of cellular proliferation within pre-existing ducts and glands as in prostate carcinoma but lacking complete disruption of the basal cell layer and stromal invasion noted with carcinoma. With increasing grades of prostatic intraepithelial neoplasia, there is an increasing degree of nuclear aberration and basal cell layer disruption. PIN is currently considered a premalignant proliferation in the prostate and is found more often within the peripheral zone. Adenocarcinoma is more often associated with high grade as opposed to low grade prostatic intraepithelial neoplasia and multifocality of concurrent carcinoma (5).

Autopsy and surgical pathology reviews have documented a strong association between the discovery of high grade PIN and the development of prostate cancer. In a case control study by Davidson 35% of patients with PIN had cancer in a subsequent biopsy compared to 13% in a matched control group (6). Recent studies have documented the multifocal nature of the premalignant changes in prostates with documented high-grade prostatic intraepithelial neoplasia. Repeat biopsies of men with PIN have demonstrated the appearance of adenocarcinoma in the gland contra lateral to the initial biopsy showing PIN in a high proportion

of patients demonstrating the multifocality of the premalignant changes.

Brawer evaluated 21 men in whom prostate biopsy of a palpable abnormality revealed isolated prostatic intraepithelial neoplasia and 12 (57%) had cancer on repeat biopsy (7). In each case carcinoma was identified on the side of the palpable abnormality. Contra lateral cancer was also noted in 6 cases (50%), Weinstein and Epstein reported that 10 to 19 men (53%) with isolated prostatic intraepithelial neoplasia on initial biopsy had cancer on repeat biopsy (8). In only 5 of these 10 men with cancer (50%) was the tumour ipsilateral to the prostatic intraepithelial neoplasia. Langer and Rovner found that 15 of 52 men (29%) with isolated prostatic intraepithelial neoplasia on needle biopsy had cancer on repeat biopsy (9). The site of carcinoma on repeat biopsy corresponded to the site of previously diagnosed prostatic intraepithelial neoplasia in only six cases (40%), a transrectal ultrasound abnormality in 3 (20%) and a site of random biopsy in 6 (40%). Close clinical follow up and repeat biopsy of the prostate are recommended for men with high-grade prostatic intraepithelial neoplasia. These data suggest that the changes that precede the development of prostate cancer are not relegated to a specific area within the prostate (the palpable nodule, site of PIN, etc.) and that prostate cancer is a multifocal disease.

Patients diagnosed with PIN who are of the appropriate age and health to benefit from intervention are usually assessed by one of two methods. One method is to follow the patient with "close clinical follow up" which usually translates into repeat digital rectal exams (DRE) and serum PSA determinations at set intervals (usually every three to six months) to see if there are signs of progression and at that time to rebiopsy the prostate. If cancer is discovered, intervention is undertaken; otherwise the policy of surveillance is continued. Others advocate a more aggressive policy of immediate rebiopsy with the discovery of PIN and a continuing rebiopsy policy at any suggestion of clinical progression. In any case because of the fluctuating nature of serum PSA determinations, the subjective nature of the DRE, and the fear of a progressing but missed cancer, many patients undergo repeat biopsies at an interval that approximates six months in the 24 months following the initial diagnosis of PIN.

Neither the natural history, the molecular changes accompanying the change from the premalignant state to frank malignancy, nor strategies to prevent these changes are definitely known (10,11). This human model of evolving carcinogenesis is a fertile bed to determine these important events and possibly develop means to arrest them before frank cancer develops.

Methods

We have proposed a randomized blinded study to assess the natural history of men found to have PIN by classical clinical parameters (PSA and DRE) and regular (every six month) trans rectal ultrasound guided biopsies of the prostate. These biopsies will be assessed for histological changes as well as a series of molecular markers associated with cancer progression. It is hoped that alone or in combination these markers would characterize progression of the prostate from the premalignant PIN stage to frank cancer earlier than the classical clinical measures above and allow for early intervention. In addition, the antiandrogen bicalutamide would be randomly assigned to patients to determine if this known minimally toxic agent can arrest or delay the development of cancer in this group of susceptible men.

Multiple volume determined systematic needle cores taken from each patient at biopsy will be immediately fixed in 20% formalin overnight and paraffin-embedded using standard procedures. Sections will be cut from the blocks and collected onto positively charged slides. Every second

slide will be stained with haematoxylin and eosin for histological examination to confirm the presence of PIN and to determine if adenocarcinoma is present. All sections will be reviewed using criteria for diagnosing PIN and differentiating the grade as described by Epstein (13). If carcinoma is detected, the subject will be withdrawn from the study and treated. The remaining intervening slides will be processed for determining the expression of the various molecular markers by immunocytochemistry. We have chosen a series of markers that will help to define changes in androgen production and utilization, angiogenesis, and epithelial-stromal interactions.

One of the high-throughput technologies that has come out of the Human Genome Project is that of the production of DNA arrays on solid supports for large-scale hybridization experiments. The resulting micro array, or "DNA chip" technology, has allowed large-scale gene discovery, expression, mapping and sequencing studies as well as detection of mutations or polymorphisms. Hybridization of complex mRNA-derived probes to an array of cDNA PCR products or oligonucleotides representing specific cDNAs spotted onto modified glass slides allows the simultaneous analysis of the differential expression of thousands of genes. This technology has been applied to gene expression studies in inflammatory diseases and in melanoma. The goal of this component of the study is to perform expression profiling to identify patterns of differential gene expression that contribute to cancer progression.

The high-density micro array consortium at the University Health Network-OCI is addressing the technical problems associated with the reproducibility of microarrays and the bioinformatics required to understand complex patterns of gene expression. Presently, the OCI array has 17,000 sequences tethered to glass microscope slides. For screening of this high-density DNA chip, total RNA from tumour samples (obtained under RNAase free conditions) will be labelled by reverse transcription in the presence of primers. The labelled product is purified, precipitated and dissolved in H₂O. Following pre-hybridization, the DNA chip is incubated with labelled probes, yeast tRNA and denatured salmon sperm DNA. The slides are washed and the expression profile scanned and analyzed. Differential gene expression within the study group will fall into two main classes: 1) those genes expressed preferentially in prostate cancer with recurrent or progressive disease; and 2) those genes expressed preferentially in prostate cancer which remains indolent or in which there has been an extended disease-free period. One of the limitations of this study is the amount of tissue available for RNA. We are therefore applying mRNA amplification methods [15] for increasing the yield of cDNA for high density microarray analysis.

We will closely examine expression levels of genes in each class in both the placebo and bicalutamide treated patients and will use the data derived from the scanning software to focus on genes, which show the most extreme difference i.e. the most over- and under-expressed genes in those tumours which subsequently develop disease both with and without drug treatment. For such profile analyses to be successful, the relative patterns of expression differences must be proven to have appropriate biological information. Biological variation may arise from clinically irrelevant heterogeneity of the tissue source so we will closely monitor morphologic parameters to control for these potential variables. To extract and detect relationships between differences we will apply analytical approaches that will define the grade-specific and/or outcome-determining 'signatures' of expression. Clearly some of these changes or 'signatures' of gene expression will simply be associated with phenotypes induced by the antiandrogen whereas

others will play a direct causal role in response and, as such, will be candidates for study and new approaches to future drug intervention.

Conclusion

PIN is felt by many to be a precursor lesion to prostate cancer. This experimental program will attempt to define its natural history and susceptibility to androgen ablation by conventional histologic methods as well as immunohistochemical and high throughput gene microarray technology. This program may not only define which cases of PIN progress and which do not but also suggest treatment opportunities by their differences in molecular expression.

References

1. Bowersox, J. Experts debate PSA screening for prostate cancer. *J. Natl Cancer Inst.* 84:1856-1857, 1992.
2. Wilt, T.J. Prostate cancer screening: practice what the evidence preaches. *Am J Med.* 104:602-604, 1998.
3. Bostwick, D.G. Brawer M.K. Prostatic intra-epithelial neoplasia and early invasion in prostate cancer. *Cancer.* 59:788-794, 1987.
4. Bostwick D.G. High grade prostatic intra-epithelial neoplasia: The most likely precursor of prostate cancer. *Cancer* 75 1823-1836, 1995.
5. Epstein, J.I. Pathology of prostatic intraepithelial neoplasia and adenocarcinoma of the prostate: prognostic influences of stage, tumor volume, grade, and margins of resection. *Seminars in Oncol.* 21:527-541, 1994.
6. Davidson D, Bostwick DG, Qian J, Wollan PC, Oesterling JE, Rudders RA, Siroky M, Stilmant M: Prostatic intraepithelial neoplasia is a risk factor for adenocarcinoma: Predictive accuracy in needle biopsies. *J Urol.* 154: 1295-1299, 1995.
7. Brawer, M.K. Prostatic intraepithelial neoplasia: a premalignant lesion. *Hum. Pathol.* 23:242-248, 1992.
8. Weinstein, M.H. and Epstein, J.I. Significance of high-grade prostatic intraepithelial neoplasia on needle biopsy. *Hum. Pathol.* 24:624-629, 1993.
9. Langer, J.E., Rovner, E.S., Coleman, B.G., Yin, D., Arger, P.H., Malkowicz, S.B., Nisenbaum, H.L., Rowling, S.E., Tomaszewski, J.E., Wein, A.J., and Jacobs, J.E. Strategy for repeat biopsy of patients with prostatic intraepithelial neoplasia detected by prostate needle biopsy. *J. Urol.* 155:228-231, 1996.
10. Lipski, B.A., Garcia, R.L., and Brawer, M.K. Prostatic intraepithelial neoplasia: significance and management. *Semin. Urol. Oncol.* 14:149-155, 1996.
11. Brawer, M.K., Bigler, S.A., Sohlberg, O.E. Nagle, R.B. and Lange, P.H. Significance of prostatic intraepithelial neoplasia on prostate needle biopsy. *Urology* 38:103-107, 1991.
12. Berner, A., Harvei, S., Tretli, S., Fossa, S.D., and Nesland, J.M. Prostatic carcinoma: a multivariate analysis of prognostic factors. *Br. J. Cancer* 69:924-930, 1994.

13. Epstein J.I. Prostate Biopsy Interpretation. (Biopsy Interpretation Series), Lippincott-Raven, Philadelphia, PA, 1995.
14. Simmons, D.M., Arriza, J.L., and Swanson, L.W. A complete protocol for in situ hybridization of messenger RNAs in brain and other tissues with radiolabeled single-stranded RNA probes. *The J. Histotechnol.* 12:169-181, 1989.
15. Wang, E., Miller, L. D. Ohnmacht, G. A. Liu, E. T. Marincola, F. M., High-fidelity mRNA amplification for gene profiling. *Nat Biotechnol*, 2000. **18**(4): p. 457-9.

Resolution of genotypic heterogeneity in prostate tumors using DOP-PCR and CGH on microdissected carcinoma and PIN foci.

Ben Beheshti^{1,3}, Paula Marrano³, Jeremy A. Squire^{1,2,3}, and Paul C. Park^{1,3}.

Departments of Laboratory Medicine and Pathobiology¹, and Medical Biophysics², University of Toronto; Ontario Cancer Institute/Princess Margaret Hospital³, the University Health Network, Toronto, Ontario, Canada

Key words: Prostate cancer, comparative genomic hybridization, degenerate oligonucleotide primed PCR, laser capture microdissection, genomic heterogeneity.

Running title: CGH and FISH analysis of early stage CaP patients.

Financial support for this project is funded by the U.S. Army Medical Research and Materiel Command (USAMRMC) Prostate Cancer Research Program (PCRP). PCP was supported by the AFUD and the Imclone Systems, Inc.

Corresponding author:

Jeremy Squire, Ph.D.

Senior Scientist

Ontario Cancer Institute, the University Health Network

610 University Avenue

Toronto, Ontario M5G 2M9

CANADA

Tel.: 416-946-4509 (direct)

Tel.: 416-978-2628 (office)

Tel.: 416-946-4501 x5012 (lab)

Fax.: 416-946-2065

e-mail: jeremy.squire@utoronto.ca

ABSTRACT

BACKGROUND: Prostate cancer (CaP) is a multifocal heterogeneous disease. A major challenge in CaP research is to identify genetic biomarkers that herald aggressive transformation.

METHODS: To investigate the effect of tumor heterogeneity on the analysis of genomic aberration, we compared the results of comparative genomic hybridization analysis of DNA extracted from tumor bulk, against that of DNA amplified by DOP-PCR from homogeneous cell population obtained by laser capture microdissection of discrete, individual tumor foci.

RESULTS: Sampling by microdissection, positive aberrations were observed in 3 of 3 foci of carcinoma involved with prostatic capsule, and in 2 of 3 PIN foci examined. Carcinoma foci consistently exhibited more extensive aberrations than the PIN samples obtained from the same tumor. Within these samples, the different tumor foci exhibited gain of 8q while PIN showed no consistent aberration. Using bulk extracted DNA, CGH detected aberrations in only 3 of the 21 samples interrogated, despite the known trisomy 8 status, as revealed by fluorescence *in situ* hybridization.

CONCLUSIONS: The results of the present study demonstrate that CGH analysis using bulk dissected fresh tissue is not sufficiently sensitive to fully detect the chromosomal numerical aberrations in CaP. Given the considerable intratumor genomic heterogeneity, CGH in conjunction with microdissection and DOP-PCR amplification provides a more complete repertoire of aberrations as well as a better phenotype-genotype correlation in prostate tumors.

INTRODUCTION

In North America, prostate cancer (CaP) is the leading cancer incidence in men and the second most common cause of male cancer mortality [1]. While the etiology of CaP remains unknown, both environmental and genetic contributions have been associated with its carcinogenesis [1, 2]. However, our understanding of the molecular genetic changes that underlie the progression of this disease remains at an early stage, as CaP exhibits both inter- and intratumor genotypic and phenotypic heterogeneity that complicates molecular and histopathological assessment and outcome prediction [3-6]. Clinically, localised CaP is often slow-growing and latent and its diagnosis sometimes may not even impact survival for 10 to 15 years, further complicating disease assessment and prognosis [2, 7, 8]. In a small but significant number of cases, however, the disease progresses to advanced stages. Advanced androgen-refractory disease is ultimately incurable and terminal. Identification of an early stage CaP-specific progression marker will allow delineation of tumor subsets that will stay indolent requiring no clinical intervention, and those that will progress to metastasis.

Progress in identifying consistent structural rearrangements in CaP has been slow. Furthermore, no consistent picture of the total chromosomal aberrations in early-stage CaP has emerged and it remains conceivable that technical difficulties in obtaining representative cytogenetic preparations derived from primary tumor material have precluded identification of causative chromosomal alterations in the early presentation of CaP. CaP is characterized by multifocal presentation. Consistent with this idea it was recently shown that a much greater frequency of chromosomal aberrations can be detected if microdissection and specialized culture methods are utilized [9]. A newly

diagnosed man with CaP will have an average of five apparently independent lesions [10]. In addition, there is growing evidence [6, 11-13] that both cancerous and pre-cancerous lesions within a given prostate tissue are non-clonal, further indicating the multifocal nature of this disease. Genetic dosage changes can be analyzed easily by comparative genomic hybridization (CGH) [14]. CGH studies of CaP that have been published generally have examined late stage, metastatic disease [15-18]. These studies have shown that there are frequent chromosomal aberrations in late stage CaP tumors, and that chromosomal copy number losses are five times more prevalent than gains [15].

Currently, the histopathological assessment of CaP is based on the Gleason system, which assigns a clinical grade to a given tumor based on the most prominent and representative histological features. This system not only has a significant clinical impact in predicting the outcome of the disease, but much of the current research effort in CaP is also directed towards identifying the molecular changes as a function of the Gleason grade.

In this study, we used the genome-wide scanning technique of CGH in combination with degenerate-oligonucleotide primed PCR (DOP-PCR) and laser capture microdissection (LCM) to demonstrate the genotypic heterogeneity among distinct foci within tumor samples, and to identify the karyotypic changes associated with the prostatic capsule invasion. Furthermore, we evaluated the effectiveness this technique against the traditional CGH method, using bulk-extracted DNA, in identifying the chromosomal gains and losses in early stage CaP specimens. In addition, we employed fluorescence *in situ* hybridization (FISH) technique to investigate the genotypic heterogeneity as a feature of early stage (pT1-T2) CaP.

MATERIALS AND METHODS

Tissue Accrual and Sample Preparations

Samples were collected from patients undergoing radical prostatectomy at the University Health Network (UHN). All samples utilized for this study were from patients presenting with evidence of high tumour volume (rising PSA levels, DRE findings, multiple positive biopsies) and no history of radiation or chemotherapy. For each prostate, a wedge of tissue was excised and analyzed histologically by frozen section. Criteria for inclusion in this study was based on the presence of a widely ranging variation in the Gleason pattern. A small wedge (approximately 1-2 cm³) of tumor tissue was dissected from the excised prostate, and the resected prostatic capsule was analyzed for extracapsular tumor extension by the pathologist on duty. The tissue wedge was quick-sectioned and hematoxylin and eosin (H&E)-stained. Samples assessed by the pathologist as having high tumor volume (> 80%) within the surrounding stroma were designated for study inclusion. A fresh wedge of tissue which directly apposes the H&E section was excised from the prostate and returned to the laboratory for research.

The obtained tissue sample was processed following two different protocols. In one set of experiments (21 patient samples), the tissue was bisected, and one of the pieces was used to establish a short term tissue culture (see below) for interphase FISH analysis. The remaining piece was placed in DNA extraction buffer and the genomic DNA from the tumor bulk extracted following standard protocols [19, 20]. This bulk-extraction method typically yielded approximately 200ug of high molecular weight DNA.

In a second set of experiments (3 patient samples), the tissue was immediately fixed in 70% ethanol (4°C, overnight) and embedded in paraffin. Serial sections, 10µm

in thickness, were obtained from the paraffin embedded tissue and stained with H&E. Homogeneous populations of epithelial cells were obtained from the sections using laser capture microdissection system (Arcturus, Mountain View, CA), from two different regions in each tumor sample, including: 1) acini of epithelial cells of Gleason pattern 3, which have infiltrated the prostatic capsule, and 2) acini of high grade PIN situated nearby (<3mm) which were not associated with the capsule. Typically 200-400 cells were collected from the serial sections for each region, and processed for genome amplification by DOP-PCR.

Amplification of the genomic DNA by DOP-PCR

The dissected cells were incubated in 20 μ L of digestion buffer (0.1% SDS, 1 μ g/ μ L proteinase K in Tris-Cl, pH 8.0) overnight. Following incubation at 90°C to inactivate the proteinase, the product containing the genomic DNA was serially diluted tenfold to concentrations of 1/10, 1/100, and 1/1000 of the original solution. One microlitre of each dilution was used as the template in separate PCR reactions.

The PCR amplification and labeling of the probe were carried out in 3 steps, using the Clontech cDNA PCR enzyme mix. In the first step, 0.1 μ L of dNTP (10mM), 0.5 μ L of the primer (5'-CCGACTCGAGNNNNNNATGTGG-3', 10 μ M), 0.5 μ L of PCR buffer (10X, Clontech, Palo Alto, CA) and 0.2 μ L of enzyme mix (Clontech) were added to the template DNA, and the volume adjusted to 5 μ L. In addition, a series of reaction mixtures containing 30ng, 3ng or 300pg of normal male DNA, obtained from human spleen tissue, were prepared in parallel for generation of reference probes for CGH. The reaction mixtures were denatured at 95°C for 5 min., and carried through eight cycles of denaturation (94°C, 1min.), annealing (30°C, 1min.) and extension (72°C, 3min).

Following a final extension of 10min at 72°C, each reaction mixture was supplemented with 20μL of reaction mixture containing 0.6μL of dNTP (10mM), 1.25μL of primer (25μM), 2.5μL of PCR buffer and 0.5μL of the enzyme. The reaction mixture was denatured at 95°C for 5min., and further cycled through 30 rounds of denaturation (94°C, 1min.), annealing (56°C, 1min.) and extension (72°C, 3min), followed by a final extension of 10min at 72°C. The product was purified by column chromatography (Qiaquick PCR Purification kit; Qiagen) and the amplification verified by electrophoresis on 1% agarose gel. Typically, the optimal product, as determined by the largest product size, was obtained from the initial template of 3ng or 300pg of normal male DNA, or from the tenfold or the hundred fold dilutions of the digest of the microdissected sample.

Probe preparation

For labeling of the PCR amplified DNA, 4μL of the selected product was added to 46μL of reaction mixture containing 1μL of dNTP (10mM), 2.4μL of primer (25μM), 5μL of PCR buffer, 1μL of the enzyme, and either 2μL of 0.4mM biotin-14dATP (tumor DNA) or 0.8μL of 1mM digoxigenin-11dUTP (normal reference DNA). The labeled probe was generated by 16 rounds of amplification using the parameters specified in the second step. The final product was purified by column chromatography, quantified by spectroscopy and sized by gel electrophoresis.

Alternatively, 2ug each of normal and bulk-extracted tumor DNA were labeled by nick translation with digoxigenin-11 dUTP (Roche) and biotin-14 dATP (Gibco BRL) respectively, as previously described [14, 21]. All final labeled probes ranged between 500bp to 2kb in size.

Comparative Genomic Hybridization (CGH)

CGH was performed as previously described [14, 21]. Images were captured using the Vysis PathVysion software, and analysis performed using the Vysis Karyotype software (Vysis, Downers Grove, IL). Results at telomeric or centromeric regions due to the presence of highly repetitive genomic sequences at these sites were not analysed. Ten metaphases were analysed to create the final CGH profile with 99% confidence intervals. Negative controls in which normal DNA was compared to itself, and positive controls using IMR32 neuroblastoma cell line, which has been previously characterised in our laboratory, were routinely included in the experiments. In addition, controls in which the DOP-PCR-amplified normal DNA was compared to nick-translated normal DNA were employed to ensure that the DOP-PCR amplification did not introduce artefactual gains or losses in the results.

Short term tissue culture

For 15 of the 21 samples in which the DNA was bulk-extracted, tissue cultures were prepared and maintained for short term (< 1 week) for interphase FISH analysis. For this, the tissue sample was dissociated into small pieces and digested in 250U/ml collagenase IV (Gibco BRL) in culture media (RPMI 1640, 10% fetal bovine serum, antibiotics) for 2-3 hours. Resulting cell suspension was centrifuged gently and washed with phosphate buffer saline, seeded into tissue culture flasks for attachment (usually 1-3 days) and subsequently harvested for interphase FISH analysis.

Fluorescence in situ Hybridization (FISH)

Harvested cytogenetic preparations from patients were dropped onto glass slides as previously described [22] using 1.5 hour colcemid treatment and 75 mM KCl

hypotonic treatment. Normal cytogenetic control slides were made from phytohaemagglutinin-stimulated normal male lymphoblasts. Denaturation of the centromere enumeration probe 8 (CEP8) and 8q24 (MYCC) FISH probes (Vysis, Downers Grove, IL) and application of the probe(s) to the slides were as per manufacturer's instructions (Vysis, Downers Grove, IL). At least 100 nuclei were used for enumerating the co-hybridized probes for each sample.

RESULTS

CGH Analysis of Bulk Extracted Tumor

CGH analysis of the bulk-extracted tumor samples revealed no chromosomal imbalances in 16 of the 21 samples examined. In 2 of the 5 samples which showed copy number changes, two were considered inconclusive given that the only changes observed were associated with the large heterochromatic region of the Y chromosome (Yq12) which is an established cytogenetic polymorphism. In contrast, three patient samples, namely patient CaP13, CaP14 and CaP26 revealed a gain of the long arm of chromosome 8 (8q). Furthermore, a concurrent loss of the short arm of chromosome 8 (8p) was observed in CaP13 and CaP14, suggestive of isochromosome 8q formation. Both CaP13 and CaP14 also showed loss of 13q, while the latter showed additional loss of 16q and 18q (Fig 1). The positive control IMR32 neuroblastoma line prepared for CGH showed high-level amplification at the 2p22 and 2p24 chromosomal regions, as expected (not shown). The negative control (normal male DNA) showed no CGH imbalance, as expected.

CGH Analysis of Microdissected DOP-PCR Derived Tumor

In contrast, extensive chromosomal gains and losses were observed by CGH in 2 of the 3 microdissected samples of PIN foci, as well as in 3 of the 3 carcinoma foci infiltrating into the capsule (Fig 2). The control experiment which compared the PCR amplified normal DNA with the nick translated normal DNA showed no chromosomal imbalances (not shown), suggesting that the changes observed in the microdissected samples were not artifacts of the PCR amplification. Within a given tumor specimen, the carcinoma foci consistently exhibited a more complex pattern of changes than the

corresponding PIN (Table 1). Moreover, in 2 of the 3 tissue samples analyzed, a subset of the changes observed in PIN were also represented in the adjacent carcinoma sample from the same patient (Table 1). This occurrence of common genomic imbalances in both PIN and carcinoma provides support for the view that the PIN may be a precursor lesion of carcinoma. A gain of 8q was a consistent feature observed among the carcinoma foci from all 3 patients, while 2 of the 3 samples also consistently exhibited +13q14.3-21.2 and -16p (Fig 2; Table 1). No consistent pattern of changes was noted among the PIN samples.

Cellular Heterogeneity of Chromosome 8 Determined by Interphase FISH

Dual-color interphase FISH was used to examine tumor preparations to determine the extent of cellular heterogeneity for chromosome 8 copy number alteration (Fig 1). Centromere 8 probe (CEP8, green) was used together with *MYCC* (8q24, orange) probe to interrogate the extent of chromosome 8q gain in the patient samples (Table 2). *MYCC* was found to always correlate in a 1:1 ratio with CEP8 in the normal control and the patient material nuclei. In control normal male lymphocytes, trisomy 8, as determined by 3 CEP8/*MYCC* signals, was observed in less than 1% of the cells. In contrast to this baseline frequency, all the patient samples for which cytogenetic preparations were established, including those in which CGH failed to identify a gain of chromosome 8, exhibited a frequency of trisomy ranging from 5% to 44% (Table 2). In addition, low levels of monosomy and polysomy of chromosome 8 were also detected in all patient samples (Table 2).

DISCUSSION

There is mounting evidence that CaP is a multifocal, heterogeneous disease. Studies examining allelic imbalances reveal that tumor foci within a given prostate are genotypically heterogeneous [6, 11, 12, 23]. Moreover, similar studies of PIN indicate heterogeneity exists at early stage of tumor progression, indicating that several foci of carcinoma may arise independently within a given tumor [12]. It is becoming increasingly important to develop and refine techniques to examine chromosomal imbalances that may contribute to genomic destabilization leading to neoplasia and progression [24, 25].

CGH is a FISH-based technique which measures the genome-wide dosage changes in a tumor sample relative to the reference sample. CGH is well suited to detect the copy number changes in homogeneous cell samples. Prostate tumors obtained from radical prostatectomy exhibit variable histological patterns, ranging from PIN to high Gleason patterns, within close spatial proximity. Moreover, the tumor foci are often closely associated with the stroma. In conventional CGH it is probable that both genotypic and phenotypic heterogeneity within the tumor, as well as the contamination by the stromal component lead to over-representation of homogenous aberrations and under-representation of more heterogeneous elements [14, 21]. In this study, CGH analysis using bulk extracted DNA detected significant aberrations in only 3 of the 21 tumor samples examined. This figure is significantly lower than the previous CGH report of aberrations in 74% of the studied samples [17]. This difference may in part be a result of our analysis focusing on earlier stages [15, 17, 18, 26]. Our FISH analysis showed considerable cell-by-cell heterogeneity at the CEP8/*MYCC* loci in all 15 cytogenetic

preparations. It is particularly interesting that in the patient sample which exhibited the most pronounced degree of trisomy 8 (44%; CaP10), the corresponding CGH analysis failed to detect a gain (Fig 1). The poor correlation between imbalances detected by CGH analysis of bulk extracted DNA and the parallel cell-by-cell analysis by FISH is an indication that this technique is not adequate for detecting the heterogeneous changes of CaP.

Recently several investigators have reported a significant advantage in combining the CGH with the techniques of DOP-PCR and LCM in identifying the aberrations in prostate and other tumor types [13, 27-35]. With this approach, Kim et al. have reported positive identification of aberrations in 100% of the tumor samples they screened [34]. This figure is consistent with the data presented herein, where all 3 of 3 tumor foci and 2 of 3 PIN foci exhibited positive aberrations. It is also noteworthy that a subset of these aberrations were uniquely present in only one of the pair of foci obtained from the same tissue sample, and would likely have gone undetected if the tissue were sampled as a whole using bulk extraction methods. Therefore, the complete repertoire of genomic aberrations in a given tumor is better represented by the sum of the changes in individual foci, rather than the averaged profiles indicated by the conventional CGH. Moreover, analysis at the level of individual foci provides a better correlation of the genomic changes with the phenotypic features.

Of the several reported chromosomal changes associated with CaP, including those on chromosomes 7, 8, 10, 13q, 16, 17, 18q, and Y [16-18, 36-43], aberrations on chromosome 8 have received the most attention. Allelotyping experiments have demonstrated frequent involvement of chromosome 8 in CaP tumorigenesis, and analysis

of extensive loss of heterozygosity (LOH) loci along 8p in CaP patients [6, 44-47]] have narrowed three tumor suppressor gene loci along the region 8p12, 8p21, and 8p22. Recent studies by Macoska et al. [48] and Virgin et al. [49] using human papillomavirus (HPV) E6/E7 and simian virus 40 (SV40) Large T antigen immortalised CaP patient cell lines, showed a direct correlation between 8p LOH allelotyping data and isochromosome 8q formation or other structural rearrangements of 8p by molecular cytogenetics. However, it was also shown that 8q gain could occur independently of 8p loss through complex structural rearrangements [48]. Alers et al. [50] demonstrated by FISH in localised prostate tumors, lymph node metastases, and distant metastases samples that +8 was more frequent than -8. Subsequent examination of the lymph node metastasis sample allowed correlation of +8 in interphase FISH with 8q gain as determined by CGH, and conversely -8 by FISH with 8p loss by CGH [50]. Together, these observations suggest that 8q gain may be independent of, and contributes to the 8p- genotype in the tumorigenic process, but can also sometimes occur through isochromosome 8q formation. This view is consistent with the data presented herein, in which 2 of the 3 patients (CaP13, CaP14) examined by CGH using bulk extracted DNA exhibited chromosome 8q gain and 8p loss concomitantly (Fig 1). In contrast, CGH analysis of all the microdissected specimens revealed a gain of 8q, in absence of 8p loss, to be a consistent feature of the invasive foci. This apparent discrepancy may be reconciled by the possibility that the 8p loss may be a recurrent aberration represented in several independent microfoci. This loss may be sufficient for detection by conventional CGH but appears to be irrelevant to the development of the invasive phenotype.

There is evidence which suggests that these foci may be genomically unstable, giving rise to further variant foci during tumor progression [51-53]. Genomic instability may be genotypically expressed as microsatellite instability as a result of failing DNA repair at the nucleotide level leading to replication errors [24, 25, 52, 53], or as chromosomal instability due to aberrations in the mitotic machinery leading to chromosomal copy number and structural changes, that ultimately lead to aneuploidy and destabilization of the tumor karyotype [24, 25, 51, 54, 55]. Given the slow rate of tumor growth in CaP, it may be speculated that the disease progression involves independent evolution of several individual foci that have acquired different genotypic changes in response to the selective pressure of the microenvironment of the prostate [56, 57]. In this regard, it is feasible that the repertoire of the individual foci within a tumor, rather than the most representative feature, may have a greater impact on the stage, and the outcome of the disease than the Gleason score *per se*. Thus in this view, the genomic profile of each tumor focus likely represents a unique endpoint of a complex interplay between genomic divergence through the multistep accumulation of genetic changes [6, 44, 46, 47, 55, 58-61], and convergence through selection. Taken together, these observations, together with the present data further support the notion of independent evolution of individual microfoci within tumors, and further suggest that the disease progression may be impacted by the individual, unique evolution of each foci rather than the tumor as a whole.

CONCLUSION

The present study demonstrates that CGH analysis using bulk dissected fresh tissue is not sufficiently sensitive to fully detect the chromosomal numerical aberrations in CaP. Given the considerable intratumor genomic heterogeneity, CGH in conjunction with microdissection and DOP-PCR amplification provides a more complete repertoire of aberrations as well as a better phenotype-genotype correlation in prostate tumors.

ACKNOWLEDGEMENTS

The authors gratefully acknowledge the support and technical expertise of Dr. J.M. Sweet, Dr. M.A.S. Jewett, Dr. J. Trachtenberg, Dr. M. Beheshti, and Jane Bayani. Financial support for this project is funded by the U.S. Army Medical Research and Materiel Command (USAMRMC) Prostate Cancer Research Program (PCRP). PCP was supported by the AFUD and the Imclone Systems, Inc.

FIGURE LEGEND

Figure 1. Representative metaphase spreads analysed by CGH, using bulk extracted DNA from patients CaP14 and CaP10 (panel A, D respectively), and corresponding karyogram (panel B, E). Regions of gains and losses in tumor DNA are represented as shifts to higher and lower green to red ratios, respectively. Note the lack of 8q gain in the CGH profile of CaP10 (E), despite the evidence of high frequency of trisomy 8, as detected by FISH analysis using CEP8 (green) and *MYCC* (8q24; orange) probes (panel C, F)

Figure 2. H&E images, and corresponding CGH analysis of focus of carcinoma (panel A, B) and PIN (panel C, D), microdissected by laser capture from the same representative tissue sample (patient C). Note the extension of the carcinoma into the capsular margin, demarcated by a large blood vessel (arrow, A). Panel E summarizes the gains (shown right of the chromosome) and losses (left of the chromosome) in the carcinoma (red) and PIN (blue) foci from this and two other patient samples.

Table 1. Summary of aberrations in microdissected foci of carcinoma and PIN from three patients.

Patient	Gleason Pattern 3	PIN
A	+3	+3p24-pter
	+4q13.3	+3p12.2-q13.2
	+4q23-q24	+8q
	+8q	+15q15-q21.2
	+13q14.3-q21.1	-20
	+14q13-q22.3	
	-16p	
	-17p	
	+Xq	
B	+2q31.1-31.2	+2q24.1-q31.2
	+5q11.1-12	+8q21.3-q22.3
	+8q	+Xq21.3-q22.2
	+10q21.1-22.2	-Y
	+13q14.2-21.2	
	-16	
	+Xq	
C	-Y	
	+8q12.1-qter	
	+Xp21.3-pter	

Table 2. Interphase FISH analyses of the centromere 8/*MYCC* copy number in the CaP patients. In each case, the number of *MYCC* signals equaled that of the centromere 8 signals. Note the variability in the centromere 8 copy number around the diploid modal value, and the significantly greater frequency of trisomy in all the patient samples compared to the baseline frequency observed in the normal lymphocyte. Boldface indicates interesting chromosome 8 copy changes observed by this method.

Sample	Chromosome 8 Copy Number			
	1	2	3	≥4
Normal	1%	96%	0%	3%
Lymphocytes				
1	4%	84%	6%	6%
2	7%	76%	5%	12%
3	1%	90%	7%	2%
4	1%	86%	7%	6%
5	5%	76%	18%	1%
6	5%	80%	8%	7%
7	1%	85%	11%	3%
8	10%	80%	7%	3%
9	5%	86%	8%	1%
10	4%	49%	44%	3%
11	10%	83%	4%	3%
12	3%	90%	6%	1%
13	8%	70%	14%	8%
14	2%	92%	6%	0%
15	3%	92%	4%	1%

REFERENCES

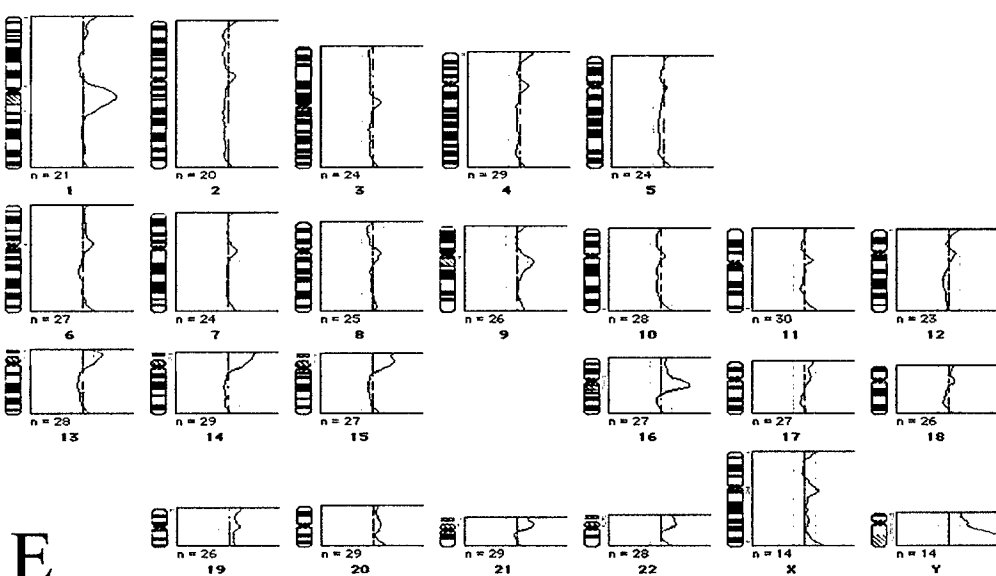
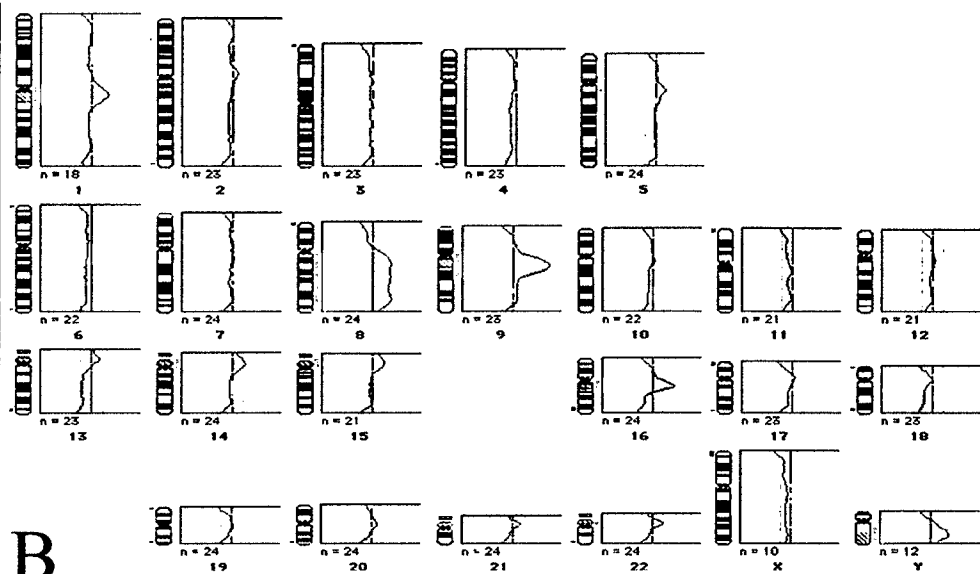
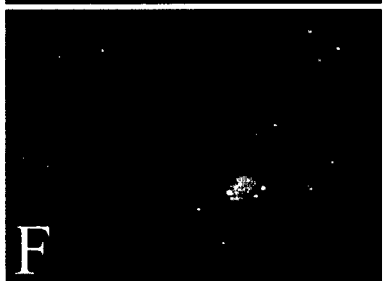
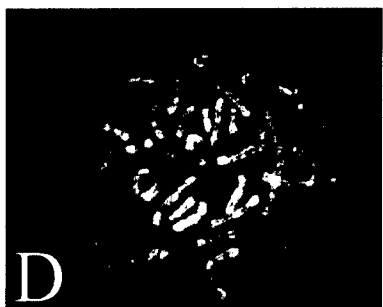
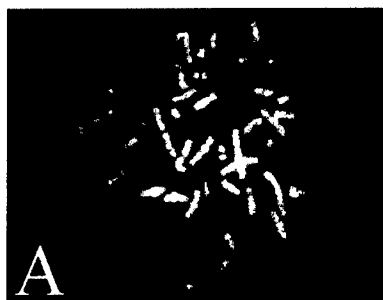
1. Haas GP, Sakr WA. Epidemiology of prostate cancer. *CA Cancer J Clin* 1997;47:273-87.
2. Scher HI, Isaacs JT, Fuks Z, et al (1995). Prostate Cancer. In *Clinical Oncology*. Eds. Churchill Livingstone Inc., New York. pp.
3. Wullich B, Breitkreuz T, Zwergel T, Unteregger G, Seitz G, Zang KD. Cytogenetic evidence of intratumoral focal heterogeneity in prostatic carcinomas. *Urologia Internationalis* 1992;48:372-7.
4. Micale MA, Sanford JS, Powell IJ, Sakr WA, Wolman SR. Defining the extent and nature of cytogenetic events in prostatic adenocarcinoma: paraffin FISH vs. metaphase analysis. *Cancer Genetics & Cytogenetics* 1993;69:7-12.
5. Aihara M, Wheeler TM, Ohori M, Scardino PT. Heterogeneity of prostate cancer in radical prostatectomy specimens. *Urology* 1994;43:60-6; discussion 66-7.
6. Macintosh CA, Stower M, Reid N, Maitland NJ. Precise microdissection of human prostate cancers reveals genotypic heterogeneity. *Cancer Research* 1998;58:23-8.
7. Lalani EN, Stubbs A, Stamp GW. Prostate cancer; the interface between pathology and basic scientific research. *Semin Cancer Biol* 1997;8:53-9.
8. Oesterling J, Fuks Z, Lee CT, Scher HI (1997). Cancer of the prostate. In *Cancer: Principles & Practice of Oncology*. Eds. Lippincott-Raven Publishers, Philadelphia. pp. 1322-1385.
9. Teixeira MR, Waehre H, Lothe RA, Stenwig AE, Pandis N, Giercksky KE, Heim S. High frequency of clonal chromosome abnormalities in prostatic neoplasms sampled by prostatectomy or ultrasound-guided needle biopsy. *Genes Chromosomes Cancer* 2000;28:211-9.
10. Bastacky SI, Wojno KJ, Walsh PC, Carmichael MJ, Epstein JI. Pathological features of hereditary prostate cancer. *J Urol* 1995;153:987-92.
11. Ruijter ET, Miller GJ, van de Kaa CA, van Bokhoven A, Bussemakers MJ, Debruyne FM, Ruiter DJ, Schalken JA. Molecular analysis of multifocal prostate cancer lesions. *J Pathol* 1999;188:271-7.
12. Bostwick DG, Shan A, Qian J, Darson M, Maihle NJ, Jenkins RB, Cheng L. Independent origin of multiple foci of prostatic intraepithelial neoplasia: comparison with matched foci of prostate carcinoma. *Cancer* 1998;83:1995-2002.
13. Zitzelsberger H, Kulka U, Lehmann L, Walch A, Smida J, Aubele M, Lorch T, Hofler H, Bauchinger M, Werner M. Genetic heterogeneity in a prostatic carcinoma and associated prostatic intraepithelial neoplasia as demonstrated by combined use of laser- microdissection, degenerate oligonucleotide primed PCR and comparative genomic hybridization. *Virchows Arch* 1998;433:297-304.
14. Kallioniemi A, Kallioniemi OP, Sudar D, Rutovitz D, Gray JW, Waldman F, Pinkel D. Comparative genomic hybridization for molecular cytogenetic analysis of solid tumors. *Science* 1992;258:818-21.
15. Cher ML, MacGrogan D, Bookstein R, Brown JA, Jenkins RB, Jensen RH. Comparative genomic hybridization, allelic imbalance, and fluorescence in situ

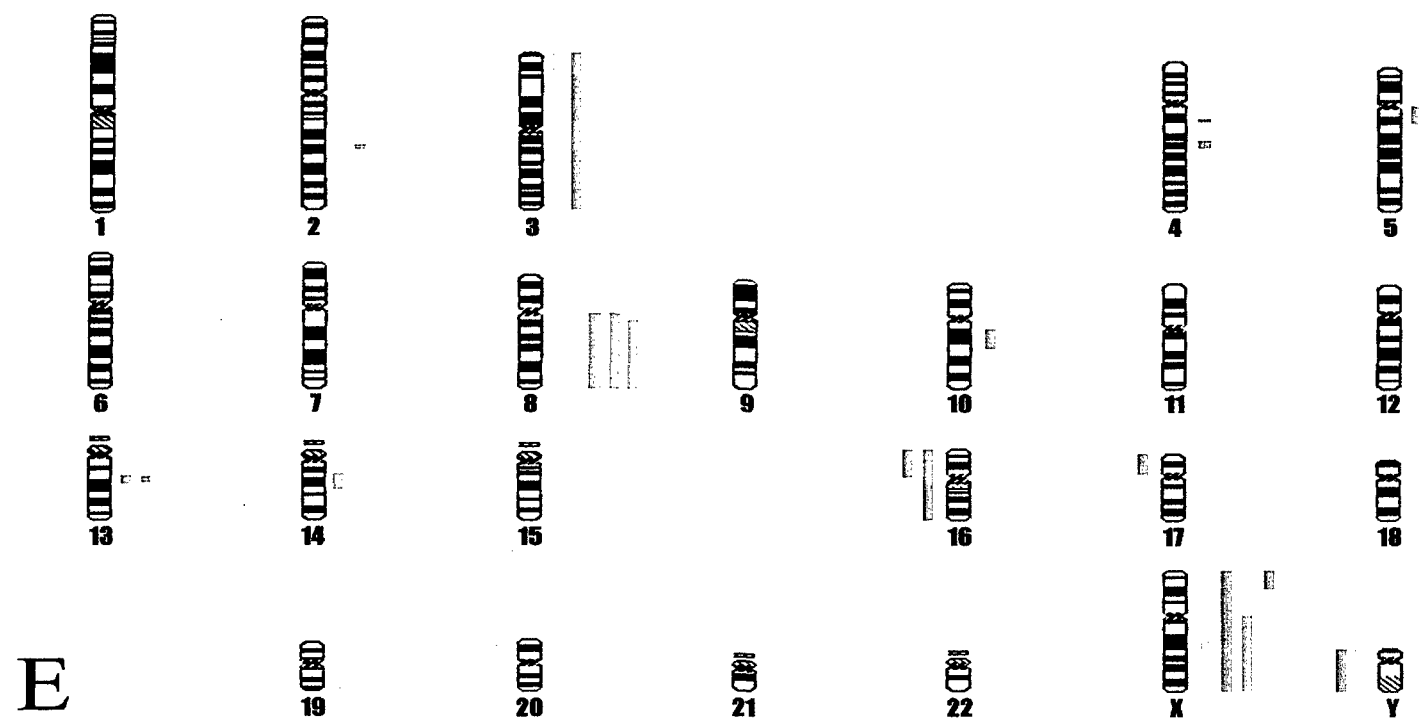
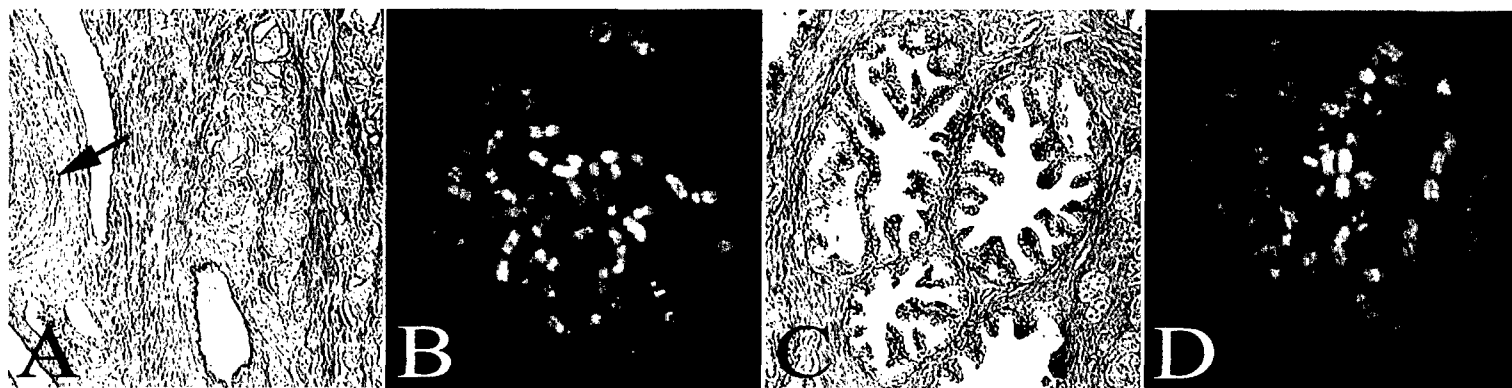
- hybridization on chromosome 8 in prostate cancer. *Genes, Chromosomes & Cancer* 1994;11:153-62.
16. Joos S, Bergerheim US, Pan Y, Matsuyama H, Bentz M, du Manoir S, Lichter P. Mapping of chromosomal gains and losses in prostate cancer by comparative genomic hybridization. *Genes, Chromosomes & Cancer* 1995;14:267-76.
 17. Visakorpi T, Kallioniemi AH, Syvanen AC, Hyytinen ER, Karhu R, Tammela T, Isola JJ, Kallioniemi OP. Genetic changes in primary and recurrent prostate cancer by comparative genomic hybridization. *Cancer Research* 1995;55:342-7.
 18. Cher ML, Bova GS, Moore DH, Small EJ, Carroll PR, Pin SS, Epstein JI, Isaacs WB, Jensen RH. Genetic alterations in untreated metastases and androgen-independent prostate cancer detected by comparative genomic hybridization and allelotyping. *Cancer Research* 1996;56:3091-102.
 19. Ausubel F, Brent R, Kingston R, Moore D, Seidman J, Smith J, Sturhl K (1998). *Current Protocols in Molecular Biology*. John Wiley & Sons, Inc., New York, USA.
 20. Dracopoli NC (1998). *Current Protocols in Human Genetics*. John Wiley & Sons, Inc., New York, USA.
 21. Kallioniemi OP, Kallioniemi A, Piper J, Isola J, Waldman FM, Gray JW, Pinkel D. Optimizing comparative genomic hybridization for analysis of DNA sequence copy number changes in solid tumors. *Genes, Chromosomes & Cancer* 1994;10:231-43.
 22. Gustashaw KM (1997). Chromosome Stains. In *The AGT cytogenetics laboratory manual*. Eds. Lippincott-Raven Publishers, Philadelphia. pp. 259-324.
 23. Takimoto Y, Shimazui T, Akaza H, Sato N, Noguchi M. Genetic heterogeneity of surgically resected prostate carcinomas and their biopsy specimens is related to their histologic differentiation. *Cancer* 2001;91:362-70.
 24. Cahill D, Lengauer C, Yu J, Riggins G, Willson J, Markowitz S, Kinzler K, Vogelstein B. Mutations of mitotic checkpoint genes in human cancers. *Nature* 1998;392:300-3.
 25. Lengauer C, Kinzler KW, Vogelstein B. Genetic instabilities in human cancers. *Nature* 1998;396:643-9.
 26. El Gedaily A, Bubendorf L, Willi N, Fu W, Richter J, Moch H, Mihatsch MJ, Sauter G, Gasser TC. Discovery of new DNA amplification loci in prostate cancer by comparative genomic hybridization. *Prostate* 2001;46:184-90.
 27. Speicher MR, du Manoir S, Schrock E, Holtgreve-Grez H, Schoell B, Lengauer C, Cremer T, Ried T. Molecular cytogenetic analysis of formalin-fixed, paraffin-embedded solid tumors by comparative genomic hybridization after universal DNA-amplification. *Human Molecular Genetics* 1993;2:1907-14.
 28. Wiltshire RN, Duray P, Bittner ML, Visakorpi T, Meltzer PS, Tuthill RJ, Liotta LA, Trent JM. Direct visualization of the clonal progression of primary cutaneous melanoma: application of tissue microdissection and comparative genomic hybridization. *Cancer Res* 1995;55:3954-7.
 29. Kuukasjarvi T, Tanner M, Pennanen S, Karhu R, Visakorpi T, Isola J. Optimizing DOP-PCR for universal amplification of small DNA samples in comparative genomic hybridization. *Genes Chromosomes Cancer* 1997;18:94-101.

30. Aubele M, Mattis A, Zitzelsberger H, Walch A, Kremer M, Welzl G, Hofler H, Werner M. Extensive ductal carcinoma In situ with small foci of invasive ductal carcinoma: evidence of genetic resemblance by CGH. *Int J Cancer* 2000;85:82-6.
31. Aubele M, Mattis A, Zitzelsberger H, Walch A, Kremer M, Hutzler P, Hofler H, Werner M. Intratumoral heterogeneity in breast carcinoma revealed by laser-microdissection and comparative genomic hybridization. *Cancer Genet Cytogenet* 1999;110:94-102.
32. Aubele M, Zitzelsberger H, Schenck U, Walch A, Hofler H, Werner M. Distinct cytogenetic alterations in squamous intraepithelial lesions of the cervix revealed by laser-assisted microdissection and comparative genomic hybridization. *Cancer* 1998;84:375-9.
33. Kim SH, Godfrey T, Jensen RH. Whole genome amplification and molecular genetic analysis of DNA from paraffin-embedded prostate adenocarcinoma tumor tissue. *J Urol* 1999;162:1512-8.
34. Kim S-H, Kim MS, Jensen RH. Genetic alterations in microdissected prostate cancer cells by comparative genomic hybridization. *Prostate Cancer and Prostatic Diseases* 2000;3:110-14.
35. Verhagen PC, Zhu XL, Rohr LR, Cannon-Albright LA, Tavtigian SV, Skolnick MH, Brothman AR. Microdissection, DOP-PCR, and comparative genomic hybridization of paraffin-embedded familial prostate cancers. *Cancer Genet Cytogenet* 2000;122:43-8.
36. Alcaraz A, Takahashi S, Brown JA, Herath JF, Bergstralh EJ, J. L-KJ, Lieber MM, Jenkins RB. Aneuploidy and aneusomy of chromosome 7 detected by fluorescence in situ hybridization are markers of poor prognosis in prostate cancer. *Cancer Research* 1994;54:3998-4002.
37. Brothman AR, Watson MJ, Zhu XL, Williams BJ, Rohr LR. Evaluation of 20 archival prostate tumor specimens by fluorescence in situ hybridization (FISH). *Cancer Genetics & Cytogenetics* 1994;75:40-4.
38. Deubler DA, Williams BJ, Zhu XL, Steele MR, Rohr LR, Jensen JC, Stephenson RA, Changus JE, Miller GJ, Becich MJ, Brothman AR. Allelic loss detected on chromosomes 8, 10, and 17 by fluorescence in situ hybridization using single-copy P1 probes on isolated nuclei from paraffin-embedded prostate tumors. *American Journal of Pathology* 1997;150:841-50.
39. Hyytinen ER, Frierson HF, Jr., Boyd JC, Chung LW, Dong JT. Three distinct regions of allelic loss at 13q14, 13q21-22, and 13q33 in prostate cancer. *Genes Chromosomes Cancer* 1999;25:108-14.
40. Macoska JA, Trybus TM, Sakr WA, Wolf MC, Benson PD, Powell IJ, Pontes JE. Fluorescence in situ hybridization analysis of 8p allelic loss and chromosome 8 instability in human prostate cancer. *Cancer Research* 1994;54:3824-30.
41. Li C, Larsson C, Futreal A, Lancaster J, Phelan C, Aspenblad U, Sundelin B, Liu Y, Ekman P, Auer G, Bergerheim US. Identification of two distinct deleted regions on chromosome 13 in prostate cancer. *Oncogene* 1998;16:481-7.
42. Qian J, Bostwick DG, Takahashi S, Borell TJ, Brown JA, Lieber MM, Jenkins RB. Comparison of fluorescence in situ hybridization analysis of isolated nuclei and routine histological sections from paraffin-embedded prostatic adenocarcinoma specimens. *American Journal of Pathology* 1996;149:1193-9.

43. Sauter G, Bubendorf L, Moch H, Gasser TC, Mihatsch MJ. Cytogenetic changes in prostatic carcinoma. *Pathologe* 1998;19:63-8.
44. Prasad MA, Trybus TM, Wojno KJ, Macoska JA. Homozygous and frequent deletion of proximal 8p sequences in human prostate cancers: identification of a potential tumor suppressor gene site. *Genes Chromosomes Cancer* 1998;23:255-62.
45. Wang JC, Radford DM, Holt MS, Helms C, Goate A, Brandt W, Parik M, Phillips NJ, DeSchryver K, Schuh ME, Fair KL, Ritter JH, Marshall P, Donis-Keller H. Sequence-ready contig for the 1.4-cM ductal carcinoma in situ loss of heterozygosity region on chromosome 8p22-p23. *Genomics* 1999;60:1-11.
46. Haggman MJ, Wojno KJ, Pearsall CP, Macoska JA. Allelic loss of 8p sequences in prostatic intraepithelial neoplasia and carcinoma. *Urology* 1997;50:643-7.
47. Perinchery G, Bukurov N, Nakajima K, Chang J, Hooda M, Oh BR, Dahiya R. Loss of two new loci on chromosome 8 (8p23 and 8q12-13) in human prostate cancer. *Int J Oncol* 1999;14:495-500.
48. Macoska JA, Beheshti B, Rhim JS, Hukku B, Lehr J, Pienta KJ, Squire JA. Genetic characterization of immortalized human prostate epithelial cell cultures. Evidence for structural rearrangements of chromosome 8 and i(8q) chromosome formation in primary tumor-derived cells. *Cancer Genet Cytogenet* 2000;120:50-7.
49. Virgin JB, Hurley PM, Nahhas FA, Bebachuk KG, Mohamed AN, Sakr WA, Bright RK, Cher ML. Isochromosome 8q formation is associated with 8p loss of heterozygosity in a prostate cancer cell line. *Prostate* 1999;41:49-57.
50. Alers JC, Krijtenburg PJ, Rosenberg C, Hop WC, Verkerk AM, Schroder FH, van der Kwast TH, Bosman FT, van Dekken H. Interphase cytogenetics of prostatic tumor progression: specific chromosomal abnormalities are involved in metastasis to the bone. *Lab Invest* 1997;77:437-48.
51. Pihan GA, Purohit A, Wallace J, Malhotra R, Liotta L, Doxsey SJ. Centrosome defects can account for cellular and genetic changes that characterize prostate cancer progression. *Cancer Res* 2001;61:2212-9.
52. Egawa S, Uchida T, Suyama K, Wang C, Ohori M, Irie S, Iwamura M, Koshiba K. Genomic instability of microsatellite repeats in prostate cancer: relationship to clinicopathological variables. *Cancer Res* 1995;55:2418-21.
53. Dahiya R, Lee C, McCarville J, Hu W, Kaur G, Deng G. High frequency of genetic instability of microsatellites in human prostatic adenocarcinoma. *Int J Cancer* 1997;72:762-7.
54. Pihan GA, Doxsey SJ. The mitotic machinery as a source of genetic instability in cancer. *Semin Cancer Biol* 1999;9:289-302.
55. Beheshti B, Park PC, Sweet JM, Trachtenberg J, Jewett MAS, Squire JA. Evidence of chromosomal instability in prostate cancer determined by spectral karyotyping (SKY) and interphase FISH analysis. *Neoplasia* 2001;3:62-69.
56. Olumi AF, Grossfeld GD, Hayward SW, Carroll PR, Tlsty TD, Cunha GR. Carcinoma-associated fibroblasts direct tumor progression of initiated human prostatic epithelium. *Cancer Res* 1999;59:5002-11.
57. Hayward SW, Rosen MA, Cunha GR. Stromal-epithelial interactions in the normal and neoplastic prostate. *Br J Urol* 1997;79 Suppl 2:18-26.

58. Suzuki H, Freije D, Nusskern DR, Okami K, Cairns P, Sidransky D, Isaacs WB, Bova GS. Interfocal heterogeneity of PTEN/MMAC1 gene alterations in multiple metastatic prostate cancer tissues. *Cancer Res* 1998;58:204-9.
59. Hugel A, Wernert N. Loss of heterozygosity (LOH), malignancy grade and clonality in microdissected prostate cancer. *Br J Cancer* 1999;79:551-7.
60. Saric T, Brkanac Z, Troyer DA, Padalecki SS, Sarosdy M, Williams K, Abadesco L, Leach RJ, O'Connell P. Genetic pattern of prostate cancer progression. *Int J Cancer* 1999;81:219-24.
61. Rohrbach H, Haas CJ, Baretton GB, Hirschmann A, Diebold J, Behrendt RP, Lohrs U. Microsatellite instability and loss of heterozygosity in prostatic carcinomas: comparison of primary tumors, and of corresponding recurrences after androgen-deprivation therapy and lymph-node metastases. *Prostate* 1999;40:20-7.





Microarray CGH

Ben Beheshti, Paul C. Park, Ilan Braude, Jeremy A. Squire

Ontario Cancer Institute, Princess Margaret Hospital, University Health Network, and Departments of Laboratory Medicine and Pathobiology, and Medical Biophysics, Faculty of Medicine, University of Toronto, Ontario, Canada.

From: "Methods In Molecular Medicine" Humana Press (to be published 2002)

Editor Yao Shan Fan

"Molecular Cytogenetics: Protocols and Applications"

Chapter title: "Microarray CGH"

*Corresponding Author:

JA Squire, Ph.D.
Ontario Cancer Institute
Division of Cellular and Molecular Biology
610 University Ave. Room 9-721
Toronto, Ontario, Canada
M5G 2M9
E-mail: jeremy.squire@utoronto.ca
Fax 416-920-5413

1. Introduction

Comparative genomic hybridization (CGH) to metaphase chromosome targets (1,2) has significantly contributed to our understanding of the cancer cytogenetics of more complex malignancies such as the solid tumours (*see* chapter 9; reviewed in (3,4)). This molecular cytogenetics-based technique (hereafter referred to as “chromosome CGH”) is capable of defining genome-wide DNA copy number imbalances in sample cells relative to a normal reference in a single experiment. Chromosome CGH has greatly increased our understanding of tumour biology and progression since the minimal recurrent regions of chromosomal gain and loss are likely to contain novel oncogene(s) and tumour suppressor gene(s) respectively.

Limitations of Chromosome CGH

The unique advantage of chromosome CGH is its whole-genome screening capability which is significantly faster and less laborious than low-throughput methods for examining single-target dosage changes such as Southern analysis, PCR, and fluorescence *in situ* hybridization (FISH). Chromosome CGH is now a well-established molecular cytogenetic method, but there are two technical limitations that restrict its usefulness as a comprehensive screening tool. First, because the target DNA within the chromosome is highly condensed and supercoiled, the resolution for determining copy number changes is no less than 10 Mb for loss (1). For copy number gains, the minimal detectable size is probably no less than 2 Mb, which is a function of both amplicon size and copy number (1,5). This resolution, while capable of providing a starting point for positional cloning studies, will still encompass too many genes to precisely localize a sequence of interest. Second, the analysis of the images obtained following chromosome

CGH is only partly automated and experienced cytogeneticists must identify each chromosome to determine regions of imbalances.

Microarray CGH: Application of Microarray Technology to CGH

Recent developments in microarray methods have circumvented some of the limitations of chromosome CGH. Complementary DNA (cDNA) microarray technology, realized through advances in the Human Genome Project (HGP) as well as robotic arraying technology on glass slides, has facilitated high-throughput analysis of differential gene expression in tumours (6-8). An emerging platform that addresses the shortcomings of chromosome CGH couples the technique to microarray expression technology, and is generally referred to as “microarray CGH”. Instead of using metaphase chromosomes, CGH is applied to arrayed short sequences of DNA bound to glass slides (herein defined as the “targets” for hybridization) and probed with genomes of interest (herein defined as the “probe”) (*see* Note 1). With sufficient representation on the microarray, this system significantly increases resolution for localizing regions of imbalance. Furthermore, just as with expression microarray screening, analysis is straightforward and automated. Two technology platforms have recently been published: 1) cDNA-based array CGH (9,10); and 2) genomic DNA-based array CGH (also referred to as “matrix CGH” and “array CGH”) (11,12). This chapter will provide an overview of the currently published methods, but readers should be aware that microarray CGH is an emerging technology and there are likely to be continual refinements to the protocols described below.

1.1. cDNA Array CGH

Microarray CGH using cDNA targets (hereafter referred to as “cDNA array CGH”) was first described by Pollack et al. (9). This platform makes use of conventional cDNA microarrays, normally employed in expression screening, for examining genomic copy number imbalances. As depicted in Figure 1, this has the advantage that duplicate arrays may be used in parallel to provide a comprehensive overview of both expression and gene copy number change in a tissue (9). The increasing availability of a variety of different cDNA microarray expression formats means that modification of protocols to interrogate these cDNA targets by CGH is immediately accessible for high-throughput analysis of gene dosage changes.

1.1.1. Application of cDNA Array CGH to Cancer Genomics

Pollack et al. examined breast cancer cell lines and tissues using a 3,360 feature microarray by cDNA array CGH (9). With optimization, they demonstrated that the technique was capable of detecting copy number gains and single deletion losses. Analysis of the tumours and cell lines showed that not all amplified genes were overexpressed, nor were most highly overexpressed genes amplified; however, a subset of the genes, including *ERBB2*, were observed to be both amplified and overexpressed. They proposed that these genes might be important mediators of the tumour initiation and progression.

The utility of cDNA array CGH for detecting gene amplifications was recently shown by Heiskanen et al. (13). In this study, cell lines with known gene amplifications were used to establish the sensitivity limits of the technique. In contrast to the protocol used by others (9,10), genomic DNA is biotin-labeled and a tyramide amplification protocol (14) is employed (13). Progressive dilution from 100% to 2% of genomic DNA

from the neuroblastoma cell line NGP with normal DNA during labeling corresponded to decreasing *MYCN* signal intensity on the microarray. Amplifications of 5-fold and greater were readily detected by this method, and at 2% dilution *MYCN* intensity was observed at 2.5-fold relative to other non-amplified genes. However, the main limitation of this method is its inability to allow two-colour CGH and thus necessitates the use of two microarrays (test, control) per experiment.

Recently, we have demonstrated the suitability of cDNA array CGH for gene amplification screening of patient samples (10). In this study, the *MYCN* (chromosome region 2p24) amplification status in neuroblastoma patients and cell lines was confirmed by cDNA array CGH on a high-density 19,200 feature microarray. In the cell line IMR32, cDNA array CGH confirmed a recently described co-amplified oncogene, *MEIS1* (15,16). Importantly, the technique was able to distinguish three tumour genotypes in patient samples not previously described (Figure 2). This study demonstrates not only the high-throughput advantage of examining thousands of genes by cDNA array CGH over conventional methods such as FISH and Southern analyses, but also the increase in resolution in contrast to chromosome CGH.

In another study by Pei et al. (17), the increased resolving power of cDNA array CGH for delineating amplicon boundaries was demonstrated in pediatric carcinomas. This work clearly shows the limited resolution of chromosome CGH when contrasted to cDNA array CGH. These results are depicted in Figure 3.

1.1.2. Current Limitations of cDNA Array CGH

There are at least three limitations to current cDNA array CGH methods. Firstly, target cDNA sequences are of low complexity in content in comparison to genomic

sequences, lacking intronic and other non-transcribed elements such as repetitive DNA and control sequences. Thus many regions of the genome being interrogated will not hybridize with uniform efficiency so that the specificity of the technique may be low or poorly reproducible. Secondly, target cDNA sequences are typically only 0.5-2 kilobases in size (9,10,13). This is on a scale of many orders of magnitude smaller than the smallest chromosome, and 1-2 orders of magnitude smaller than genomic insert sequences in bacterial artificial chromosomes (BACs), P1-derived artificial chromosomes (PACs), and cosmids. Although this may be suitable for expression mapping by microarray where the probe is comparable in size, reduced signal sensitivity may become a concern when using labeled genomic probes. Although Pollack et al. (9) describe detection of both copy number gains and losses by cDNA array CGH, it is likely that genomic DNA-based arrays are more robust for detection of single copy changes, including copy losses. Finally, a last issue with cDNA microarray technology, and therefore also with cDNA array CGH, is that currently there is a significant number of gene misannotations in the commercially available clone sets (18). This may take the form of wrongly identified sequences, incorrect chromosomal locations or even the complete absence of human sequences in the cDNA targets (eg. due to clone contamination, heterologous sequences). In practical terms this manifests as inconsistent results or findings that cannot be substantiated when other methods are applied. To eliminate this shortcoming, commercial sources of clone sets and many institutions with array fabrication capabilities are sequence-confirming their clone sets. Overall, these limitations contribute to the high rate of false positive (15%) and false negative (15%) results reported for this technique (9).

1.2. Array CGH

The second microarray CGH platform (hereafter referred to as “array CGH”) uses genomic DNA sequences as targets on the microarray. Array CGH was first established by Solinas-Toldo et al. (11), and further refined by Pinkel et al. (12). As described in these studies, the DNA targets for the microarray can be derived from genomic clones including yeast artificial chromosome (YAC; 0.2-2 Mb in size), BAC (up to 300 kb), P1 (~ 70-100 kb), PAC (~ 130-150 kb), and cosmid (~ 30-45 kb), and are of several orders of magnitude smaller than chromosome targets. This decrease in target size increases the resolution of copy number imbalance detection over chromosome CGH (Figure 4). Given the differences in the structural complexity in the target DNA with respect to chromosome CGH, modifications to the hybridization conditions are necessary (11,12). The advantage of array CGH over cDNA array CGH is that there is more uniformity in hybridization and subsequent signal fidelity because the DNA targets have a greater complexity and coverage, containing intronic and other non-transcribed genomic sequences.

1.2.1. Application of Array CGH to Cancer Genomics

To date, several groups have published results using array CGH (11,12,19-25). Pinkel et al. (12) detected genomic imbalances within a sub-band of chromosome 20 in breast cancer that had failed to be observed using chromosome CGH. Using array CGH, precise genomic mapping of the position of amplicon boundaries within 20q13.2 was performed (19). This allowed *CYP24* to be localized within the minimal amplified region, identifying it as a new candidate oncogene in breast cancer (19). In another

study, array CGH was used to examine neurofibromatosis type 2 (NF2) patients and determined the extent and frequency of deletions around the *NF2* locus on chromosome 22q (20). This microarray was constructed from a 7 Mb tiling path of 104 BAC and PAC genomic clones around *NF2*, and included smaller cosmids for mapping copy number changes at higher resolution. Both single copy losses and homozygous deletions were detectable in the patient samples by this system (Figure 5). Further refinements have permitted retrospective analysis using genomic DNA from archival samples. Daigo et al. (21) have adapted array CGH for amplicon profiling of laser capture microdissected (Arcturus, Mountain View, CA; <http://www.arctur.com>) formalin-fixed paraffin-embedded tumour samples, using degenerate oligonucleotide-primed (DOP)-PCR (26) for whole genome amplification of the extracted DNA.

1.2.3. Applications in Other Fields

Microarray CGH is a versatile technique that may be used to examine genetic disorders other than cancer. A recent study by Geschwind et al. (23) demonstrated the use of array CGH for investigating the molecular basis of laterality of the human cerebral hemispheres. Gene dosage changes in patients with Klinefelter's syndrome (karyotype: XXY) were examined with a DNA microarray constructed with cosmids covering the pseudoautosomal region of the sex chromosomes, and findings were correlated with anomalous dominance and other cognitive or behavioural phenotypes.

1.2.4. Current Issues with Genomic DNA-based Array Fabrication

Although array CGH still has some limitations, most of these relate to array production and will be addressed as the technology matures. While modifications to existing array fabrication systems are possible, current production limitations are mainly

associated with difficulties in automating batch preparation DNA from genomic clones. For example, published array CGH studies involve the use of laborious DNA extraction methods such as maxi prep kits (Qiagen) and phenol/chloroform extractions from genomic clones (11,12). However, commercially available batch extraction kits (eg. R.E.A.L. System™, Qiagen) from genomic clones coupled with DOP-PCR may aid in automation (*see* Note 2). A second difficulty is related to the generation of adequate amounts of DNA for batch microarray production. While cDNA expression clones have universal primer sites amenable to large scale PCR synthesis of genes and expressed sequence tags for subsequent purification and arraying, the same is not true for genomic clones. In addition, the larger genomic inserts require long PCR which has more exacting amplification conditions (27) and these may be confounded by the presence of repetitive DNA elements in template sequences. The third difficulty is the viscosity of large size genomic sequences in solution that may cause clogging of spotting pins of some arrayers, although new split pin designs may circumvent this problem (28). Finally, as with the cDNA clone sets, there is also the concern that a small but significant number of commercially available genomic clones are misannotated in their localization (eg. due to source clone plate contamination, mislabeling). Currently the solution is to FISH-confirm cytogenetic mappings of clones used for array CGH, although this is not a trivial task when dealing with tens or hundreds of genomic clones. The BAC/PAC resources (<http://www.chori.org/bacpac/>), further described in chapter 27, is an ongoing project to FISH-map all clones (25) that will largely alleviate this problem.

1.2.5. Current Accessibility to Genomic DNA-based Arrays

While cDNA microarrays can be obtained both commercially and from array fabrication core facilities within research institutions, array CGH is not yet immediately accessible to most researchers. At present, scientists wanting to study a chromosomal region of interest by array CGH will require custom array production. Progress in the HGP has facilitated construction of a tiling path of genomic clones that cover chromosomal loci of interest (eg. MapViewer resource at the National Center for Biotechnology Information: <http://www.ncbi.nlm.nih.gov/>). While the associated costs of genomic DNA-based microarray production are not practical for individual research laboratories, it is likely that institutional core microarray facilities will be able to modify production to address this need. Conceivably, the post-HGP era will facilitate production of whole genome arrays (29), and even higher-resolution chromosome-specific and chromosome band-specific microarrays. Notably, the first high-density whole genome microarray (approximately 2,000 BAC clones) was recently introduced (25) and demonstrated its ability to precisely delineate genome-wide segmental aneuploidy breakpoints in tumour cells.

1.2.6. Commercial Sources of Genomic DNA-based Arrays

An alternative to custom arraying of genomic targets may be to obtain commercially available microarrays. Currently, the only such system is produced by Vysis Corporation (<http://www.vysis.com>), called the GenoSensor System™. The AmpliOnc I™ array from Vysis contains BAC, PAC, and P1 genomic clones from 59 known oncogenes spotted in triplicate (30), and has been used by groups studying breast cancer (21) and glioblastoma multiforme (24). This microarray complements their GenoSensor™ microarray reader and analysis software package. The next generation

genomic microarray from Vysis will comprise 250-300 features, including genomic clones from the AmpliOnc I™ array, subtelomeric regions of all chromosomes, major tumour suppressor genes, and major microdeletion syndrome loci (30).

1.3. Detection and Analysis

Analysis of microarray CGH involves three components, namely: 1) image acquisition; 2) quantification of fluorescence intensity; and 3) interpretation. These can be accomplished using the system developed for expression microarrays with minimal or no modification.

1.3.1. Image Acquisition

Image acquisition for microarray CGH requires systematic scanning of all gridded features on the microarray. Commercially available microarray scanners are typically laser-based scanning systems that can acquire the two differential wavelengths sequentially (eg. Packard BioScience, <http://www.packardbiochip.com>) or simultaneously (eg. Virtek Vision Inc., <http://www.virtek.ca>; Axon Instruments Inc., <http://www.axon.com>). Alternatively, resources for the development of in-house microarray scanning systems are also available (eg. <http://brownlab.stanford.edu/>; (31)). The technical details underlying these systems are specific to the hardware package, and are beyond the scope of this chapter.

1.3.2. Fluorescence Quantification and Ratio Analysis

Software for fluorescence quantification and ratio analysis of gridded spots is usually included with the scanner hardware. Alternatively, there are less sophisticated softwares publicly available (eg. ScanAlyze: <http://rana.stanford.edu/>; (32)). Quantified

fluorescence intensities requires normalization and establishment of the fluorescence ratio baseline. Often, microarray features are spotted in duplicate or triplicate for assessing result reproducibility. For array CGH, inclusion of genomic clones onto the microarray from regions that are known not to be involved in copy number change are recommended as internal controls for these purposes. In addition, parallel experiments in which differentially labeled normal genomic DNA is compared against itself can serve to establish the specificity of the system. Overall, there is an obvious need for statistical analysis of the conformity of the results (33). Global normalization approaches such as those used in expression microarray experiments may also be used for establishing baseline thresholds (10,34).

Previous reports indicate that the relationship between the fluorescence ratio and copy number changes (1,9,11,12) deviates from linearity at low copy numbers. For this reason, it is important for users to independently establish this relationship for interpretation of CGH results and to confirm imbalances by direct FISH analysis of tissue sections.

1.3.3. The Role of Bioinformatics in Microarray CGH

As representation on the microarrays increases in density, data storage (35) and bioinformatics will become an important aspect of the CGH analysis. In addition, the increase in resolution will make the task of identifying consensus regions of genomic imbalance amongst samples more challenging. Overall, this will necessitate datamining techniques that can handle many data points on multiple dimensions between experiments. Moreover, for cDNA array CGH, *in silico* determination of chromosomal localisations of cDNA targets is essential for providing a comprehensive ideogram-type

schematic of chromosomal copy number changes (Figure 3) (10). As microarray CGH technology becomes more prevalent, more standardized informatics and analysis tools will appear.

Acknowledgments

The authors are grateful to Paula Marrano, Bisera Vukovic, Monique Albert, and Pascale Macgregor for critical reading of the manuscript. This work was supported by Canadian Cancer Society through the National Cancer Institute of Canada, and the U.S. Army Medical Research and Materiel Command (USAMRMC) Prostate Cancer Research Program (PCRP). PCP was supported by the AFUD and the Imclone Systems, Inc.

2. Materials

2.1. cDNA array CGH

2.1.1. Array preparation

1. 20X sodium saline citrate (SSC): Dissolve 175.32 g of NaCl, 88.23 g of sodium citrate-2H₂O in 1 L water, titrate to pH 7.0. Store at room temperature.
2. cDNA microarray. Store in dessicator at room temperature.
3. Blocking solution: 3% BSA, 4X SSC, 0.1% Tween-20. Store at -20°C.
4. Glass coverslips.

2.1.2. Probe preparation by random primer labeling of genomic DNA

1. High molecular weight genomic DNA.
2. *EcoRI* or *DpnII* (New England Biolabs).
3. Qiaquick PCR purification kit (Qiagen).
4. BioPrime labeling kit (Gibco BRL). Store at -20°C.
5. dNTP mixture: 4.8 mM each of dATP, dGTP, dTTP.
6. 2.4 mM dCTP.
7. 1 mM Cy5-dCTP, Cy3-dCTP (Amersham). Store in the dark at -20°C.
8. Microcon 30 filter (Amicon).
9. Yeast tRNA (Gibco BRL). Store at -80°C.
10. Poly(dA-dT) (Sigma). Store at -20°C.
11. Cot-1 DNA (Gibco BRL).

12. Hybridization buffer: 3.4X SSC and 0.3% SDS. Prepare fresh per experiment.

2.1.3. Probe denaturation and hybridization

1. Rubber cement.
2. Hybridization oven.

2.1.4. Washes

1. Heated water bath.
2. Coplin jars.
3. Slide centrifuge.

2.2. Array CGH

2.2.1. Array preparation

1. DNA extracted and purified from genomic clones.
2. Maxiprep DNA extraction kit (Qiagen).
3. Glass slides.
4. Glass capillary tubes or robotic arrayer.
5. Blocking solution: 10 µg/µL salmon sperm DNA (Life Technologies) in 50% formamide (Gibco BRL), 10% dextran sulphate, 2X SSC, 0.2% SDS, 0.2% Tween-20. Store at -20°C.

2.2.2. Probe preparation by nick translation of genomic DNA

1. High molecular weight genomic DNA.
2. DNA polymerase I (Roche).
3. DNase I (Gibco BRL).

4. 10X Cy3 dNTPs: 0.1 mg/mL BSA (Sigma), 0.1 M β -mercaptoethanol (Sigma), 0.5 M Tris-HCl, 50 mM MgCl₂, 0.08 mM Cy3-dCTP (Amersham), 0.2 mM dATP, 0.12 mM dCTP, 0.2 mM dTTP, 0.2 mM dGTP; dissolved in water. Store in the dark at -20°C.
5. 10X Cy5 dNTPs: 0.1 mg/mL BSA, 0.1 M β -mercaptoethanol, 0.5 M Tris-HCl, 50 mM MgCl₂, 0.08 mM Cy5-dCTP, 0.2 mM dATP, 0.12 mM dCTP, 0.2 mM dTTP, 0.2 mM dGTP; dissolved in water. Store in the dark at -20°C.
6. DNase I dilution buffer: 50 mM Tris-HCl, 5 mM MgCl₂, 1 mM β -mercaptoethanol, 100 μ g/mL BSA; dissolved in water. Store at -20°C.
7. DNA size standard ladder (eg. *Hind*III ladder).
8. 0.3M Ethylenediaminetetracetic acid (EDTA) (Gibco BRL).
9. Sephadex G50 spin column (Amersham).
10. Cot-1 DNA (Gibco BRL).
11. Hybridization buffer: 50% formamide, 10% dextran sulphate, 2X SSC, 2% SDS. Store at -20°C.

2.2.3. Probe denaturation and hybridization

1. Hybridization oven.

2.2.4. Washes

1. Heated water bath.
2. 0.1 M sodium phosphate buffer.
3. NP-40 (Vysis).

3. Methods

3.1. cDNA array CGH

3.1.1. Array preparation

1. Block cDNA microarray under a glass coverslip for 1 hour at 37°C with blocking solution prior to hybridization with denatured probe (*see* Note 3).

3.1.2. Random primer labeling of genomic DNA

1. 2 µg each of high molecular weight tumour and normal genomic DNA is separately digested with *DpnII* for 1-1.5 hours (*see* Notes 4-6). The digestion products are purified (Qiaquick PCR kit), vacuum-dried, and resuspended in 25 µL of water.
2. Random primer labeling is performed using the Bioprime Labeling kit, according to manufacturer's instructions, with modifications. Denature the DNA and 20 µL Random Primers (included in kit) at 100°C for 5 minutes. Immediately chill on ice, and add 2.5 µL dNTPs, 1.25 µL dCTP, 1 µL Cy5/Cy3-dCTP, and 1 µL Klenow fragment (included in kit). Incubate at 37°C for 90 minutes.
3. Combine Cy3- and Cy5-labeled products and load onto a microcon 30 filter. After centrifuging at 2,000 g for 10 minutes, check the sample reservoir for the presence of labeled product (purple colour). Add directly to the sample reservoir 30 µg Cot-1 DNA, 100 µg yeast tRNA, and 20 µg poly(dA-dT), and centrifuge for 20 minutes at 5,000 g. To recover the sample, add 15 µL

hybridization buffer, and invert microcon filter into a fresh collection tube and centrifuge for 1 minute at 16,000 g.

3.1.3. Probe denaturation and hybridization

1. Denature the probe at 100°C for 90 seconds in heated water bath or PCR machine. Chill probe on ice, and allow probe to preanneal at 37°C for 0.5-1 hour.
2. The probe is added to the microarray, covered with a glass coverslip and sealed with rubber cement. Hybridization is at 65°C for 16-20 hours in a moist chamber humidified with hybridization buffer (*see* Notes 3 and 7).

3.1.4. Washes

1. The cDNA microarray is washed at 65°C (*see* Note 7) for 5 minutes in 2X SSC, 0.03% SDS, followed by successive washes in 1X SSC and 0.2X SSC at room temperature (5 minutes each).
2. The microarray is centrifuged at low speed (50 g) for 5 minutes to dry.

3.2. Array CGH

3.2.1. Array preparation

1. Genomic clones (BACs, PACs, cosmids, etc.) are grown with appropriate antibiotic and isolated using commercially available maxi kits. Typical yield is tens of micrograms of DNA. Standard protocols using phenol/chloroform may be used to further purify the DNA (*see* Note 2).
2. Size and quality of DNA is assessed by 1% agarose gel electrophoresis, and quantified with a UV spectrophotometer.

3. This target DNA is sonicated to 1.5-15 kb fragments, precipitated, diluted to appropriate concentrations and spotted down on glass slides in a clean environment with capillary tubes at approximately 200–400 μm diameter spots (*see* Note 8).
4. Arrays are preannealed for 1 hour at 37°C with 20 μL blocking solution under a glass coverslip in a hybridization chamber (*see* Notes 3 and 9).

3.2.2. Probe preparation by nick translation of genomic DNA

1. 2 μg each of high molecular weight tumour and normal genomic DNA (*see* Note 5) is separately labeled by nick translation. The reaction mixtures are as follows:

A) Cy3 reaction (to total 100 μL with water):

- i. Tumour genomic DNA: 2 μg
- ii. 10X Cy3 dNTPs: 10 μL
- iii. DNA polymerase I: 1 μL
- iv. DNase I (*see* Note 10)

B) Cy5 reaction (to total 100 μL with water):

- i. Normal genomic DNA: 2 μg
- ii. 10X Cy5 dNTPs: 10 μL
- iii. DNA polymerase I: 1 μL
- iv. DNase I (*see* Note 10)

2. The labeling reaction proceeds for 1.5 hours at 16°C (refrigerated water bath or PCR machine), following which the reaction mixtures are put on ice.

3. The size of the labeled product is assessed by 1% agarose gel electrophoresis (*see* Note 11). Optimum fragment length for CGH is 500-2,000 base pairs. If the size range is too large, reaction mixtures are returned to 16°C with additional DNase I and polymerase I to incubate further.
4. Labeling reaction is stopped with addition of 0.1 volume 0.3M EDTA.
5. Unincorporated nucleotides are removed from the labeling mixtures using a Sephadex G50 spin column.
6. Labeled products are mixed together, supplemented with 50 µg Cot-1 DNA, and precipitated with 0.1 volume 3M sodium acetate and 2 volumes cold 100% ethanol. Precipitate is rinsed with 70% ethanol and air dried, then redissolved in 20 µL hybridization buffer.

3.2.3. Probe denaturation and hybridization

1. Denature probe for 5 minutes at 75°C, and allow preannealing of the probe for 0.5-1 hour at 37°C to ensure sufficient blocking of repetitive elements.
2. Apply the probe to the microarray after preannealing of the microarray is completed, cover with glass coverslip and seal with rubber cement. Arrays are hybridized for 24 hours at 37°C in a chamber humidified with hybridization buffer (*see* Note 3).

3.2.4. Washes

1. Arrays are washed at 55°C in 50% formamide, 2X SSC pH 7.0 (3X, 10 minutes each), then in 0.1 M sodium phosphate buffer with 0.1% NP-40 pH 8 at room temperature, 5-10 minutes.

2. Drain excess liquid and mount slide in DAPI/Antifade under a glass coverslip.

4. Notes

1. Controversy exists in establishing a standard nomenclature. Although the term “probe” correctly refers to the known nucleic acid sequence tethered on the microarray while “target” is the unknown sequence in the sample (36), for the sake of conformity this chapter is following the convention used by all current microarray CGH publications.
2. Until automated and practical batch methods are developed, many groups are using maxi kits for obtaining target DNA for genomic DNA-based microarrays. This is a labor- and time-intensive process that needs repeating when the target DNA is exhausted over multiple arrayings. If purified target DNA is available (at least several hundred nanograms template, from either maxi or mini preps), DOP-PCR (26) may be used to ensure an indefinite supply of target DNA.
3. It is very important that the microarray does not dry during any hybridization step. Ensure that the hybridization chamber remains humidified with hybridization buffer to prevent evaporation of the probe or blocking mixture. If the microarray does dry, the results are invariably unusable.
4. The protocol herein is optimized for cDNA microarrays with approximately 3,500 features arrayed over an area of approximately $18 \times 16 \text{ mm}^2$ (9,10). The amount of DNA, as well as the final hybridization volume, must be scaled up when using higher density microarrays covering a larger spotting area (10).
5. As expected, the size and purity of the unlabeled genomic DNA is very important for obtaining high quality results using microarray CGH. Low quality DNA used in labeling can result in high background and low signal intensity on the

microarray. The protocol stated herein is optimized for genomic DNA extracted from fresh tissues.

6. The choice of restriction enzyme for digestion is important for labeling efficiency. It has been noted that decreasing the average fragment size prior to labeling may increase labeling efficiency (9). This has to be balanced against excessive digestion producing fragments that are too small to be suitable for hybridization to the cDNA targets. In our hands *EcoRI* has produced consistently satisfactory results for human genomic DNA.
7. When beginning the technique, a range of different hybridization and wash temperatures should be tested to determine the optimal sensitivity and specificity for the specific cDNA microarrays used. In our hands (10) we have found that hybridization at 37°C and wash at 55°C allows sufficient sensitivity for detection of high copy number gains and amplifications. We have observed that 65°C washes reduced signal intensity on our microarrays. Too low a wash temperature will result in non-specific binding (too many yellow signals). We recommend that these tests be performed using differentially labeled DNAs from different samples to ensure optimization of the technique specificity.
8. To date, the protocols for array fabrication have not yet been standardized. The published works specify target DNA concentrations of 400-1000 µg/mL hand-spotted on glass slides coated with poly-L-lysine (11), or 2 µg/µL target DNA on aminopropyltrimethoxy silane-coated slides (12). It is important to note that both the concentration as well as the slide preparation is likely to change as automation procedures with robotic arrayers emerge.

9. The protocol specified herein for array CGH assumes a maximum gridded feature area that can be covered with a 22 x 20 mm² glass coverslip. In addition, it is assumed that the target DNA are denatured during array fabrication (12). Otherwise, a microarray denaturation step of 2 minutes in 70% formamide/4X SSC (11) must be included prior to probe hybridization.
10. The final probe length depends on the DNase I concentration. For CGH, the suitable length for hybridization ranges from 500-2,000 base pairs. Initially, stock solutions of 1×10^{-4} U/ μ L, prepared fresh in DNase I dilution buffer, may be used to obtain the final concentration of 5×10^{-5} U/ μ L. However, this should be adjusted as necessary to obtain optimal fragment length.
11. Approximately 0.05 – 0.1 volume of each labeling mixture is loaded onto the gel with DNA stain (eg. ethidium bromide). Assessment of labeling by agarose gel is recommended as it can aid in troubleshooting array CGH results.

5. References

1. Kallioniemi, A., Kallioniemi, O. P., Sudar, D., Rutovitz, D., Gray, J. W., Waldman, F., Pinkel, D. (1992) Comparative genomic hybridization for molecular cytogenetic analysis of solid tumors. *Science* **258**, 818-821.
2. Kallioniemi, O. P., Kallioniemi, A., Sudar, D., Rutovitz, D., Gray, J. W., Waldman, F., Pinkel, D. (1993) Comparative genomic hybridization: a rapid new method for detecting and mapping DNA amplification in tumors. *Semin. Canc. Biol.* **4**, 41-46.
3. Forozan, F., Karhu, R., Kononen, J., Kallioniemi, A., Kallioniemi, O. P. (1997) Genome screening by comparative genomic hybridization. *Trends Genet.* **13**, 405-409.
4. James, L. A. (1999) Comparative genomic hybridization as a tool in tumour cytogenetics. *J. Pathol.* **187**, 385-395.
5. Parente, F., Gaudray, P., Carle, G. F., Turc-Carel, C. (1997) Experimental assessment of the detection limit of genomic amplification by comparative genomic hybridization CGH. *Cytogenet. Cell Genet.* **78**, 65-68.
6. Lennon, G., Auffray, C., Polymeropoulos, M., Soares, M. B. (1996) The I.M.A.G.E. Consortium: an integrated molecular analysis of genomes and their expression. *Genomics* **33**, 151-152.
7. Schena, M., Shalon, D., Davis, R. W., Brown, P. O. (1995) Quantitative monitoring of gene expression patterns with a complementary DNA microarray. *Science* **270**, 467-470.
8. DeRisi, J., Penland, L., Brown, P. O., Bittner, M. L., Meltzer, P. S., Ray, M., Chen, Y., Su, Y. A., Trent, J. M. (1996) Use of a cDNA microarray to analyse gene expression patterns in human cancer. *Nat. Genet.* **14**, 457-460.
9. Pollack, J. R., Perou, C. M., Alizadeh, A. A., Eisen, M. B., Pergamenschikov, A., Williams, C. F., Jeffrey, S. S., Botstein, D., Brown, P. O. (1999) Genome-wide analysis of DNA copy-number changes using cDNA microarrays. *Nat. Genet.* **23**, 41-46.
10. Beheshti, B., Braude, I., Marrano, P., Zielenska, M., Squire, J. A. (2001) Survey of DNA amplifications in neuroblastoma tumors using cDNA microarrays. *Canc. Res.*
11. Solinas-Toldo, S., Lampel, S., Stilgenbauer, S., Nickolenko, J., Benner, A., Dohner, H., Cremer, T., Lichter, P. (1997) Matrix-based comparative genomic hybridization: biochips to screen for genomic imbalances. *Genes Chr. Canc.* **20**, 399-407.
12. Pinkel, D., Segraves, R., Sudar, D., Clark, S., Poole, I., Kowbel, D., Collins, C., Kuo, W. L., Chen, C., Zhai, Y., Dairkee, S. H., Ljung, B. M., Gray, J. W., Albertson, D. G. (1998) High resolution analysis of DNA copy number variation using comparative genomic hybridization to microarrays. *Nat. Genet.* **20**, 207-211.
13. Heiskanen, M. A., Bittner, M. L., Chen, Y., Khan, J., Adler, K. E., Trent, J. M., Meltzer, P. S. (2000) Detection of gene amplification by genomic hybridization to cDNA microarrays. *Canc. Res.* **60**, 799-802.

14. Raap, A. K., van de Corput, M. P., Vervenne, R. A., van Gijlswijk, R. P., Tanke, H. J., Wiegant, J. (1995) Ultra-sensitive FISH using peroxidase-mediated deposition of biotin- or fluorochrome tyramides. *Hum. Mol. Genet.* **4**, 529-534.
15. Jones, T. A., Flomen, R. H., Senger, G., Nizetic, D., Sheer, D. (2000) The homeobox gene MEIS1 is amplified in IMR-32 and highly expressed in other neuroblastoma cell lines. *Eur. J. Canc.* **36**, 2368-2374.
16. Spieker, N., van Sluis, P., Beitsma, M., Boon, K., van Schaik, B. D., van Kampen, A. H., Caron, H., Versteeg, R. (2001) The MEIS1 oncogene is highly expressed in neuroblastoma and amplified in cell line IMR32. *Genomics* **71**, 214-221.
17. Pei, J. (2001) cDNA array CGH analysis of pediatric osteosarcomas identifies regions of amplification on chromosome 17. *Canc. Res.*
18. Halgren, R. G., Fielden, M. R., Fong, C. J., Zacharewski, T. R. (2001) Assessment of clone identity and sequence fidelity for 1189 IMAGE cDNA clones. *Nucleic Acids Res.* **29**, 582-588.
19. Albertson, D. G., Ylstra, B., Segraves, R., Collins, C., Dairkee, S. H., Kowbel, D., Kuo, W. L., Gray, J. W., Pinkel, D. (2000) Quantitative mapping of amplicon structure by array CGH identifies CYP24 as a candidate oncogene. *Nat. Genet.* **25**, 144-146.
20. Bruder, C. E., Hirvela, C., Tapia-Paez, I., Fransson, I., Segraves, R., Hamilton, G., Zhang, X. X., Evans, D. G., Wallace, A. J., Baser, M. E., Zucman-Rossi, J., Hergersberg, M., Boltshauser, E., Papi, L., Rouleau, G. A., Poptodorov, G., Jordanova, A., Rask-Andersen, H., Kluwe, L., Mautner, V., Sainio, M., Hung, G., Mathiesen, T., Moller, C., Pulst, S. M., Harder, H., Heiberg, A., Honda, M., Niimura, M., Sahlen, S., Blennow, E., Albertson, D. G., Pinkel, D., Dumanski, J. P. (2001) High resolution deletion analysis of constitutional DNA from neurofibromatosis type 2 (NF2) patients using microarray-CGH. *Hum. Mol. Genet.* **10**, 271-282.
21. Daigo, Y., Chin, S. F., Gorringe, K. L., Bobrow, L. G., Ponder, B. A., Pharoah, P. D., Caldas, C. (2001) Degenerate oligonucleotide primed-polymerase chain reaction-based array comparative genomic hybridization for extensive amplicon profiling of breast cancers : a new approach for the molecular analysis of paraffin-embedded cancer tissue. *Am. J. Pathol.* **158**, 1623-1631.
22. Weber, T., Weber, R. G., Kaulich, K., Actor, B., Meyer-Puttlitz, B., Lampel, S., Buschges, R., Weigel, R., Deckert-Schluter, M., Schmiedek, P., Reifenberger, G., Lichter, P. (2000) Characteristic chromosomal imbalances in primary central nervous system lymphomas of the diffuse large B-cell type. *Brain Pathol.* **10**, 73-84.
23. Geschwind, D. H., Gregg, J., Boone, K., Karrim, J., Pawlikowska-Haddal, A., Rao, E., Ellison, J., Ciccodicola, A., D'Urso, M., Woods, R., Rappold, G. A., Swerdloff, R., Nelson, S. F. (1998) Klinefelter's syndrome as a model of anomalous cerebral laterality: testing gene dosage in the X chromosome pseudoautosomal region using a DNA microarray. *Dev. Genet.* **23**, 215-229.
24. Hui, A. B., Lo, K. W., Yin, X. L., Poon, W. S., Ng, H. K. (2001) Detection of multiple gene amplifications in glioblastoma multiforme using array-based comparative genomic hybridization. *Lab. Invest.* **81**, 717-723.

25. Cheung, V. G., Nowak, N., Jang, W., Kirsch, I. R., Zhao, S., Chen, X. N., Furey, T. S., Kim, U. J., Kuo, W. L., Olivier, M., Conroy, J., Kasprzyk, A., Massa, H., Yonescu, R., Sait, S., Thoreen, C., Snijders, A., Lemyre, E., Bailey, J. A., Bruzel, A., Burrill, W. D., Clegg, S. M., Collins, S., Dharni, P., Friedman, C., Han, C. S., Herrick, S., Lee, J., Ligon, A. H., Lowry, S., Morley, M., Narasimhan, S., Osoegawa, K., Peng, Z., Plajzer-Frick, I., Quade, B. J., Scott, D., Sirotkin, K., Thorpe, A. A., Gray, J. W., Hudson, J., Pinkel, D., Ried, T., Rowen, L., Shen-Ong, G. L., Strausberg, R. L., Birney, E., Callen, D. F., Cheng, J. F., Cox, D. R., Doggett, N. A., Carter, N. P., Eichler, E. E., Haussler, D., Korenberg, J. R., Morton, C. C., Albertson, D., Schuler, G., de Jong, P. J., Trask, B. J. (2001) Integration of cytogenetic landmarks into the draft sequence of the human genome. *Nature* **409**, 953-958.
26. Telenius, H., Carter, N. P., Bebb, C. E., Nordenskjold, M., Ponder, B. A., Tunnacliffe, A. (1992) Degenerate oligonucleotide-primed PCR: general amplification of target DNA by a single degenerate primer. *Genomics* **13**, 718-725.
27. Cheng, S., Fockler, C., Barnes, W. M., Higuchi, R. (1994) Effective amplification of long targets from cloned inserts and human genomic DNA. *Proc. Natl. Acad. Sci. USA* **91**, 5695-5699.
28. Lichter, P., Joos, S., Bentz, M., Lampel, S. (2000) Comparative genomic hybridization: uses and limitations. *Semin. Hematol.* **37**, 348-357.
29. Wilgenbus, K. K., Lichter, P. (1999) DNA chip technology ante portas. *J. Mol. Med.* **77**, 761-768.
30. King, W., Proffitt, J., Morrison, L., Piper, J., Lane, D., Seelig, S. (2000) The role of fluorescence in situ hybridization technologies in molecular diagnostics and disease management. *Mol. Diagn.* **5**, 309-319.
31. Cheung, V. G., Morley, M., Aguilar, F., Massimi, A., Kucherlapati, R., Childs, G. (1999) Making and reading microarrays. *Nat. Genet.* **21**, 15-19.
32. Eisen, M. B., Spellman, P. T., Brown, P. O., Botstein, D. (1998) Cluster analysis and display of genome-wide expression patterns. *Proc. Natl. Acad. Sci. USA* **95**, 14863-14868.
33. Brazma, A., Vilo, J. (2000) Gene expression data analysis. *FEBS Lett.* **480**, 17-24.
34. Kerr, M. K., Martin, M., Churchill, G. A. (2000) Analysis of variance for gene expression microarray data. *J. Comput. Biol.* **7**, 819-837.
35. Sherlock, G., Hernandez-Boussard, T., Kasarskis, A., Binkley, G., Matese, J. C., Dwight, S. S., Kaloper, M., Weng, S., Jin, H., Ball, C. A., Eisen, M. B., Spellman, P. T., Brown, P. O., Botstein, D., Cherry, J. M. (2001) The Stanford Microarray Database. *Nucleic Acids Res.* **29**, 152-155.
36. Phimister, B. (1999) Going Global (Editorial). *Nat. Genet.* **21**, 1.
37. Alon, U., Barkai, N., Notterman, D. A., Gish, K., Ybarra, S., Mack, D., Levine, A. J. (1999) Broad patterns of gene expression revealed by clustering analysis of tumor and normal colon tissues probed by oligonucleotide arrays. *Proc. Natl. Acad. Sci. USA* **96**, 6745-6750.

6. Figure Legends

Figure 1. Schematic depiction of the utility of cDNA microarrays in expression and CGH analyses. cDNA microarrays are screened with labeled probes derived from RNA and/or DNA of normal (Cy5) and tumour (Cy3) tissue. Analysis of the red:green signal intensity ratios indicate the level of A) gene expression or B) gene dosage change, respectively. Analyses may require datamining techniques for optimal interpretation of the results. A) Two-dimensional hierarchical clustering (32,37) is applied to the results to identify patterns of gene expression and establish clinical correlates. B) *in silico* cDNA chromosome localisation and arrangement into sequential order allows the results of cDNA array CGH to be depicted as an ideogram-type plot across the genome, facilitating identification of regions of gene dosage change.

Figure 2. Normalized cDNA array CGH of neuroblastoma patients identified three tumour genotypes: A) No high copy gains or amplification of genomic DNA; B) *MYCN* amplification as the sole genomic copy number imbalance; and C) *MYCN* amplification with previously undetected co-amplified 2p24 genes and high copy number gains of numerous other genes, suggesting an underlying genetic instability. This third clinical genotype was not previously described, as these regions are not resolvable by chromosome CGH (10).

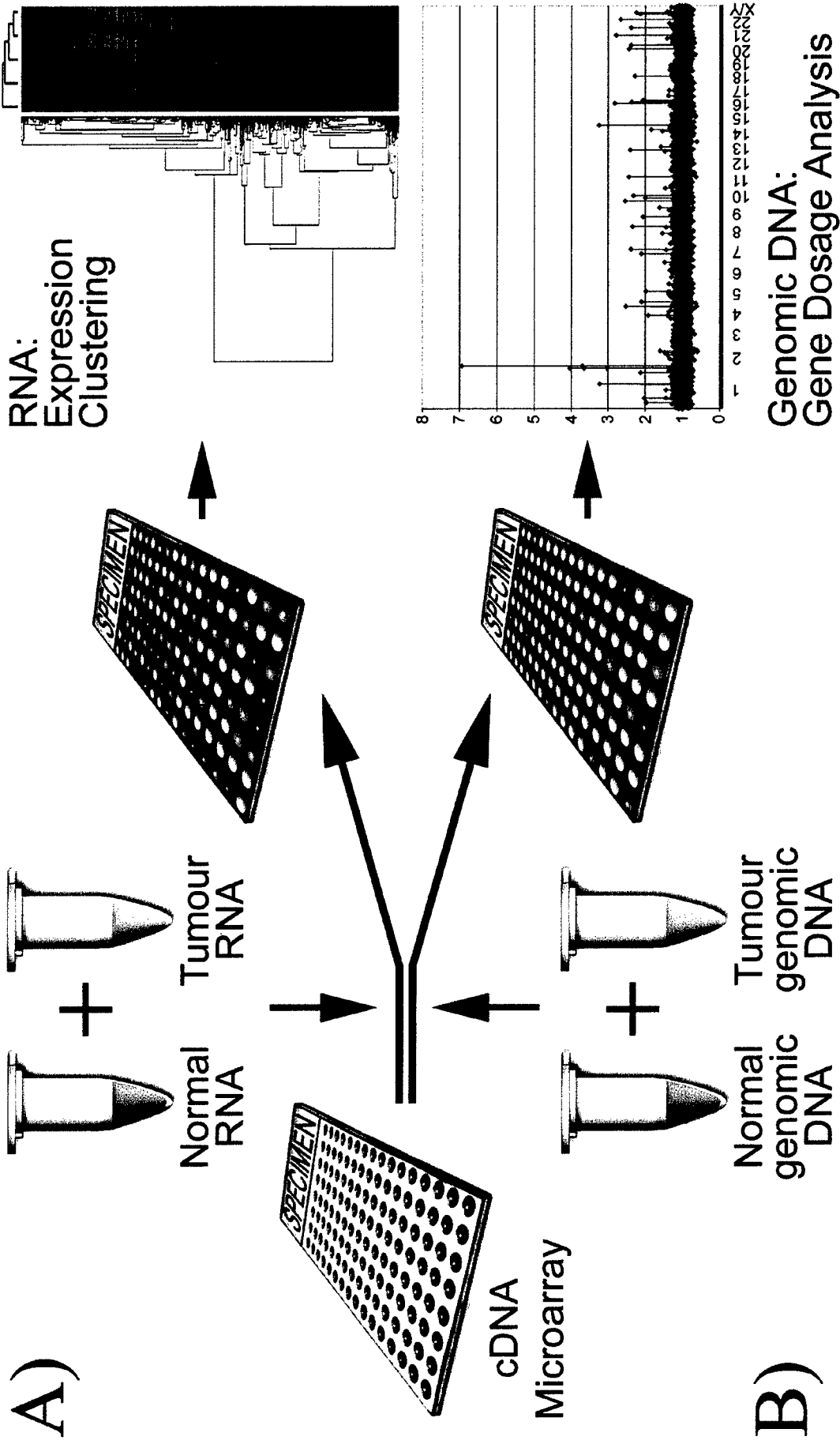
Figure 3. High resolution detection of gene dosage changes on chromosome 17 using high-density cDNA array CGH. Chromosome CGH detected high copy gain of the

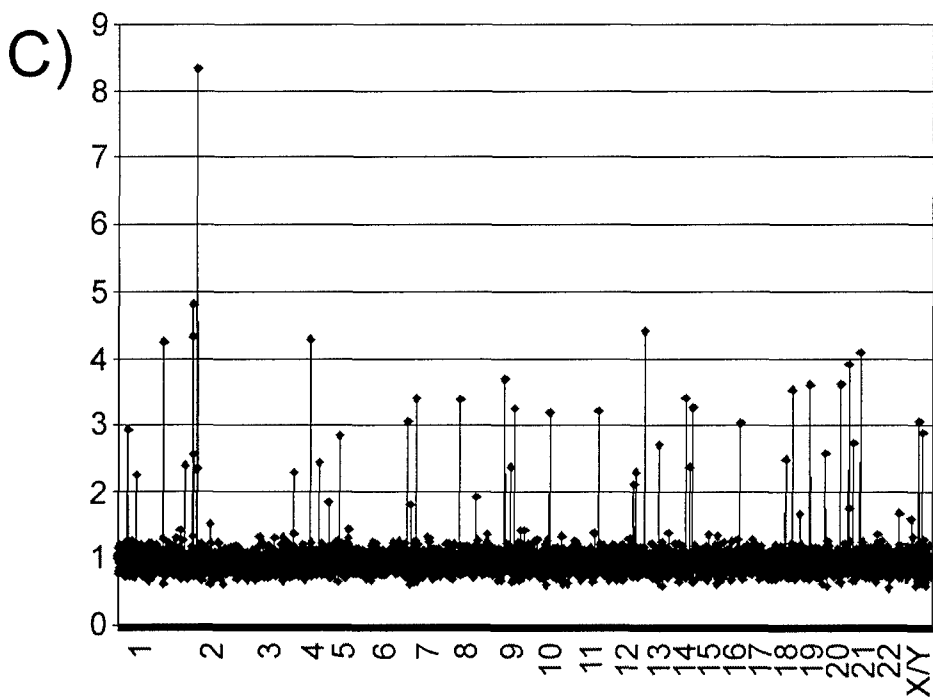
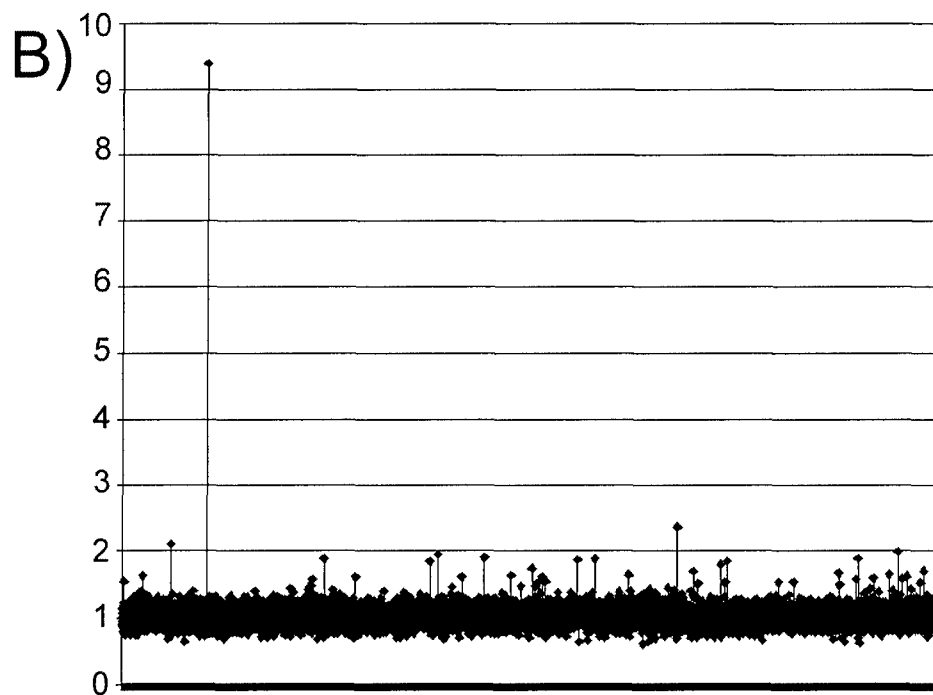
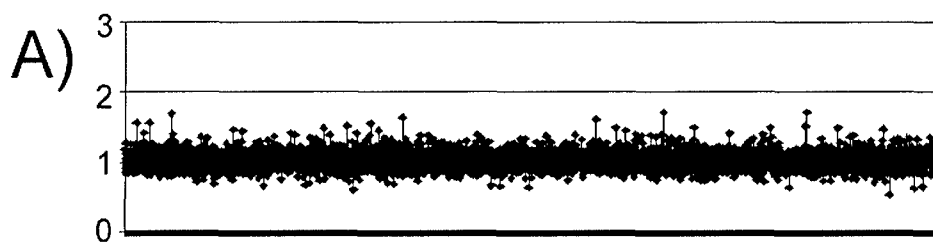
chromosome region 17p-17q21 (vertical gray bar) in an osteosarcoma sample. Corresponding normalized cDNA array CGH using genomic DNA from the same sample significantly resolved the boundaries of this gain to the region 17p12-17p11.2 (horizontal gray bar). Chromosome ideograms are constructed by *in silico* assignment of microarray cDNAs to chromosomes, then arranging cDNAs into sequential order along each chromosome (10).

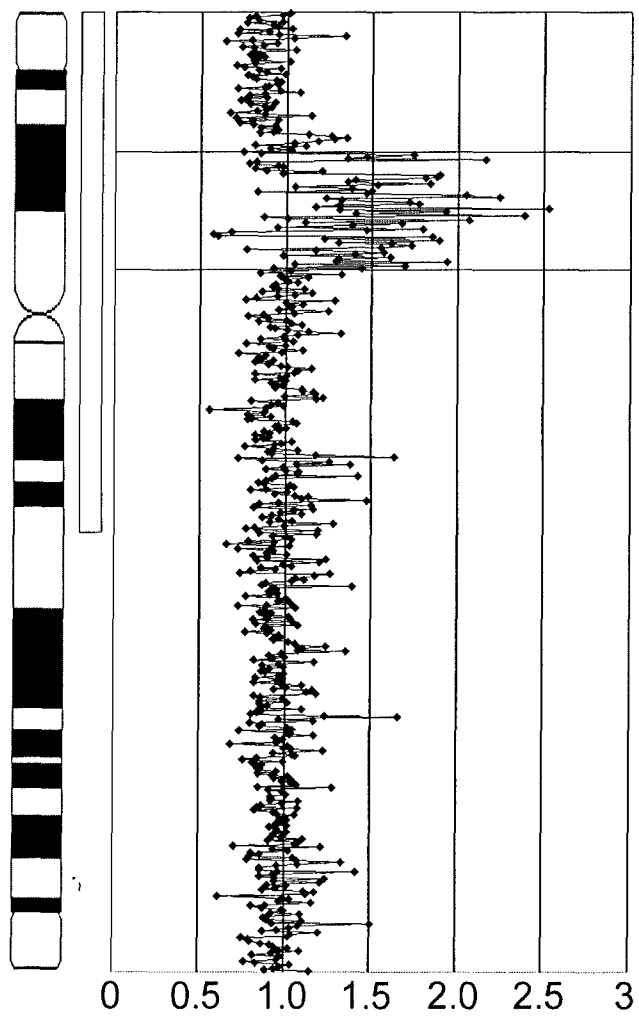
Figure 4. Schematic representation of the array CGH technique for a focused analysis of copy number imbalances along a region of interest (eg. 8q21.1). A) A tiling path of genomic clones (eg. BACs, PACs, P1s, cosmids) is generated to cover the region. After extraction and purification, these genomic DNA targets are arrayed onto glass slides. B) Array CGH is performed by hybridizing labeled normal (Cy3) and tumour (Cy5) genomic DNA to the microarray, and detected using a microarray scanner. C) Each array spot, realigned *in silico* as a single contiguous map to correspond with the tiling path, can be analysed by fluorescence ratio to identify the regions of copy number changes. These results may be correlated with *in silico* techniques to identify candidate genes of interest.

Figure 5. Histogram showing the copy number of the genomic clones comprising a 7 Mb tiling path on chromosome 22q, represented from the centromeric (left) to the telomeric (right) direction. Each black bar represents an individual genomic clone. Chromosome X and Y control genomic clones are separated (gray bar) on the right of the histogram. A) Array CGH comparing normal male and female DNA shows expected single copy loss of chromosome X clones (arrows). B) Comparison of a male NF2 patient against

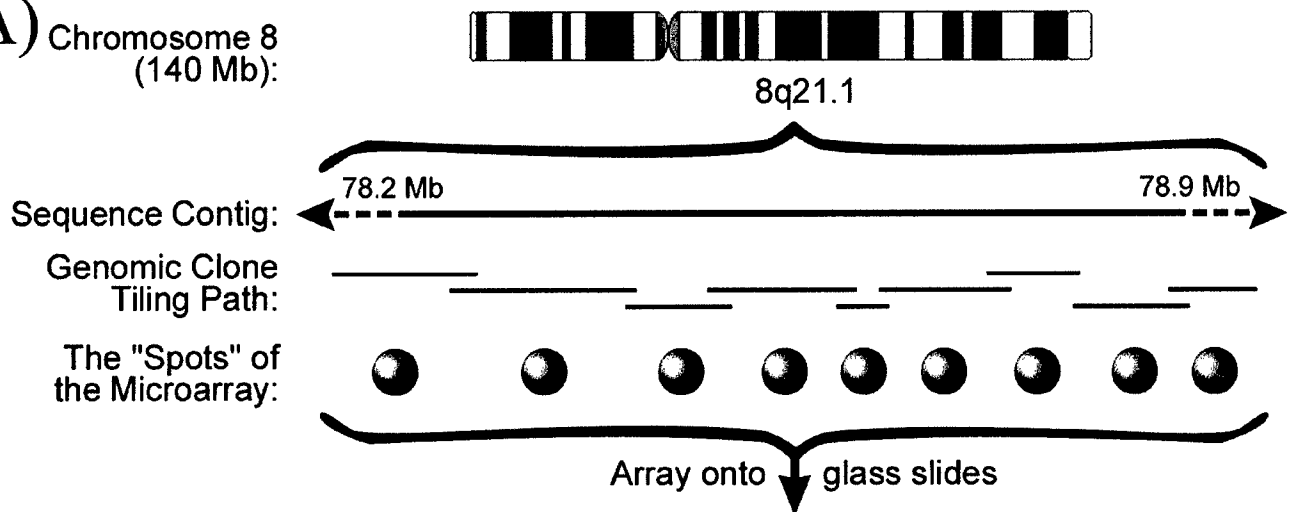
normal female control delineates boundaries of heterozygous loss along the *NF2* locus and surrounding region (stippled region). C) The detection of homozygous interstitial deletion (asterisk) within a region of single copy loss in a heterozygous female *NF2* patient against a normal female control demonstrates the sensitivity and the resolution of array CGH. The accuracy of the technique is reflected by the deviation of the ratio from the expected values. Adapted from Bruder et al., 2001 (20) with permission.



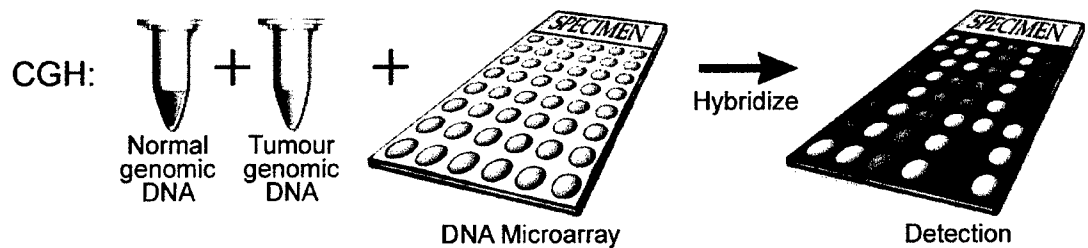




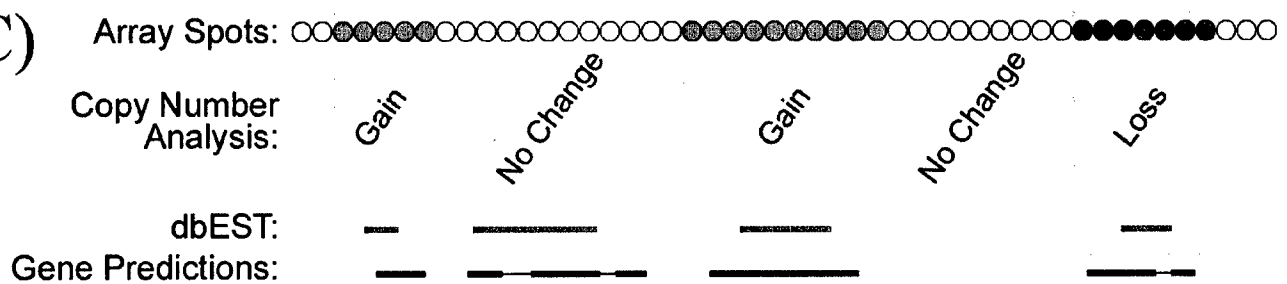
A) Chromosome 8
(140 Mb):

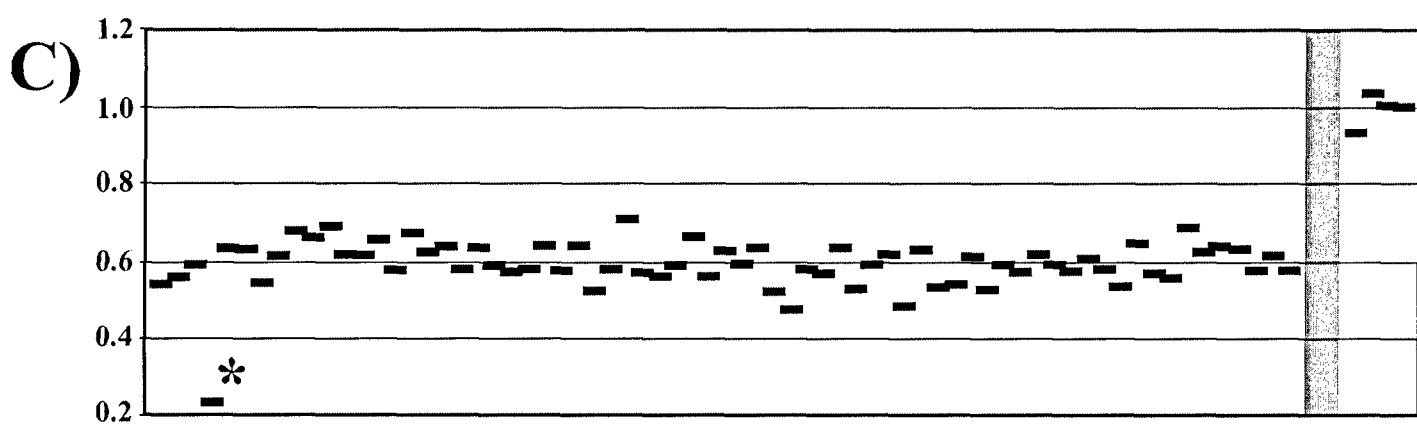
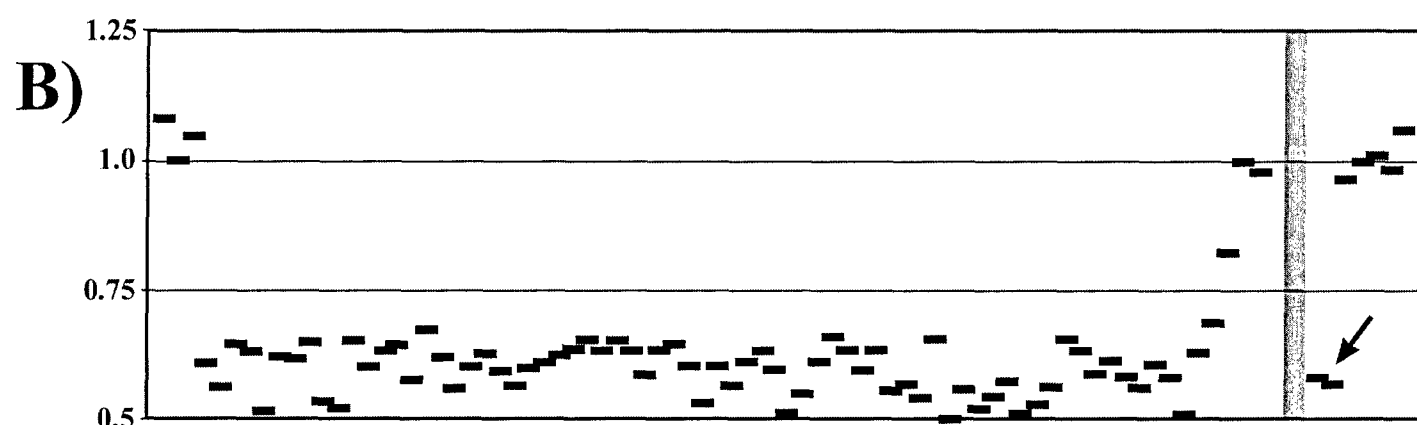
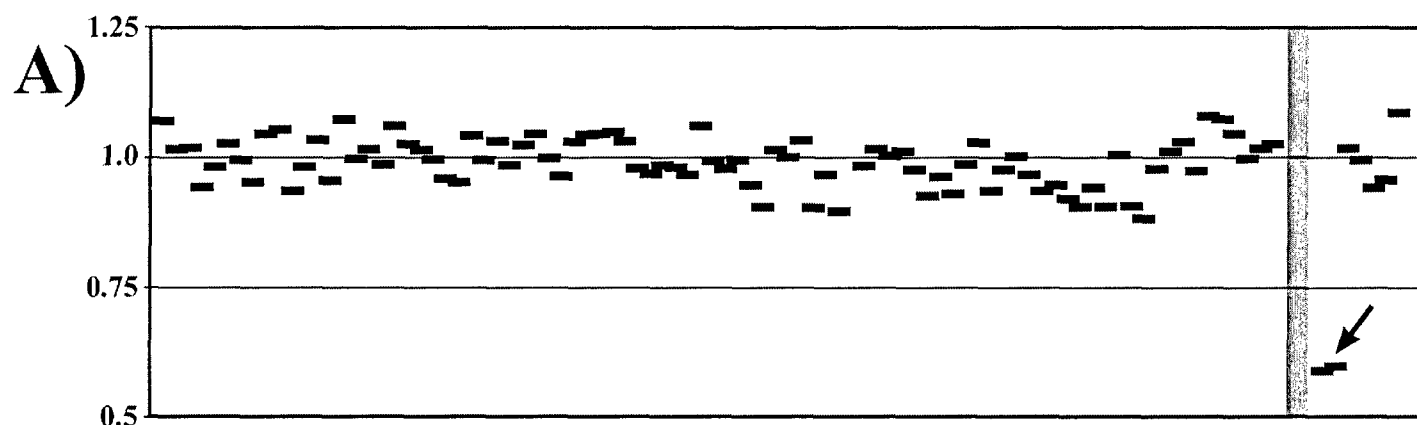


B)



C)







DEPARTMENT OF THE ARMY
US ARMY MEDICAL RESEARCH AND MATERIEL COMMAND
504 SCOTT STREET
FORT DETRICK, MARYLAND 21702-5012

REPLY TO
ATTENTION OF:

MCMR-RMI-S (70-1y)

21 Feb 03

MEMORANDUM FOR Administrator, Defense Technical Information
Center (DTIC-OCA), 8725 John J. Kingman Road, Fort Belvoir,
VA 22060-6218

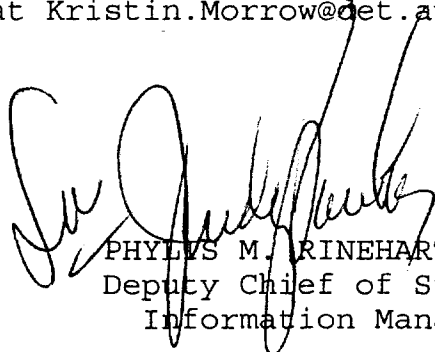
SUBJECT: Request Change in Distribution Statement

1. The U.S. Army Medical Research and Materiel Command has reexamined the need for the limitation assigned to technical reports written for this Command. Request the limited distribution statement for the enclosed accession numbers be changed to "Approved for public release; distribution unlimited." These reports should be released to the National Technical Information Service.

2. Point of contact for this request is Ms. Kristin Morrow at DSN 343-7327 or by e-mail at Kristin.Morrow@det.amedd.army.mil.

FOR THE COMMANDER:

Encl


PHYLLIS M. RINEHART
Deputy Chief of Staff for
Information Management

ADB263458	ADB282838
ADB282174	ADB233092
ADB270704	ADB263929
ADB282196	ADB282182
ADB264903	ADB257136
ADB268484	ADB282227
ADB282253	ADB282177
ADB282115	ADB263548
ADB263413	ADB246535
ADB269109	ADB282826
ADB282106	ADB282127
ADB262514	ADB271165
ADB282264	ADB282112
ADB256789	ADB255775
ADB251569	ADB265599
ADB258878	ADB282098
ADB282275	ADB232738
ADB270822	ADB243196
ADB282207	ADB257445
ADB257105	ADB267547
ADB281673	ADB277556
ADB254429	ADB239320
ADB282110	ADB253648
ADB262549	ADB282171
ADB268358	ADB233883
ADB257359	ADB257696
ADB265810	ADB232089
ADB282111	ADB240398
ADB273020	ADB261087
ADB282185	ADB249593
ADB266340	ADB264542
ADB262490	ADB282216
ADB266385	ADB261617
ADB282181	ADB269116
ADB262451	
ADB266306	
ADB260298	
ADB269253	
ADB282119	
ADB261755	
ADB257398	
ADB267683	
ADB282231	
ADB234475	
ADB247704	
ADB258112	
ADB267627	